2006

Some Factors Affecting the Interfacial Interaction at Thermomechanical Pulp Fiber and Polypropylene Interphase

Sangyeob Lee
Louisiana State University and Agricultural and Mechanical College

SOME FACTORS AFFECTING THE INTERFACIAL INTERACTION AT THERMOMECHANICAL PULP FIBER AND POLYPROPYLENE INTERPHASE

A Dissertation
Submitted to the Graduate School of the
Louisiana State University and
Agricultural and Mechanical College
In partial fulfillment of the
Requirements for the degree of
Doctor of Philosophy

in

The School of Renewable Natural Resources

by
Sangyeob Lee
B.S. Youngnam University, Korea, 1993
M.S. Youngnam University, Korea, 1995
M.S. University of Idaho, U.S.A. 2002

August 2006

ACKNOWLEDGEMENTS

Numerous individuals provided invaluable help throughout this project, which cannot be successfully completed without their assistance. I am sincerely grateful to Dr. Todd F. Shupe, my major professor, for his guidance, advice, and assistance. My deep appreciation is also extended to my other committee members. Specifically, I would like to express my sincere gratitude to Dr. Chung Y. Hse for his guidance and advice throughout this study. I am grateful to Dr. Ben S. Bryant, for his support and invaluable advice on numerous subjects. I also would like to thank Dr. C. F. "Niels" DeHoop, Dr. Richard P. Vlosky and Dr. John Fleeger for their assistance and support.

I wish to express my appreciation to Dr. Leslie H. Groom (Project Leader, USDA-Forest Service Southern Research Station, Pineville, LA) and his research unit (Research Scientists; Dr. Thomas L. Eberhardt, Dr. Thomas Elder, Dr. Chi-Leung So and technicians; Dale E. Huntsberry, Donna M. Edwards, Karen Reed, Gary W. Smith, and Janie R. Gurgainers) for their help and guidance on the instrumental operations of this project. I am grateful to Dr. John Bostick at Norac Inc. for benzoyl peroxide. I also thank Mr. Henry C. Brown and C. Becker at Huntman Inc. for supplying the maleic anhydride and many helpful discussions concerning the experimental applications. Further appreciation is given to the following persons: Dr. Brain Via, Xiaobo Li, Yaojian Liu, Dr. Cheng Piao, Hui Pan, and my colleagues in the School of Renewable Natural Resources.

I thank my parents (Sungwoo Lee, Chungrang Han, and Youngsoon Kim), my wife, Wehrawn Kang, whose patience and support through out my study, and my children (Linda, Lisa and Todd), who provided a constant source of encouragement and a joyful life.

I am indebted to the Louisiana Forest Products Development Center for funding this study and my assistantship at the Louisiana State University Agricultural Center.

TABLE OF CONTENTS

LIST OF TABLES

LIST OF FIGURES

ABSTRACT

This dissertation focused on some selected factors that influence the interfacial interactions at the interphase between wood based materials and thermoplastic surfaces. Several treatments were applied to enhance interfacial properties. In general, interfacial properties were altered by physical and chemical surface modification. Study of the interfacial interactions between wood fiber surfaces as a reinforced material and thermoplastics as a matrix material is important to understand fundamentals of wood fiber-plastic composites (WPC). This study represents fundamental research to define treatment effects on surfaces of wood pulp fibers and polypropylene (PP) film.

Two thermosets, ion implantations, and maleic anhydride (MA) grafting were used to increase interfacial adhesion between wood based materials and PP. Thermoset resins were applied at three levels to fiber handsheets and PP film laminates. The surface treatment increased shear and tensile strength properties and PP crystallinity (X_C) as determined by differential scanning calorimetry (DSC). The ion implantation method using oxygen and argon as ion sources proved to be one of the most effective treatments to improve interfacial bonding between thermomechanical pulp (TMP) fibers and PP film. Oxygen plasma treatment was more effective than argon to increase tensile strength due to the electron donor and accepter mechanism generated by magnetic fields between two electrodes. The MA grafting effect also improved the tensile strength of TMP fiber handsheets and PP film laminates fabricated with a 50/50 weight fraction. A brittle failure was observed by scanning electron microscopy (SEM) at the fracture surface of tensile specimens made from TMP fiber handsheets and PP film laminates (TPL). It was found by using extraction with CH_2Cl_2 and H_2O as solvents that the PP nucleation ability on fiber surfaces was extremely reduced due to the removal of deposit materials from the surface.

Thus, the extractives on the wood/non-wood fiber surface played a potential role for surface induced nuclei and lamella deposits for the PP melts.

In conclusion, the surface treatments of ion implantations, thermoset treatment, and MA modification enhanced interfacial strength of TPL. Electron interaction and mechanical interlocking in the wood fiber handsheet improved interfacial interactions between the wood-based materials and PP.

CHAPTER 1

LITERATURE REVIEW

1.1. Introduction

Natural fiber-reinforced composites have attracted increased interest because of the advantages of the bio-based fibers, such as low density, relatively high toughness, high strength and stiffness, good thermal properties and biodegradability (Rezai and Warner 1997, Wu et al. 2000, Joseph et al. 2003). Lignocellulosic materials are widely utilized in wood fiber and thermoplastic composites (WPC) because of their low density, relatively high strength and stiffness, and machinability (Maldas and Kokta 1991b, Rievld and Simon 1992, Kolosik et al. 1992, Stark 1999, Wolcott et al. 2000, Xue and Tao1 2005**)**. Wood fibers as a reinforcing component for thermoplastics open up further possibilities for use of lignocellulosic fiber resources. However, the main disadvantage of natural fibers in thermoplastics is the poor compatibility between hydrophilic fiber surfaces and hydrophobic thermoplastics. Therefore, chemical and mechanical modifications are used to increase the interfacial adhesion characteristics at the wood fiber and thermoplastic interface. A study of the properties of composites made with the natural fibers of sisal, coir, and jute with unsaturated polyester resin demonstrated that compatible structural properties were obtained and that, using a modified rule of mixtures, the properties of the fiber reinforced composites could be predicted (Lin 1986, Bryant et al. 2003).

Composite materials consist of two or more components and phases. The interface is a key component, which, among other roles, provides a means of stress transfer from fiber to fiber through the matrix and serves to protect the fibers from environmental degradation. Although the concept of a perfect interface took root in conventional mechanics, which has treated the

interface as an infinitely thin layer with no physical properties of its own, it is generally agreed today that the interfacial region of a composite extends a considerable distance from the fiber surface into the matrix, and has a complex chemical structure and a broad range of physical properties (Caldwell 1993). It is appropriate to call this region "interphase." Depending on the subjects discussed, the terms "interface" and "interphase" or "interfacial region" may be used interchangeably.

Research on the strength properties of WPC have been directed toward overcoming the structural weakness and dimensional stability of the material in an outdoor exposure environment. However, there are still problems to overcome. The problems have stimulated research on the improving interfacial bonding between the hydrophilic and hydrophobic materials through chemical and mechanical modifications. They continue to address many WPC problems such as structural deformation caused by thermal expansion (softening), decay, and marine borer attack (FPL 1999, Pendleton et al. 2002, Wolcott 2003, Verhey and Laks 2002). Selected categories of the thermoplastics are often based on plastic properties, product requirement, copolymer application, cost, availability, and machinery (Clemons 2002). Sources of wood fillers from hardwood and pines such as short fibers (aspect ratio less than 10) have been studied in combinations of thermoplastics such as polypropylene (PP), low- and high-density polyethylene (LDPE and HDPE), polyvinyl chloride (PVC), and polystyrene (PS).

Considerable effort has been placed to study chemical and physical modifications to improve the interfacial adhesion between the wood fibers and the polymer matrix (Karlsson et al. 1996, Espert and Karlsson 2004). The interfacial segregation (separation of fibers from polymer matrix) at the wood fiber surface and PP interface resulted in lower adhesion strength (Beshay and Hoa 1990, Alexy et al. 2000, Amash and Zugenmaier 2000). Therefore, interfacial failure

occurred as the PP matrix began to pull away from the fiber surface producing voids and cracks (Angles et al. 1999, Bledzki et al. 2005). The material grafting system led to alter thermoplastic properties and surface chemistry of the wood material (Demir et al. 2005). Coupling agents such as maleic anhydride (Maldas and Kokta 1990b, Raj et al. 1990, Mohanakrishnan et al. 1993, Collier et al. 1996, Hristov et al. 2004, Mahlberg et al. 2001) and silane (Beshay 1989, Kokta et al. 1990) have been used for chemical modification of both wood fiber and the thermoplastics. With regards to mechanical properties of WPC, the modifications of both natural fiber and thermoplastic interface are important.

1.2. Chronological Development of Wood-based Composites

Leo Bakeland developed "Bakelite" in 1909 which was used for decades to make telephones. He also developed phenolic resin impregnated Kraft paper laminates before the day transistors. When decorative overlay impregnated with melamine and a clear melamine impregnated sulfite paper were added to the top layer of the phenolic base sheets, the products were called "Formica" or high-pressure laminates. Terms of "impreg" and "compreg" were used by the US Forest Products Laboratory to describe phenolic resin impregnated wood and compressed phenolic resin impregnated wood to achieve both hardness and dimensional stability (Bryant 1966). The effectiveness of the methods depended on the microscopic structure and surface chemistry of wood as well as molecular weight of the synthetic polymer. During World War II, Germany made airplane propellers by laminating thin birch veneer with heavily impregnated paper with low-molecular weight phenolic resin to make a variation of compreg that was dimensionally stable. In 1946, dimethylol urea (DMU) was used to impregnate wood and was reported to improve hardness and moisture resistance. Polyolefins were first introduced to treat wood in 1959. Polyethylene glycols (PEG) served as an exceptional dimensional stabilizer

via cell wall diffusion. PEG permanently swelled the cell walls and the wood could not shrink. Unlikely phenolic resin impregnations, PEG treated wood is not brittle but acts like green wood. During the 1960s, olefinically unsaturated monomers were broadly accepted. The other monomeric materials were also applied to modify wood fiber surfaces and thermoplastics as cross-linking agents in late 1960s (Lu et al. 2000). In 1972, maleic anhydride (MA) was introduced as a coupling agent to wood materials combined with polyethylene (PE) or PVC. However, the monomers were not applied for wood fiber and thermoplastic modification until a continuous extrusion system was introduced in the WPC industry in 1983 (Clemons 2002).

Bryant (1966) summarized some of the problems related to resin impregnation of solid wood that must take into account wood microscopic structure, species, density, amorphous region of the cell wall, grain orientation, and the molecular weight and chemistry of the polymer or monomer stabilizers. The macroscopic nature of wood can inhibit cell wall impregnation of diffuse porous species. Solid contents and molecular size of resins were also important to increase the liquid diffusion to create intimate contact at the material interface. High density wood species, in general, had less dimensionally stable and were difficult to impregnate liquid through side-grain penetration. Low molecular weight polymers or monomers were needed to impregnate into wood cell wall because most impregnation targeted the amorphous region in the S_2 layer to fill voided spaces. Therefore, understanding surface chemistry changes during the chemical and physical treatment is important to overcome strength weakness and dimensional changes.

1.3. Wood Fibers in Wood Fiber and Thermoplastic Composites

Wood can be considered as a polymeric composite made up of three different polymers such as cellulose, hemicellulose and lignin. These polymers are responsible for most of the

physical and chemical properties exhibited by wood and wood products. One of the major disadvantages of products made from wood or wood fibers is wettability in wet environments and humid atmospheres. Free water moves into a fiber-based composite through the capillaries between the fibers that are wetted due to their hydrophilic surface area. This action is known as absorption. On the other hand, moisture can move in the vapor form into the cell wall, thus swelling the individual fibers by means of adsorption. Therefore, wood fiber surface modification is important to produce WPC. The microfibril appearance of the wood fiber surfaces, including end breaks or damaged points, and the chemical composition of wood fibers

Table 1.1. The main chemical compositions of softwood and hardwood in percent of dry wood weight; average values of common pulpwood species. (Sjöström and Alen 1999).

	Softwood		Hardwood	
	Normal wood	Compression wood	Normal wood	Tension wood
Cellulose	37-43	29-31	39-45	50-65
Galactoglucomannans	15-20	9-12	---	---
Glucuronoxylan	---	---	15-30	16-23
Glucomannan	---	---	2-5	2-4
Arabinoglucuronoxylan	5-10	6-8	---	---
Galactan	---	9-11	---	0-10
Laricinan (1,3-glucan)	---	3-5	---	---
Lignin	25-33	37-40	20-25	16-20
Extractives	2-5	2-5	2-4	2-4

of different parts of the tree varies with different species and pulping processes. Table 1.1 compares the chemical composition of softwoods and hardwoods of common pulpwood species. The major distinctions are different combinations and amounts of hemicellulose, lignin, and extractives. These differences between individual wood species are shown in Table 1.2.

Increasing the amount of caustic in the pretreatment of refined pulp fibers increases the strength of the pulp sheets. Boras and Gatenholm (1999) studied the chemical composition model of spruce fibers and measured the distribution of carbohydrates, lignin, and extractives of

Table 1.2. Fiber characteristics and chemical composition of various softwood species. (Sundholm 1999)*

Species	Black spruce (*Picea marana*)	White spruce (*Picea glauca*)	Balsam fir (*Abies balsmea*)	Jack pine (*Pinus bank-siana*)	Lodgepole pine (*Pinus contorta*)	Ponderosa pine (*Pinus ponderosa*)	Loblolly pine (*Pinus taeda*)	Slash pine (*Pinus elliottii*)	Radiata pine (*Pinus radiata*)	Caribbean pine (*Pinus caribaea*)
Fiber length (mm)	3.5	3.3	3.5	3.5	3.1	3.6	3.6	4.2	4.0	2.6-3.9
Fiber width (μm)	25-30	25-30	30-40	28-40	35-45	35-45	35-45	N/A	35-45	35-45
Cell wall thickness (μm)	2.2	2.4	2.5	2.5-2.9	3.0	2.4	3.3	4.2	3.0	6.0-7.1
Specific gravity (g/cm^3)	0.45	0.42	0.37	0.46	0.43	0.42	0.54	0.66	0.43	0.33-0.68
Lignin (%)	27.6	29.4	29.4	28.3	27.7	25.6	28.6	26.8	28.9	26.2-31.2
Extractives (EtOH-Benz) (%)	2.2	2.0	2.5	4.0-4.2	3.5	4.4-5.0	3.2-5.4	3.4-6.0	5.4	4.2

* (Values are averages, except where the ranges are shown.)

pulp after refining. On the basis of the oxygen/carbon (O/C) ratio obtained from electron spectroscopy for chemical analysis (ESCA), he suggested that the pulp surface had a composition of approximately 40% carbohydrates, 28% lignin and 32% extractives. Extractives were in the form of globular particles spread over both carbohydrates and lignin components of the fiber surfaces. The extractives were gradually removed by the sequence of treatments. Washing and extraction treatments resulted in the removal of non-carbohydrates from the fiber surfaces with the result that with their removal, the hydrophobicity of the surface decreased. Extractives in wood fibers strongly affect surface hydrophobicity and their removal makes it more difficult for non-polar polymers to bond to them.

1.4. Chemical Modification of Wood Fibers and Polyolefin

Recently, a considerable amount of research was conducted using coupling agents to build a crosslinking system between wood fibers and thermoplastic polymers. Even though many studies have shown the effectiveness of the fiber treatment, poor interfacial adhesion between the hydrophobic polymer and hydrophilic fiber remains a problem. The problems of compatibility of wood fibers can be overcome by grafting short polymer segments onto the fiber surface using coupling agents and adhesion promoting agents. Thermoplastic composite materials have both advantages and disadvantages (Table 1.3). Attempts have been made to overcome the disadvantages by using dispersing agents, elevating the mixing temperature, and extending the mixing period in the mixer (Gateholm 1996 and Maldas 1989). A number of copolymers and chemicals have been used as wood coupling or dispersing agents in combination with PE (Lu et al. 2000). He pointed out that the most common coupling agents or copolymers were maleic anhydride (MA), maleic anhydride modified polypropylene (MAPP), polyethylene-poly- (phenyl isocyanate), and silane A172 [vinyl-tris (2-methoxyethoxy) silane].

Table 1.3. Advantages and disadvantages of wood fiber compared to inorganic fillers. (Maldas and Kokta 1993, Chen and Meister 1995, Bledzki 1998).

Advantages of the wood fiber	Disadvantages of the wood fiber
• High specific strength and modulus, renewable nature, lower cost, and suffers little damage. • Possesses strength and modulus properties on an equal density basis. • Equals or exceeds the stiffness of most traditional construction materials on stiffness/weight efficiencies. • Less machine wear during mixing and fabrication (a nonabrasive material). • Easy to process with all of the processing methods for mass production.	• Poor interfacial adhesion between the hydrophobic polymer and hydrophilic fiber. • Poor dispersion of wood materials in the polymer matrix. • Breakage or damage of fiber during the mixing stage. • Variations in the quality of raw material • Limited thermal stability during processing

Common dispersing agents used were stearic acid, paraffin wax, PE wax, and mineral oil. Typical properties of the MA and MAPP are listed in Table 1.4. Kazayawoko et al. (1997b) evaluated the effect of MAPP (Epolene E-43 and Epolene G-3002) treated TMP on the mechanical properties of WPC (weight ratio of 30% wood fiber-70% PP). The tensile strength of the TMP-PP composites was increased by 40% over the untreated specimens.

Sain and Kokta (1993 a,b) found that the modifying agent is covalently bonded explosion pulp (EP) fiber and PP. The pretreated fiber or the PP with m-phenylene bismaleimide (BMI)

Table 1.4. Typical properties of two maleated polypropylene and maleic anhydride. (Kazayawoko et al. 1997b).

	Epolene E-43	Epolene G-3002	Maleic Anhydride
Acid number (mg KOH g)	47	60	-
Density (g cm^{-3})	0.934	0.959	1.48
Viscosity (cps)	400(190°C)	15,000 (225°C)	-
Mw	9100	60,000	98.06
Mn	3900	20,000	-
Maleic anhydride units	1.6	10.7	-

significantly enhanced the adhesion between PP and EP as observed on the fracture surface using scanning electron microscopy (SEM). The change in percent crystallinity of PP measured by differential scanning calorimetry (DSC) was found to be influenced by the presence of the modifier in the composite. Thorsen et al. (1979) observed that the main reaction was caused by the oxidation process of cystine to sulfonic acid. Carbon was also oxidized. Many physical properties of fibers, yarns, and fabrics were related to the scission of cystine disulfide by ozone and the formation of sulfonic acid groups at the fiber surface. The spectra obtained during the induction period suggested the occurrence of some ordered structure that was characterized by higher regularity and packing of the helical moieties (Kimura et al. 1998). This ordered structure was clearly different from an amorphous structure and close to a crystal structure.

When comparing the effectiveness of different coupling agents and treatments to enhance wood fiber-plastic compatibility, it was observed that coating by an isocyanate treatment was the most effective (Maldas and Kokta 1989). They grafted chemical-thermomechanical pulp (CTMP) fibers with a 56.2% silane level to compare it to a 3% isocyanate treatment. They also reported the influence of different pulping agents, such as poly methylene (polyphenyl isocyanate), silanes (A-172, A-174, A-1100), and grafting on the mechanical properties of composites. Raj et al. (1989a, b) used aspen fiber, wood flour, and cellulose flour as reinforcement materials with LDPE. Wood fibers were treated using isocyanate or a vinyl silane-coupling agent to improve the adhesion between the fiber and polymer. Aspen fibers were also used as a filler material in HDPE and LDPE. To improve the bonding between the fiber and polymer, different chemical treatments of the fiber such as treatment with different isocyanates and coating with maleic anhydride was examined (Raj et al. 1989a). Composites with isocyanate treated wood fibers produced higher tensile strength compared to untreated fiber composites.

But when compared to diisocyanate, the polyisocyanate treated fibers produced an even higher gain in strength. HDPE or LDPE filled with MA coated aspen fibers showed a slight decrease in strength with the increase in filler concentration. Tensile modulus generally increased with filler loading and was not affected by fiber treatment (Raj et al. 1990).

Wood fibers treated with sodium sulfite were particularly effective in improving the amount of monomer bond and the conversion of monomer to polymer when PMMA was added to wood fibers (Chen and Meister 1995). Even though chemical modification of the fiber surfaces by graft copolymerization has been extensively performed and reported, no systematic study of samples after each step of the grafting process has been reported in conjunction with the suggested procedures. To explore this point of view, a systematic infrared study of wood samples grafted with monomers by copolymerization was made. Khan et al. (1991) treated wood fibers with methylmethacrylate (MMA) and butylmethacrylate (BMA) monomers using high-energy ionizing radiation.

Han (1991) indicated that MAPP was localized at the interface between the wood filler and the PP, and it acted as a compatibilizer. Kazayawoko et al. (1999) also investigated the surface chemistry before and after treatment of black spruce TMP with MAPP, and confirmed esterification between the hydroxyl groups of wood fiber and the anhydride groups of MAPP. Thermomechanical pulp, recycled newsprint, and wood flour are comparable in terms of their surface chemistry based on the elemental composition and O/C ratio of each type of fiber surface. Mechanical pulp was found to behave differently in the xanthate grafting reaction than chemical pulps. In most cases, lower conversions and higher homopolymer contents were observed than in comparable polymerization involving chemical pulps. Decreasing fiber length

resulted in increased total formation of polymer but reduced grafting efficiency (Hornof et al. 1977).

1.5. Chemical Crosslinking

Intermolecular interactions in solution and at interfaces can be reduced to two phenomena: London dispersion forces, and electron donor-acceptor (acid-base) interactions. Earlier popular notions that all "polar" groups can interact with each other were shown to be untenable; donor-donor and acceptor-acceptor interactions were negligibly small compared to donor-acceptor interactions (Fowkes 1980). Reaction mechanisms of modified and virgin plastic polymers with wood fibers were examined by using electron spectroscopy for chemical analysis (ESCA) and Fourier transform infrared spectroscopy (FTIR). Interfacial bonding determines the characteristic properties of WPC. The main parameters influencing the formation of such bonds were material properties (type, amount, and distribution), surface and chemical modification, adequate sample preparation, and processing conditions (Bledzki 1998).

Progressive changes in the surface chemical composition of wood fibers as a function of an increasing degree of sulfonation are shown in Table 1.5 with O/C ratios of wood fibers with different percentage of the C_1 (C-H), C_2 (C-O), C_3 (O-C-O and C=O), and C_4 (-COOH). Boras and Gatenholm (1999) reported as O/C ratio was increased with washing and further increased by extraction, the fiber surfaces became enriched with carbohydrates due to removal of the hydrophobic hemicellulose, extractives, lignins, and waxes. The highly sulfonated TMP fibers were still very different from those of Kraft or sulfite fibers with a lower O/C ratio and higher content of C_1 carbon not bonded to oxygen. Extraction with acetone resulted in a further increased O/C ratio. It was also suggested that increased exposure of cellulose on the fiber surface after neutral sulfite pulping resulted in reduction of glucomannan, glucomannan

Table 1.5. The oxygen/carbon (O/C) atomic ratios and the relative amounts of different carbons (C 1s) of model compounds and components in softwood fibers. (Barry and Koran 1990, Hedenberg 1995, Sjöström 1999, Boras and Gatenholm 1999).

	O/C	C_1	C_2	C_3	C_4
Cellulose (theoretical)	0.83	--	83	17	
Bleached Kraft pulp	0.80	6	75	18	1
Arabinoglucuronoxylan (theoretical)	0.81	--	78	19	3
Xylan (from pulp)	0.83	5	67	24	4
Lignin (theoretical)	0.33	49	49	2	
Kraft lignin (from pulp)	0.32	52	38	7	3
Oleic acid (theoretical)	0.11	94	--	--	6
Extractives (from pulp)	0.12	93	5	--	2

C1= carbon bound to hydrogen or carbon atoms only (C-H).
C2=carbon with one bond to oxygen (C-O).
C3 =carbon with a double bond to oxygen or with single bonds to two oxygen atoms (O-C-O and C=O).
C4 = carbon in carboxyl groups (-COOH).

acetate, xylan, and glucuronoxylan. It is evident that after 1.5 % sulfonation, the O/C ratios remain approximately constant (Barry and Koran 1990). The O/C ratio value for different mechanical pulps reported in the order TMP (0.44)< CTMP (0.46) < RMP (0.47)< SGW (0.49)< bleached sulfite pulp (0.73) < bleached Kraft pulp (0.82). All pulps have O/C ratios lower than that of pure cellulose (0.83), but are much higher than that of pure lignin (0.33). Thus, it is apparent that slight differences in the surface carbon composition is due to the lower percentage of lignin and extractives in the wood fibers, which in turn is a direct consequence of sulfonation.

Maleic anhydride (MA) is a popular coupling agent for making WPC. It was used to modify both wood and plastic polymers by graft copolymerization (Lu et al. 2000). The reaction group [$(CO)_2O$-] of MA interacts mainly with hydroxyl groups (-OH) of cellulose, hemicellulose and lignin to form esterification or hydrogen bonding (Figure 1.1). Figure 1.2 shows how one carbon-carbon double bond (C=C) can react with thermoplastic polymers. The structure of the MA greatly increases the graft reactivity of the carbon-carbon double bond on the heterocyclic ring with the polymer matrix through the conjugate addition under a radical form and creates a

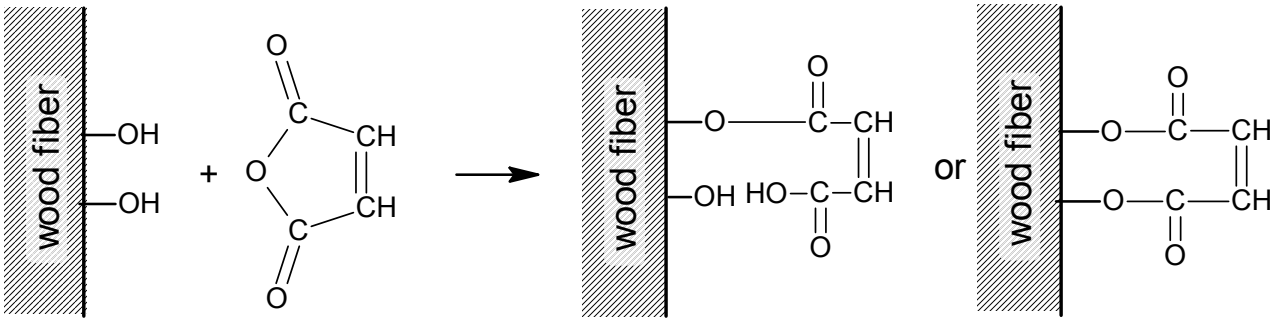

Figure 1.1. Hypothetical reaction mechanism of maleic anhydride on the surface of the cellulosic fiber. (Felix and Gatenholm 1991, Kazayawoko et al. 1999, Bledzki 1996).

crosslinking system between the two materials (Morrison 1992). Kazayawoko et al. (1997a) showed a proof of MAPP chemical reaction with bleached Kraft pulp fiber from an infrared absorption band near 1730cm^{-1}. They also found that both bleached Kraft pulp and TMP reacted chemically with MAPP because of the exposed end of the reaction groups in bleached Kraft pulp (45% yield) surfaces. From the FTIR results, Kazayawoko et al. (1997a) confirmed the esterification reaction between anhydride groups of MAPP and hydroxyl groups of wood fibers and determined the effect of wood fiber types and the presence of long PP chains. One of the most thoroughly examined chemical modifications of wood is the acetylation-esterification of hydroxyl groups on wood fiber surfaces, by a reaction with acetic anhydride, thereby forming

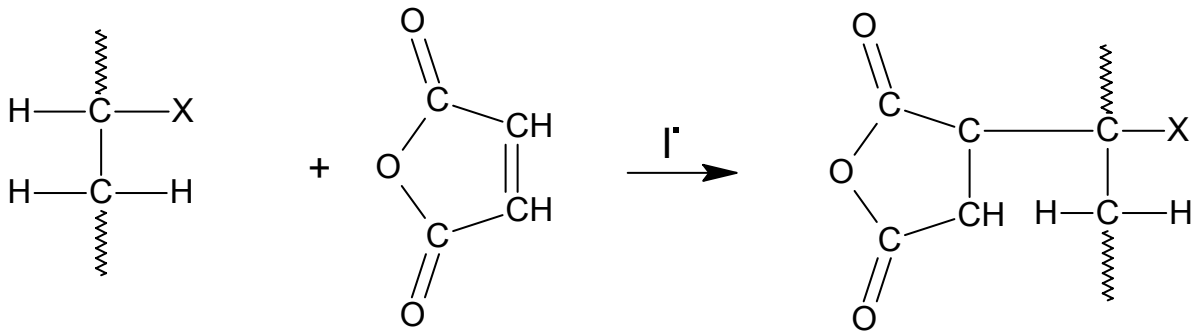

Figure 1.2. Hypothetical reaction mechanism between maleic anhydride modified polypropylene and thermoplastics. (Caldwell 1993, Trivedi and Culbertson 1982, Lu et al. 1998).

esters, mainly with hemicellulose and lignin. Acetylation is a single-site reaction where one acetyl group reacts with one-OH without polymerization. This reaction reduces hygroscopicity and swelling of wood (Bledzki 1998). Table 1.6 shows how six different investigators have tried to enhance the properties of WPC made with wood fiber, wood pulp, and wood flour by using catalyzed MA in the presence of initiators.

Table 1.6. Effect of interface modification with maleic anhydride on the mechanical properties of wood fiber and thermoplastic composites.

Modifier[1]		Initiator[2]	Matrix[3]	Fiber[4]		Properties Change[5](%)			Reference
Type	%			Type	%	MOR	MOE	Toughness	
Modification of the matrix									
MA	1	TBPB	PP	RGP pulp	50	261.0	87.6	-	Takase and Shiraishi (1989)
MA	1	TBPB	PP	RGP pulp	30	113.0	13.8	-	Takase and Shiraishi (1989)
MA	5	BPO	PS 525	CTMP	25	51.1	-7.7	-10.6	Maldas and Kokta (1990)
MA	5	BPO	PS 201	CTMP	25	32.1	9.6	32.8	Maldas and Kokta (1990)
MA	5	DCP	PP	HW pulp	30	28.5	-27.7	-	Mohanakrishnan et al. (1993)
Pretreatment of the fibers with MA and polymer									
MA	10	DBP, HDPE	HDPE	CTMP	30	20.2	36.7	26.4	Raj et al. (1990)
MA	10	DBP, LDPE	LLDPE	CTMP	30	43.6	-1.2	46.4	Raj et al. (1990)
MA	3	DCP	HDPE	NF	30	69.5	16.7	4.3	Maldas and Kokta (1991)
MA	3	BPO	HDPE	NF	30	-9.2	8.3	8.6	Maldas and Kokta (1991)
MA	1	DCP	PP	Wood fiber	20	15.2	4.3	-	Collier et al. (1996)
MA	5	DCP	PP	HW pulp	30	24.8	-18.8	-	Mohanakrishnan et al. (1993)

[1]MA; Maleic anhydride.
[2]TBPB; Tert-butyl peroxy benzonate, BPO; Benzoyl peroxide, DCP; Dicumyl peroxide, DBP; Dibuthyl phthalate.
[3]PP;polypropylene, HDPE; High density polyethylene, LDPE; Low density polyethylene, PS;Polystylene.
[4]RGP; Refiner ground pulp, CTMP; Chemi-thermomechanical pulp, HW; Hardwood, NF; Nutshell flour.
[5]Based on the properties of untreated composites. MOR; Modulus of rupture, MOE; Modulus of elasticity.

1.6. Physical Modification

Physical modification relies on controlling surface chemistry on the wood fiber surface without losing weight. The methods used to modify the fiber surfaces, included surface fibrillation, heat treatment and electrical discharges. Avelia et al. (1998) found that NaOH-extracted fibers produced by steam-explosion (SEP) presented a smooth and clean surface with strong defibrillation given to a high number of single shorter fibers. Even though, better interfacial adhesion was observed in the samples reinforced by the SEP fibers, there was less improvement in mechanical properties of the composites due to the significant fiber damage

produced during the explosion process (Avella et al. 1998). Heat treatment also caused surface chemistry changes on the wood fibers and was influenced by the type of fiber as well as by treatment procedure. Cell walls of wood fibers can be broken and fractionated into their main components (cellulose, lignin, and hemicellulose) with the steam explosion pulping (SEP) process (Bledzki et al. 1998). They showed that the hemicelluloses degraded to furan-type compounds which polymerize to produce water-insoluble polymers at high temperatures.

Liu et al. (1998) reported that the total surface free energy and polar component of rayon, cotton, and wood fibers decreased after heat treatment at 120°C for 2h. The changes were attributed to the loss of bound water and the formation of hydrogen bonds between the separate hydroxyl groups on the fiber surface. For rayon and cotton fibers, the interfacial shear strength between the wood fiber and PS also increased with the heat treatment which changed the surface energy. This was explained by the weak boundary layer at the fiber/PS interface. Coutinho et al. (1997) fabricated WPC using modified wood fibers with silane coupling agents at three different temperatures of 170°C, 180°C, and 190°C. Evidence showed that 180°C was the best mixing temperature. Kokta and Daneault (1986) studied the effect of composite treatment by an immersion system in boiling water. The grafted aspen fiber composites showed by far the best results compared to those of wood flour, mica, or glass-fiber filled LDPE. They also reported that mechanical properties of composites did not significantly change under extreme conditions, with the exception of increased stress and decreased strain, when measured at -40°C. Maximum improvements in mechanical properties occurred when the temperature was maintained at 175°C for 15 min. (Maldas and Kokta 1990b). They also stated the preferred weight fraction of both a monomer and an initiator were found to be 5% and 1%. Felix et al (1993), using PS, found that the oxygen content was raised due to the formation of carboxylic compounds on fiber surfaces at

200°C for 30 min. The tensile strength and modulus of PS-based WPC were slightly decreased, while those of PP-based WPC were not significantly affected by the heat treatment of fibers.

Heat treatment reduced the acid-base interaction potential of cellulose fibers and resulted in the decreased tensile strength of composites made with PS and PE. Acid-base interactions and chemical linkages may be all involved in the adhesion between the plasma modified fibers and plastics, but their relative contributions to the interfacial adhesion may vary greatly, depending on the nature of gases and the treatment procedures. Plasma induced polymerization and plasma state polymerization of some monomers have also been reported using a variety of surface modifications depending on the nature of the gases. Felix et al. (1994) reported that surface acidity was accentuated by forming a plasma polymer layer on the cellulose surface using methacrylic acid (MMA) as the sustaining gas. Mechanical properties of PS and PE based WPC were improved by strong acid-base interactions. Young et al. (1995) reported that the adhesion between PP film and filter paper was enhanced when the PP was treated with O_2 plasma, while the cyclohexane plasma treatment of the papers did not improve the interfacial adhesion. Plasma-state graft copolymerizations of acrylonitrile on regenerated cellulose were shown to be very effective in improving the interfacial adhesion to PP. In general, Ar and O_2 plasmas produced free radicals on lignocellulosic fiber surfaces, and higher levels of free radical intensity were achieved. Therefore, the plasma treatment was positively correlated with the increase in strength properties of WPC fabricated with treated PP film and filter papers.

Corona treatments of wood fibers and polyolefins using electro magnetic fields generated by high electronic discharges were reported to be an effective technique for improving the mechanical properties of WPC. Dong et al. (1993) had shown that the yield strength, strain, and the elongation at break of 15-30% fiber contained LDPE-based WPC were strongly improved by

the treatments. The treatment of LDPE results in more improvement in the tensile strength, while the tensile modulus and ultimate strength appeared to be insensitive to the corona treatment. Belgacem et al. (1994) reported that the tensile strengths at yield and rupture, energy at rupture, and the tensile modulus increased with the treatments. The properties increased linearly with the corona current and the treatment time at a constant current. They also suggested that the dispersive interaction plays an important role in improving the mechanical properties of WPC. Dong and Sapieha (1991) showed that increased acid-base interactions enhanced the interfacial adhesion in wood fiber/LDPE composites as measured by a single fiber fragmentation test.

CHAPTER 2

THE FOCUS OF THIS STUDY

The purpose of this study was to study selected factors affecting the interfacial bonding of whole wood fiber pulp sheets and polypropylene (PP). Unlike previous research on the wood-fiber-thermoplastic composites (WPC), this study was not oriented toward existing WPC technology. Thermomechanical pulp (TMP) fibers formed into a thin handsheet were used for this study because lignin and other components are redeposited on their surface affecting their surface chemistry. The deposition occurs when pulping is carried out in excess of the lignin glass transition temperature of 140°C. Theoretically, this promotes fiber to fiber bonding without the use of resin binders. The PP film was selected as a matrix material to obtain two advantages. In general, PP has a high melting point and provides a high elastic modulus intension and tensile strength with a density less than 1 $kg \cdot m^{-2}$. Additionally, a uniform melt-flow into handsheets should occur during the hot-pressed laminating.

In effect, this research relates to the fundamental interaction of the surface chemistry of natural, lignin-rich TMP fibers and hydrophobic thermoplastic materials. Chemical and physical surface modifications on the TMP fibers and PP film were studied. Interfacial interaction between lignin-like wood fiber surfaces and a hydrophobic thermoplastic was studied by examining the effect of chemical and physical surface modifications on the tensile properties of thin laminates made of thin TMP fiber handsheets and thin sheets of PP film.

Since wettability between polar solid and non-polar liquids is a commonly used indicator of compatibility, the behavior of macro- and micro-sized adhesive droplets on thin microtome sections of earlywood and latewood of loblolly pine (*Pinus taeda* L.) was investigated. Droplet

behavior such as changing contact angle, volume, and surface tension measurements related to interfacial shear strength properties were studied. Due to the different behavior in droplet sizes on the wood surface, droplet verses AFM scanning methods were used to measure the contacting angle and also compared between them.

The plasma treatments were used to modify the surface chemistry of thin pulp sheets by using a direct current (DC) generator to improve interfacial adhesion. The oxygen-based DC plasma was applied to the surface of TMP fiber handsheets, and PP film. Specimens were tested in tension to determine if the treatments enhanced tensile properties of the laminates.

Further study was made to elucidate an understanding of the interfacial interaction between TMP fiber and PP. The grafting effect of maleic anhydride (MA) as an interfacial bonding agent was studied and its influence on the tensile strength properties of the TMP handsheet-PP film laminates (TPL). This study included the effect of different levels of MA and benzoyl peroxide (BPO) on the TMP fiber and PP film interactions. Optical equipment was used to examine the nature of the fracture surfaces of tensile test specimens. The effect of thermal treatment of TMP pulp was also considered. Estimates were made of the porosity of TMP fiber handsheets and the number of fibers exposed at the fracture surfaces interface to see if these correlated with the tensile strength properties of TPL.

In another study, the surface of thin fiber handsheets was sprayed with thermosets, liquid resins, urea- and phenol-formaldehyde (UF and PF) resins, to enhance the tensile strength properties of TPL. This study investigated the influence of thermoset adhesive levels and other experimental factors on the tensile properties of TPL.

Finally, interfacial phenomena of PP induced heterogeneous nucleation ability was observed on the fiber surfaces of untreated, cleaning with distilled water and extracting with an

organic solvent. This study investigated the influence of surface deposit materials on the induction of heterogeneous PP nucleation.

CHAPTER 3

WETTING STUDY OF THERMOSETS AS COMPATIBILIZERS AT THE WOOD AND POLYPROPYLENE INTERFACES

3.1. Introduction

Previous wetting studies involving contact-angle measurement on wood surface wettability have shown as an old and well defined technique with model liquid called probes (Gardner et al. 1991, Wålinder 2000, Wålinder and Ström 2001). Wetting studies with wood fiber plastic composites (WPC) have evaluated qualitative surface chemistry and treatment effects on the surface determined by contact angle analysis to reveal chemical bonding evidence between fibers (Felix and Gatenholm 1991, Hedenberg and Gatenholm 1995, Geoghegan and Krausch 2003). Untreated wood materials were highly hydrophilic, but this was substantially reduced by chemical and physical surface modification (Matuana et al. 1998a, Gauthier et al. 1999, Rabinovich 2002). Improved contact angle measurements of the modified surfaces were positively correlated to shear strength properties at the interface. Single lap-shear-joint tests and peel tests (Kolosick et al. 1993, Chen et al. 1995, Matuana et al. 1998b, Oksman and Lindberg 1998) were used to investigate surface interactions at the wood-polymer interface. Assuming that the failure of samples occurred at the interface and that the stress distribution was uniform, peel and lap shear strengths can be considered as a qualitative measure of interfacial adhesion. In practice, contact-angle measurements can be readily obtained on flat wood surfaces but not on fibers. However, wetting studies using thermoset such as urea formaldehyde (UF) and phenol formaldehyde (PF) resin have rarely been reported due to the incompatibility of thermosets in contact with a thermoplastic matrix.

Some factors influencing surface wetting of wood by liquid monomers and polymers were evaluated to study their effect on flexural and shear strength properties of wood-based products as well as surface energetic properties at the interface (Hse 1972a, 1972c, Shupe et al. 1998). The previous research was based on contact-angle at the liquid-solid interface. Limited studies have been made to study wetting of solid wood by contact angle measurement of sessile or micro-droplets of thermoset resins where the effect of wood structure was considered. The dispersing area of thermoset droplets was influenced by wood structure, grain directions, glueline thickness, viscosity, molecular weight distribution, surface roughness, and surface chemistry (Hse 1968, Hse 1971, 1972a, 1972b, Gardner et al. 1996, Liu et al. 1997, Hse and Kuo 1988, Richter et al. 2002). Mathematical expressions on the droplet volume were based on the response of equivalent height and average contact angle of droplets with an assumption of the symmetric droplet dispersing on the wood surface (Chatterjee 2002a, Chatterjee 2002b). However, surface roughness at the local sites is heterogeneous due to the cellular structure of wood and different grain angles of the wood specimens.

Cazabat (1992) has shown that the wetting behavior between macro- and micro-droplets on the wood surface were different. To determine the optimum level of thermoset and thermoset wetting characteristics for the wood-based composites, more wetting studies were performed (Casilla et al. 1981, Chibowski and Perea-Carpio 2002, Sharma and Rao 2002, Paunov 2003). This examined the differences between the behavior of micro-sized adhesive droplets on the earlywood and latewood of loblolly pine (*Pinus taeda* L.). This study also addressed droplet behavior such as contact angle of thermosets on the surface of microtome sections, heterogeneous wetting, and interfacial strength properties between thermosetting resins applied

wood surface and polypropylene (PP) film. The droplet verses scanning method for the contact angle measurement on a wood surface was also examined.

3.2. Materials and Experimental

3.2.1. Materials

Earlywood and latewood from the sapwood of loblolly pine were selected from areas around Pineville, La. Wood samples were microtomed with each tangential section of 1.4 x 1.4 x 0.06 cm^3. The wet microtomed samples were placed between glass plates and dried for 48 hours at 80 °C. To minimize sample warping, a slight load was applied. PP films (Plastic Suppliers, Inc. Columbus, OH) were used to make lap-shear joints. Two liquid thermosets - urea formaldehyde (UF; Dynea Inc., Chembond® YTT-063-02, 60% solid content) and phenol formaldehyde (PF: Dynea 13B410, 100 cps, Sp. Gr.: 1.202, 56% solid content) resin were used as probe droplets.

3.2.2. Three Directional Images

Three image-capture systems (SPOT RT camera, and two of SOAR VL-7EX; Scalar, Inc. Los Gatos, CA) and an image analysis system (Image-Pro® Plus, V.5.2) were used to generate continual micro-images from sides (parallel and perpendicular to the grain direction) and top for 5 minutes. Figure 3.1 shows the experimental setup to measure wetting characteristics of UF and PF from the sides and top as a function of time. Contact angle measurement used a sessile droplet method with microscopic magnification at 50×. Two video capture systems were set up from the top and the side of the sample droplet. An auto-pipette generated 2 μl micro-droplets to observe droplet behavior on the different wood surfaces. Single images were generated from the video files every 5 seconds for 5 minutes. During this stage, droplet size and volume changes were also recorded as a function of time.

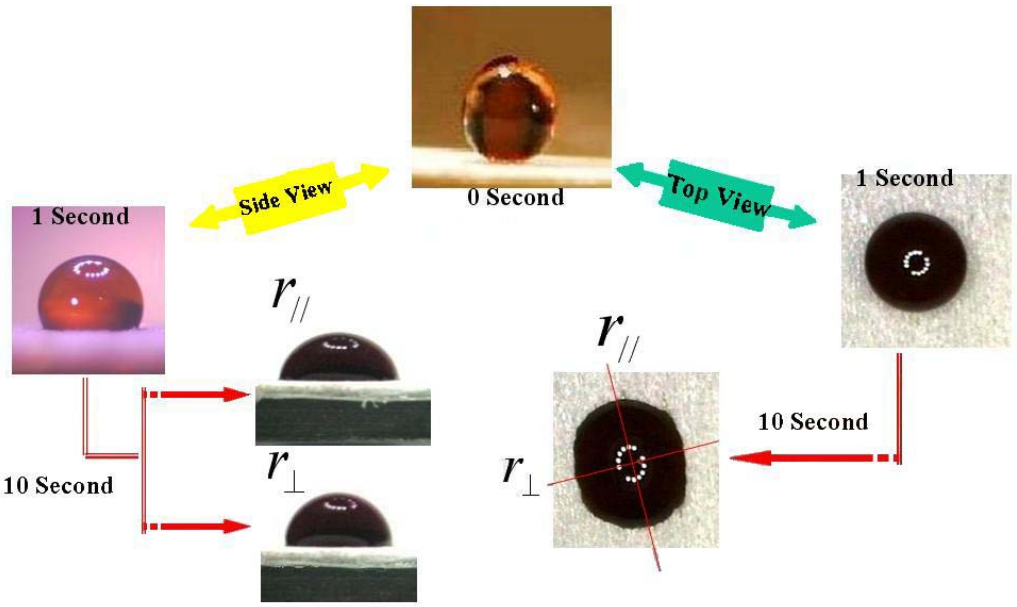

Figure 3.1. Experimental procedures to collect phenol-formaldehyde resin wetting characteristics from the sides and top of the instrumental setup as a function of time.

3.2.3. Atomic Force Microscope Scanning

The technical feasibility of using AFM as a micro-manipulator to measure micro-contact angle measurement and its difference with sessile droplets using resins as a probe material was determined. Figure 3.2 shows the 3-D plot of the surface and section analysis of the scanned surface. The measurement of the topography of a sample using AFM involves a micro-fabricated cantilever with a very small tip being scanned above the surface of the sample (Wang et al. 2001). The scanning method used a Nanoscope IIIa atomic force microscope (AFM; Digital Instruments) mounted on a pneumatic isolation table with an acoustic hood over the dried droplet surface. All AFM micrographs were taken at a resolution of 512 × 512 pixels in tapping mode™. Micro-droplets were generated using an air-automated spray, and the size range was from 1 to 100 µm. The micro-droplets were dried for 24 hours before scanning the wood surface. For the contact-angle measurements, two image analysis systems were applied. The analysis systems were section analysis from the AFM software and Image-Pro® Plus.

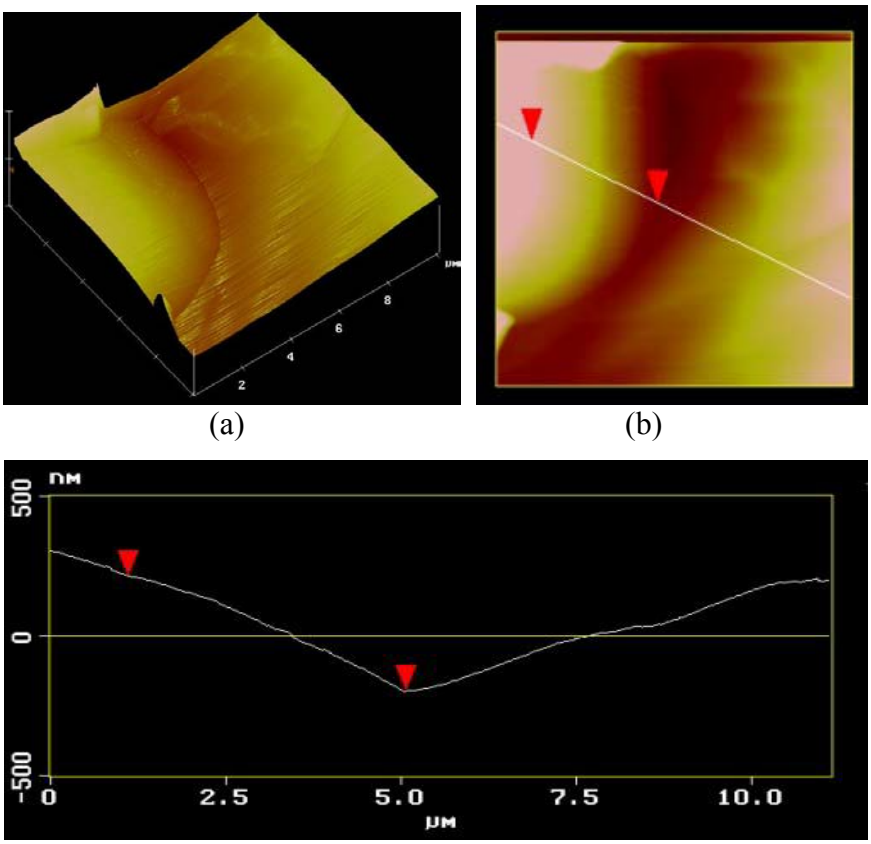

Figure 3.2. Atomic force microscopy (AFM) 3D images scanned at the edge of a micro-droplet and section analysis: (a) 3-D surface plot, (b) Section selection, and (c) Section analysis.

3.2.4. Wetting Characteristics

The geometry of droplets quickly changed into a hemisphere shape in five seconds. In another five seconds, an exact hemisphere reflected a reduced volume (V) of the droplets (Figure 3.3). Thus, experimental and mathematical efforts developed several types of simplified hemispheric models to estimate a precise droplet volume on wood surfaces. The following equation from Zwillinger (2003) described the volume, surface area, and angle of response for a hemisphere and a simplified model for the exact hemisphere:

$$V_a = \frac{1}{3}\pi h^2 (3R - h) \qquad (R = a) \qquad (3.1)$$

Where R was the hemisphere radius, determined by substituting R for droplet hight (h). However, the droplets remained as an enclosing hemisphere shape rather than an exact hemisphere. Thus, the following equation was required to generate an exact volume for an enclosing hemisphere with contact angle (θ) and droplet height (h) determined from the droplets.

$$V_b = \frac{1}{6}\pi h^2 (3\frac{h^2}{\tan^2\theta} - h^2) \tag{3.2}$$

Accuracy in the droplet volume was obtained using balance of gravity and capillary forces, and a well-applied "drop volume" method for estimating interfacial tension (Lando and Oakley 1967, Wilkinson and Aronson 1973, Holcomb and Zollweg 1990, Chatterjee 2002a, Chatterjee 2002b). A drop of resin on the wood surface changed with gravity forces and a relatively small amount of droplets penetrated into the wood surface. The surface tension equation was extracted by using capillary force response for droplet retention on the solid surface and each volume condition. The extracted critical surface tension equation (Equation. 3.3 and 3.4) was expressed as:

$$\gamma_{V_a} = \frac{\Delta\rho g R^2 (2 - 3Cos\theta + Cos^2\theta)}{6Sin\theta} \tag{3.3}$$

and

$$\gamma_{V_b} = \frac{\Delta\rho g h^2 H}{12 r Sin\theta} \quad (H = \left[3\frac{h^2}{\tan^2\theta} - h^2\right]) \tag{3.4}$$

Where $\Delta\rho$ = density difference between the drop and continuous phase;
g = gravity acceleration;
γ = interfacial tension between the two phases;
r = wetted radius; and
θ = three-phase contact angle.

3.2.5. Shape Analysis

A dimensionless shape factor (DSF: Equation 3.5 and 3.6) was also generated from the capillary forces ($C_p = \left[\frac{\left(\Delta\rho g V_{a,b}\right) - \left(2\pi\sigma \cdot rSin\theta\right)}{A}\right]$) and wet area (A) of the resin droplets (Kwok et al. 1997, Chatterjee 2002a, Chatterjee 2002b). The DSF from each volume condition was calculated and expressed as:

$$DSF_{Va} = \frac{\Delta\rho g R^2}{2\sigma} = \frac{3Sin^2\theta}{2 - 3Cos\theta + Cos^2\theta} \tag{3.5}$$

and

$$DSF_{Vb} = \frac{\Delta\rho g R^2}{2\sigma} = \frac{6Sin^2\theta}{2 - 3Cos\theta + Cos^2\theta} \tag{3.6}$$

3.2.6. Single Lap Shear Test

Shear strength properties of the single-lap laminates were tested in tension using an Instron 4465 mechanical testing at a crosshead speed of 0.05in. min.$^{-1}$ according to ASTM D5573-94 (ASTM 1994). Seventy-two PP film laminated joints were prepared to a nominal UF and PF sprayed area of 0.45 × 0.4 inch^2. On each side of the wood strips, a UF or a PF resin was sprayed and six sheets of PP film were placed in the middle of the strips. The single-lap shear specimens were pressed at 100 psi for two minutes at 400 °F. At least 18 specimens were tested for each set of samples. Analysis of variance was used to determine the potential significance of the main effects for this study with each resin and wood type. Multiple comparisons were employed to determine significant differences between the different species using SAS software 9.0e (SAS 2004).

3.2.7. Fracture Surface

Shear failure was observed using scanning electron microscopy (SEM; S-3600N) on the fracture surfaces of UF and PF-loaded microtomed wood surfaces and PP film joints, and the investigated interfacial adhesion characteristics at the resin sprayed wood surface and the PP interface. An ion sputter apparatus (Technics Hummer V) was used to coat samples with an approximately 15-nanometer thin gold layer. Images of 75x and 4,000x were generated at 10 kV.

3.3. Results and Discussion

3.3.1. Shape Transformation

Figure 3.3 shows droplets shape changes from an exact sphere of an adhesive droplet to an enclosing hemispherical dimension as a function of time on the wood surface. The droplet shapes were transformed from an exact sphere with an initial contact angle of 162° to a hemisphere over time (showing little wetting). The shape transformation occurred quickly, in 5 seconds, from an exact sphere to an exact hemisphere shape. From this result, the critical surface tension and volume were calculated using Eq. 3.1, 3.2, 3.3, and 3.4. The surface free energy

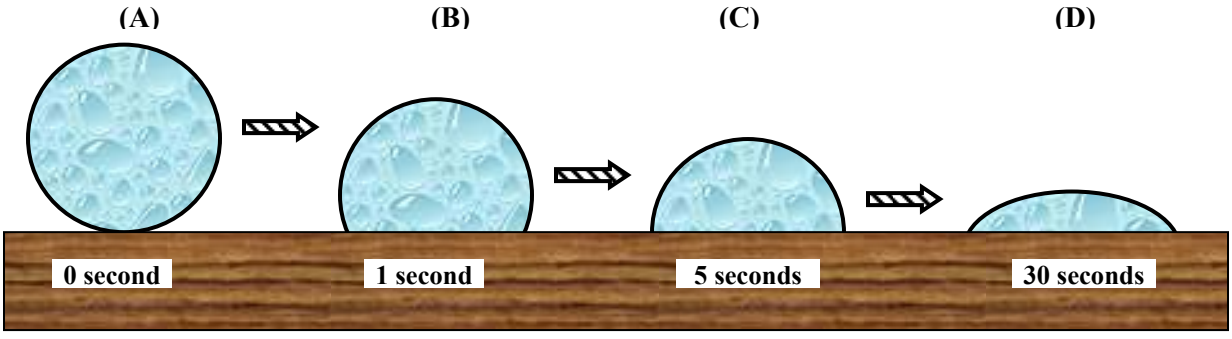

Figure 3.3. An enclosing hemispherical dimension of the micro-droplets from an exact circle of an adhesive droplet as a function of time on the wood surface. (A) Exact sphere, (B) Hemisphere, (C) Exact hemisphere, and (D) Enclosing hemisphere.

and droplet volume were obtained by using the response of equivalent height of droplet changes (Eq. 3.1) and the response of the average angle (Eq. 3.2). Where the droplets were extended by the gravity factor and surface condition of the wood surface, both methods were judged to be reliable to address substrate characteristics interfaced with the two resins. Using the two methods, an increased precision to predict volume changes was obtained.

3.3.2. Urea Formaldehyde and Phenol Formaldehyde Wetting

Wetting characteristics of UF and PF droplets on the microtomed wood surface of loblolly pine earlywood and latewood are presented in Table 3.1. Earlywood with UF droplets dispersed relatively quickly in the longitudinal direction on the surface with higher capillary pressure and the long fiber length. Weight changes were also higher than other combinations. The cell cavities of earlywood are much larger than those of latewood which has both smaller cavities and thicker cell walls (Figure 3.7c). Thus, the surface roughness influenced the dispersing factor and resulted in more resin penetration into the cell walls. The dispersing ratios ($R_{//} / R_{\perp}$) indicated that adhesives dropped on the earlywood surfaces provided more extended resin coverage than that applied on the latewood surface. In general, the critical surface tension was used to evaluate adhesive bonding characteristics at the interface (Scheikl and Dunky 1998,

Table 3.1. Wetting characteristics of micro urea-formaldehyde and phenol-formaldehyde droplets on the microtome section of loblolly pine earlywood and latewood.

Thermoset Type	Wood Type	Sp. Gr. (Dry)	Capillary Pressure ($mNcm^{-2}$)	Weight Change Rate ($\mu\ell\ sec^{-1}$)	Dispersing Factor $R_{//} / R_{\perp}$	Contact Angle @ 10 sec. (°) $\theta_{//}$	$\theta_{\perp}$	Critical Tension ($Dyn\ cm^{-1}$) $r_{//}$	$r_{\perp}$
UF	Early	0.55	14.6	0.073	2.11	68.5	70.6	61.3	37.7
	Late		12.1	0.069	1.39	67.5	72.9	48.7	40.6
PF	Early		13.0	0.068	1.42	65.2	78.6	88.7	60.2
	Late		12.2	0.045	1.27	64.1	73.9	53.2	40.2

Wålinder 2000, Khan et al. 2004). Surface tension ($r_{//}$) values were close to published values (Hse 1971) while $r_{\perp}$ was not. There was less penetration into the inner cell structure with latewood regardless of resin type. This result probably influenced the shear performance at the wood-PP interface. Volume changes of UF and PF droplets were shown as a function of time on the wood surface (Figure 3.4). The initial contact angle was 162° and decreased rapidly in five to ten seconds. After 30 seconds, the droplet volumes were fairly constant. The volume changes with UF droplets on both wood types showed a similar trend as PF except PF on earlywood surfaces. UF resin gels very quickly and has very high molecular weight (MW) distribution while PF resin has lower MW distribution.

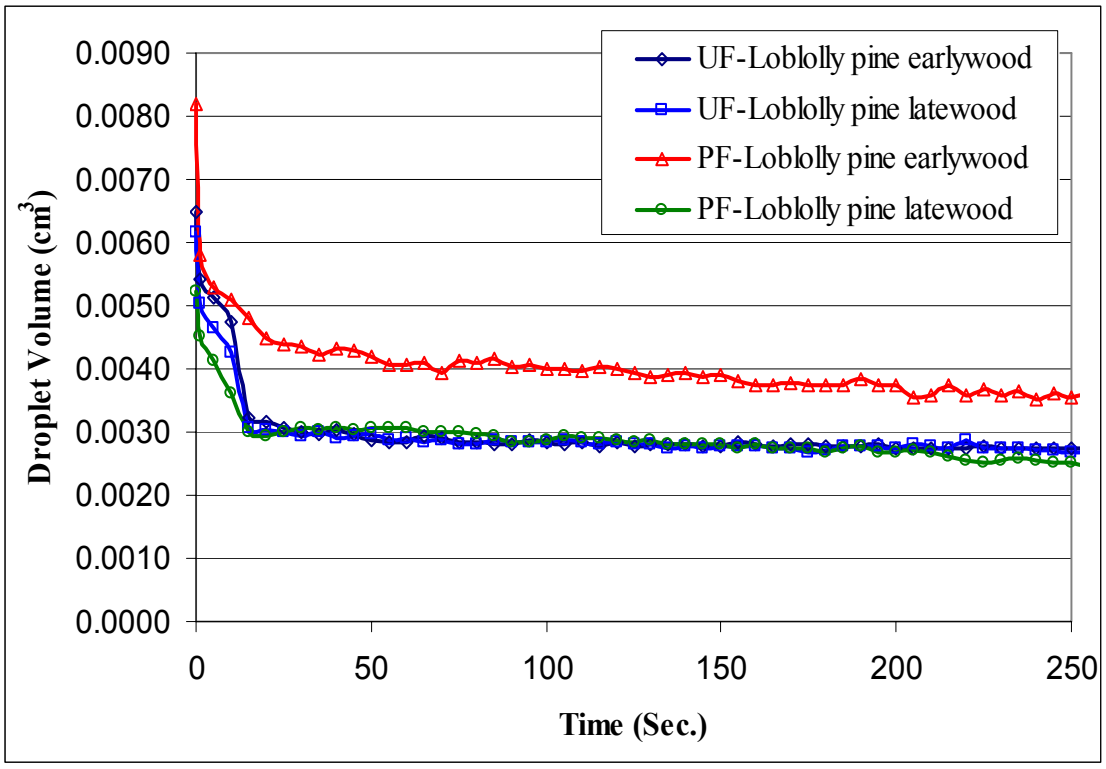

Figure 3.4. Volume changes of urea-formaldehyde and phenol-formaldehyde droplets as a function of time on the surface of microtomed loblolly pine wood.

3.3.3. Single Lap Shear Strength

Shear strength properties from single lap joints of the UF and PF sprayed wood surfaces and PP film interface are shown in Figure 3.5. Single-lap shear strength increased 53% (from 160 to 244 psi) when the latewood was sprayed with UF resin. It should be noted that 88% wood failure was observed with UF resin sprayed on two wood types while 25% wood failure was noted with PF resin. Single-lap shear tests demonstrated that the UF loading at the wood and PP film interface improved the interfacial interaction. This result is largely attributable to the surface tension of wood with UF droplets due to the inherent properties of this resin. The earlywood, which had higher dispersing ratios with both resin types, showed poor shear performances due to over penetration by capillary action. Thus, the thermoset resin remaining on the wood surface was beneficial in increasing interfacial interaction at the wood-PP interface with UF resin.

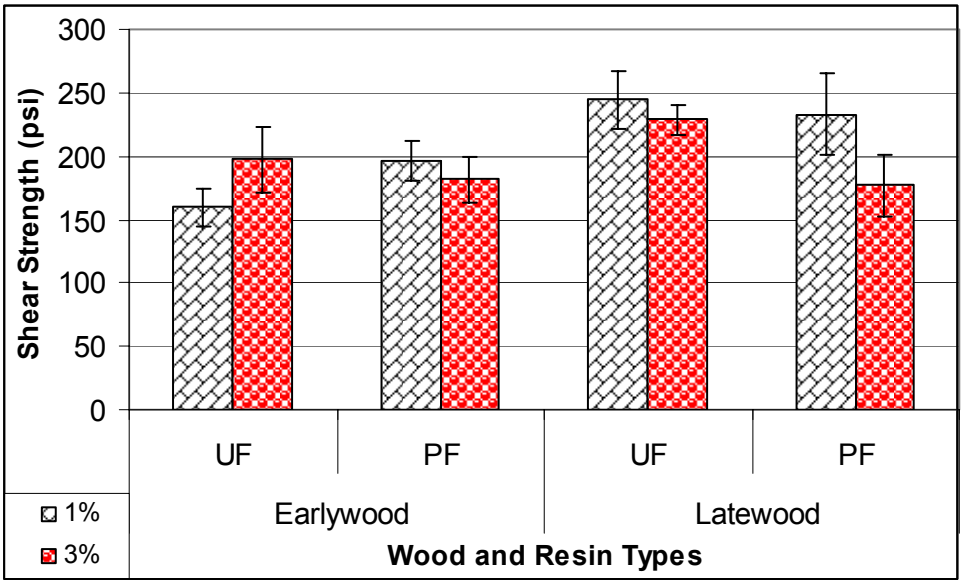

Figure 3.5. Shear strength properties from single lap joint laminated assemblies of urea-formaldehyde and phenol-formaldehyde sprayed wood surfaces and polypropylene film interface (The error bars represent one standard deviation).

3.3.4. Dimensionless Shape Factors

Figure 3.6 shows dimensionless droplet shape factors (DSF) with a critical boundary between high and low retaining regions as a function of contact angle. Loblolly pine had relatively higher retentions with UF resin than PF and influencd shape transformation of the droplets. The higher retention indicates increased resin penetration into the wood and in general, confirms the fact that high resin retention at the interface is important to obtain effective adhesion. Also shear strengths at the wood-PP interface increased and showed a lower thermoplastic failure than when thermoplastics were used for surface modification. Therefore, the capillary forces and surface tension played an important role in influencing the interfacial strength properties.

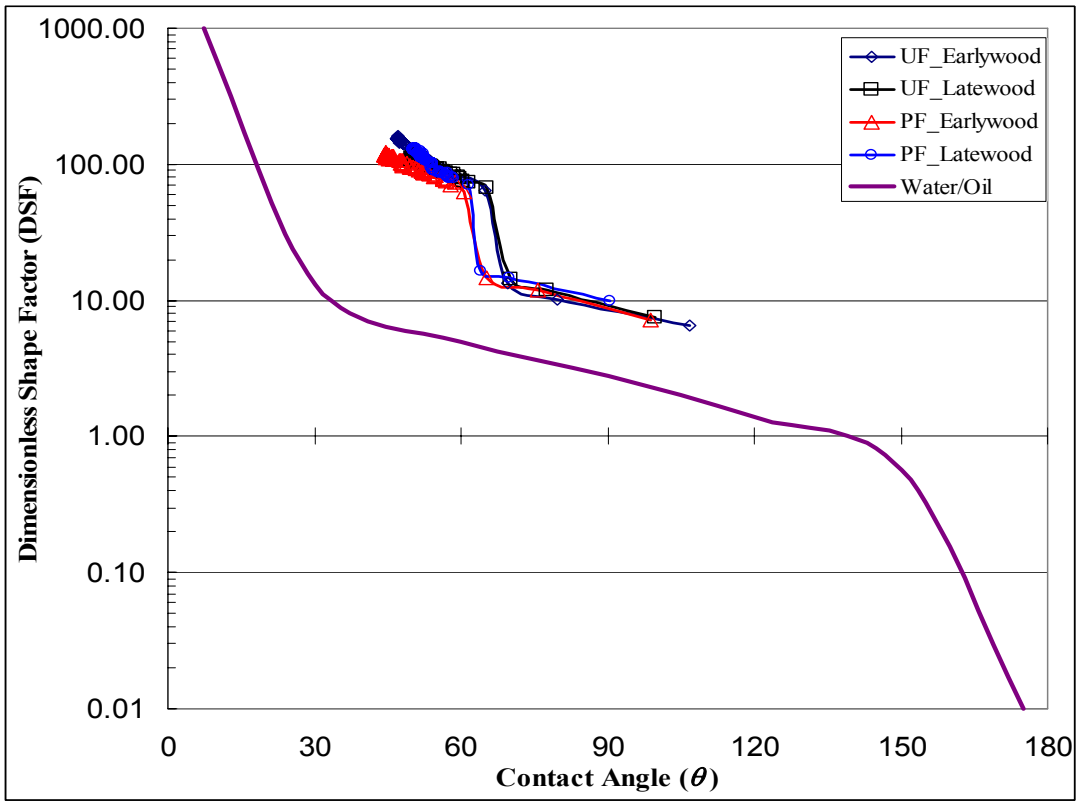

Figure 3.6. Dimensionless shape factor (DSF) changes as a function of contact angle changes of urea-formaldehyde and phenol-formaldehyde droplets on earlywood and latewood surfaces.

Table 3.2. Model-generated contact angle measurements verses scanned angle of urea-formaldehyde and phenol-formaldehyde droplets on the tangential surface of microtomed loblolly pine.

Resin and Wood Type		Sessile Droplet Model	R^2	Expected Angle	Scanned Angle
UF	Earlywood	$Angle = 88.457X^{-0.1215}$	0.88	24.2	28.3
	Latewood	$Angle = 88.334X^{-0.1051}$	0.95	28.8	31.0
PF	Earlywood	$Angle = 90.822X^{-0.0882}$	0.98	35.4	35.5
	Latewood	$Angle = 79.426X^{-0.0835}$	0.94	36.2	39.5

3.3.5. Contact Angle vs. Surface Scan

Models were developed for contact-angle measurements using two different systems. The models differentiated droplet behaviors on two different wood surfaces. Contact angles from scanned micro-droplets and predicted values with the best-fit models are presented in Table 3.2. Models were performed with α=0.05. The R^2 values obtained from the models were an excellent fit to the data collected from the microdroplet scanning method. Microdroplets sprayed on the wood surfaces showed that wetting on a small scale is strongly affected by minimal physical surface heterogeneities more than the relatively larger scale of sessile droplets and they resulted in higher contact angles. Thus, the AFM technique to scan microdroplets can be a beneficial to understand microscale droplet behavior of wood adhesives on the surface of wood materials. Experimental contact angles on the wood surfaces were measured using AFM and found to validate prediction models.

3.3.6. Shear Failure

SEM micrographs showed the fracture surface from shear load in Figure 3.7. The low magnification image shows many fibers exposed from the wood surface. The fibers were produced by PP stretching during the shear failure. PP film sheets were melted under heat and flowed into radial resin canals exposed on the tangential section and the tracheids, parenchyma

cells, transverse resin canals, and epithelial cells. The fracture behavior of joints can also be affected by many other variables such as including the fiber and matrix nature, the fiber-matrix interaction, resin distribution, cell structure, etc. Thus, the surface fibrillation of the PP matrix may add the interfacial shear strength of single lap shear joints.

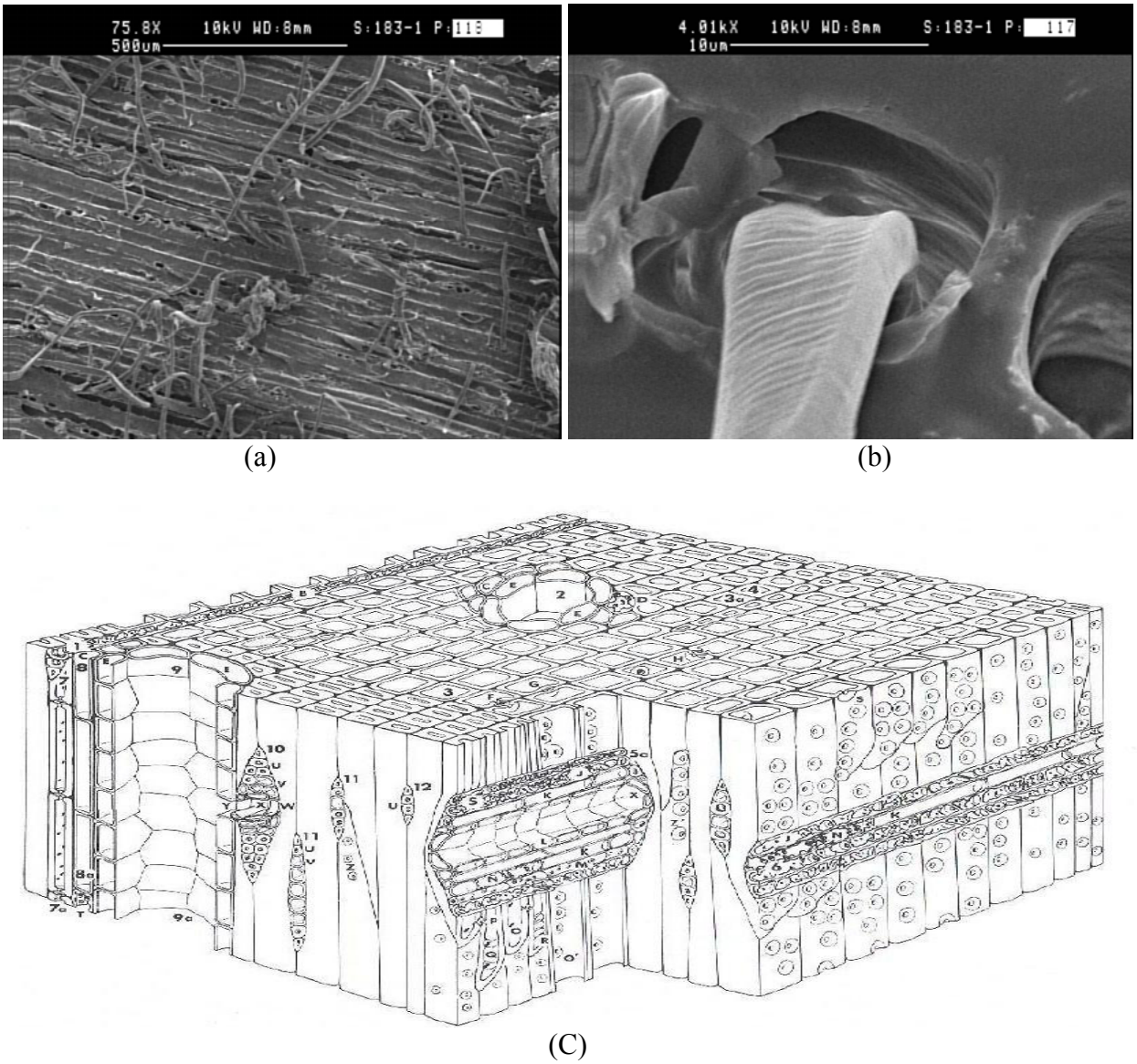

Figure 3.7. Scanning electron microscopy (SEM) micrographs generated with (a) low and (b) high magnification on the fracture surface of wood strip and polypropylene interface, and (C) anatomical structures of typical southern pine from Koch (1972).

CHAPTER 4

INFLUENCES OF ARGON- AND OXYGEN-BASED PLASMA TREATMENTS ON THE PROPERTY ENHANCEMENT OF WOOD FIBER HANDSHEET AND POLYPROPYLENE LAMINATES

4.1. Introduction

Lignocellulosic materials have been widely utilized to make wood fiber-thermoplastic composites (WPC) because of their low weight, relatively high strength and stiffness, and machinability (Lin 1986, Rievld and Simon 1992, Kolosik et al. 1992, Wolcott et al. 2000, Xue and Tao1 2005**)**. Considerable effort has been made regarding chemical and physical surface modifications to improve the interfacial adhesion between the wood fibers and the polymer matrix (Karlsson et al. 1996, Espert and Karlsson 2004). Several researchers have modified both the wood fiber and the thermoplastic surface with coupling agents (Beshay 1989, Kokta et al. 1990, Maldas and Kokta 1990a, Collier et al. 1996, Mahlberg et al. 2001, Hristov et al. 2004). Another method used was plasma modification of the surface by introducing magnetic fields and ionized gases using electronic discharges. However, surface modification using plasma on wood fiber materials remains poorly understood (Denes et al. 1999, Rehn and Viöl 2003).

Plasma treatment of polymer surfaces promotes wettability, printability, and adhesion (Chaoting et al. 1993, Mahlberg et al. 1998, Lee et al. 1999). In most applications, dielectrics are used to guarantee stable operation without material deformation. This application requires discharge power of about 100 to 400W. Useful operating frequencies are in the range of 10–30 kHz (Draou et al. 1999, Kazayawoko et al. 1999, Jang and Yang 2000). The technique provides effective surface modification and uniform surface coatings. The treatment of surfaces at low temperature and pressure is important for large-scale WPC production (Poncin-Epaillard

et al. 1997). The ion implantation is applied to both wood and non-wood materials to obtain an activation layer at the wood fiber-thermoplastic interface (Porta et al. 1990, Posadowski and Radzimaki 1993, Denes et al. 1999). Essentially, this process provides a simple surface modification of wood and wood fibers by using ionized oxygen with nitrogen or argon gas as a carrier (Brown and Mathys 1997, Montes-Morán et al. 2001).

Numerous processes take place simultaneously during plasma treatment of the surfaces of bio-based materials. These include dissociation by electron impact, ionization, and molecular excitation at low pressure and ambient temperature (Badey et al. 1996, France and Short 1997, Draou et al. 1999, Lee et al. 1999, Montes-Morán et al. 2001). Gas sources for ionization have been used in plasma treatment on the surface of fibers or plastics, such as Ar, O_2, cyclohexane, NH_3, N_2, methacrylic acid (MMA) (Felix et al. 1994, Young et al. 1996, Poncin-Epaillard et al. 1997, Rehn and Viöl 2003). Argon or oxygen plasma treatment improved interfacial adhesion properties from 5 to 15 times as measured by the peel test between polypropylene (PP) film and cellulosic filter paper. In contrast, the cyclohexane plasma was less effective in the improvement of adhesion of treated regenerated cellulose (Young et al. 1996). Thus, Ar or O_2 plasma was shown to be very effective in improving interfacial adhesion at the fiber and PP interface. The enhancement was due to the formation of a plasma associated ionized layer on the cellulose surface and resulted in strong acid/base interactions. The NH_3 or N_2 plasma treatment for 15 seconds on cellulose fibers containing 86% cellulose and 13% hemicellulose also yielded lower modulus properties in polystyrene (PS) composites (Felix et al. 1994). Oxygen and carbon (O/C) ratio of cellulose fibers with a 15 second treatment time reduced the modulus significantly. But further exposure to the plasma environment caused an increase in the O/C value due to the

induced thermal degradation and ablation of the modified surface layers (Mahlberg et al. 1998, Denes et al. 1999).

Heat generated between electrodes was not beneficial in modifying the wood surface due to the thermal effects on the chemical composition of the wood fiber (cellulose, hemicellulose, and lignin). The temperature was generally above glass transition temperatures of the wood materials as well as the melting point of thermoplastics (Maldas and Kokta 1991a, b). Therefore, many researchers have used the cold plasma system to obtain an optimum treatment effect as well as improved surface modification (Chaoting et al. 1993, Young et al. 1995, Poncin-Epaillard et al. 1997, Rehn and Viöl 2003, Bente et al. 2004). Cold plasma was generated when an electromagnetic field and gas flow at low pressure and near-ambient temperature was used from the power sources of direct current (DC), radio frequency, and microwave (NPPS 1995, Lennon et al. 2000, Ihara et al. 2001). Both the surface chemistry and morphology of the treated wood fibers and plastics provided electron donor rich and oxygen activated surfaces (Young et al. 1996, Poncin-Epaillard et al. 1997).

Physical adhesions, acid-base interactions, and chemical linkages may all be involved in the adhesion between the plasma modified TMP fibers and plastics, but their relative contributions to the interfacial adhesion may depend on the nature of ionized gases and plasma treatment procedures. The surface modification can also change mechanical interlocking between the wood fibers and thermoplastic matrix without chemical modification. The interaction of TMP fiber surfaces and a semicrystalline polymer with Ar and O_2-plasma treated interface is not clearly understood. Therefore, a major thrust of this study was to study the effect of direct current (DC)-based plasma treatment on the interfacial interaction between TMP fiber handsheets and PP.

4.2. Materials and Methods

4.2.1. Materials

Thermomechanical pulp (TMP) fibers (loblolly pine; *Pinus taeda* L.) were generated from mature wood at 8 bar digester/refining pressure in a continuous, pressurized, single-disc refiner at the Bio Composites center, University of Wales, Bangor, Wales, UK. The average moisture content of the TMP fibers was 8.2 percent. Macerated TMP fibers were prepared in the laboratory and filter papers were Sharkskin lot No. X31 from Schleicher & Schuell Inc. Keene, NH. Five grams of fibers were soaked in 500 ml water for 24 hours and formed into 5.5-inch diameter handsheets.

Polypropylene (CO-EX, Plastic Suppliers, Inc., Columbus, OH) film was used for evaluating the Ar and O_2 plasma effect on tensile strength of the TMP fiber handsheet and PP film laminates (TPL).

4.2.2. Ar and O_2 Plasma Treatment

Figure 4.1 shows the modified ion sputter (Ladd Sputter Coater, Ladd Research Industries, Inc., Williston, VT) that was used for Ar and O_2 plasma treatment on the TMP fiber handsheets and PP films. This plasma system had parallel electrodes and a DC-based power source. The distance between the two electrodes was 2 inches, and a plasma barrier plate was located 1-inch from the top and bottom electrodes. Experiments were performed on non-neutral plasma, utilizing electron trap and ion trap with an indirect plasma etching operation using a plasma barrier between electrodes. The plasma barrier provided secondary plasma overflow on wood materials and minimized thermal transfer from the top electrode to the wood samples. The simplicity of the systems also led to a better understanding of the electromagnetic field effect with ionized gas etching on the TMP fiber handsheet surface and PP film at a low pressure

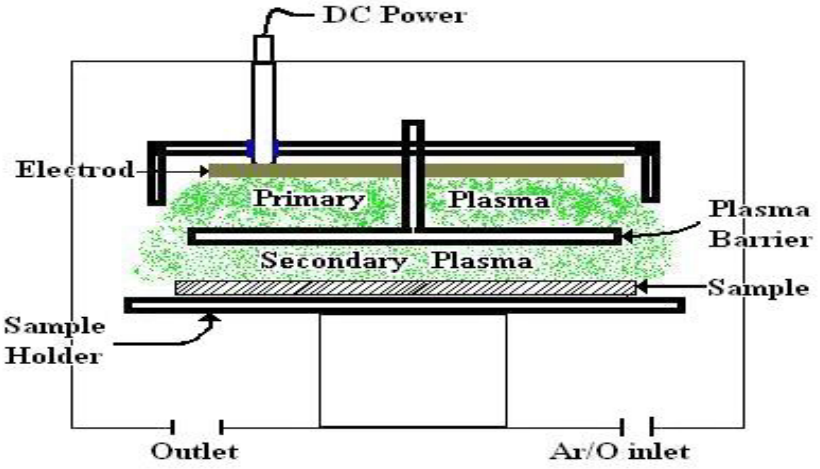

Figure 4.1. Parallel plate direct current (DC)-based dielectric discharge with a plasma barrier plate to generate secondary plasma on the substrate.

environment. The Ar and O_2 plasma treatment was performed with a 20 sccm (standard cubic centimeters per minute) gas flow rate and exposure times of 30, 60, 300, and 600 seconds. The chamber was evacuated below 30 mtorr and argon gas was purged twice at a chamber pressure of 100 mtorr to clean the chamber and the sample. Argon-based plasma was performed at the chamber pressure of 100 mtorr, 2.5 kV, and 34 mA. Oxygen-based plasma was carried out at 100 and 200 mtorr chamber pressure, 1.5 kV, and 40 mA. After the plasma treatment, the chamber was re-evacuated to 30 mtorr and slowly purged with air.

4.2.3. Atomic Force Microscopy and Fourier-Transform Infrared Spectroscopy (FTIR)

Atomic force microscopy (AFM) was applied to characterize the surface topography of substrates as well as to observe adhesion and mechanical properties on scales from hundreds of microns to nanometers. This study used a Nanoscope IIIa AFM (Digital Instruments) mounted on a pneumatic isolation table with an acoustic hood. The scanning area was 1 um^2 (360 samples) and 6.25 um^2 (120 samples). All AFM micrographs were taken at a resolution of 512 × 512 pixels in tapping mode. The images were evaluated and statistically analyzed using the

quantify root mean squire (RMS) to quantify surface roughness. FTIR (NEXUS^{TM} 670 FTIR E.S.P.; Thermo Nicolet) is equipped with "Smart Golden Gate" and mid- range (4000- 650cm^{-1}) capabilities. The data acquisition software was OMNIC 5.2.

4.2.4. Scanning Electron Microscopy

The morphology of the TMP fiber handsheet and PP films was investigated using scanning electron microscopy (SEM: Hitachi S-3600N). Mounted fibers were coated with an approximately 15-nanometer thin gold layer using an ion sputter (Technics Hummer V). The morphological characteristics were analyzed from photomicrographic images to identify the fiber surface conditions. Images were generated at 15 kV and 1,000×.

4.2.5. Fabrication of TPL

The weight fraction of TMP fiber handsheet and PP film was 50/50. Two handsheets and 12 PP films were cut into 2 × 4 inch^2 sizes to perform the plasma treatment. Treated samples were laminated and pressed at 100 psi pressure with a pressing temperature of 400 °F for two and half minutes using a 6 × 6-inch laboratory press.

4.2.6. Tensile Strength Test

One hundred and eighty dog-bone tensile samples were cut to nominal dimensions of 2 × 0.6 × 0.027 inch^3 with a neck width of 0.18 inch. Tensile strength properties were tested using an Instron 4465 mechanical testing machine at a crosshead speed of 0.05 in. min.$^{-1}$ according to ASTM D638-03 (ASTM 2003). At least 6 specimens were tested for each set of samples and the mean values as well as standard deviations were calculated.

4.2.7. Differential Scanning Calorimetery

Thermal characteristics of plasma treated samples were evaluated with differential scanning calorimetery **(**DSC; Perkin-Elmer DSC 7**)** under nitrogen atmosphere. A heating rate

of 5 °C min.$^{-1}$ from -30 °C to 200 °C and a cooling rate of 5 °C min.$^{-1}$ from 200 °C to 50 °C were applied for DSC samples. Finally, thermal characteristics of glass transition (T_g), onset (T_{om} and T_{oc}), and peak temperature (T_m and T_c) were determined by endothermic and exothermic curves during the polymer relaxation and crystallization based on ASTM E793-01 and E794-01 (ASTM 2001a, b). For calculation of the percents of crystallinity (X_C) of the plasma treated samples from the area of under the cooling curve, the following equation was used:

$$X_C = \left[\frac{\Delta H_f}{w \Delta H_f^0} \right] \times 100 \tag{4.1}$$

Where ΔH_f and ΔH_{f_0} are heat of fusion (J g^{-1}) from the area under the crystallization curve and heat of fusion from 100% crystalline PP (207.14 J g^{-1}). The w is the mass fraction of PP in the TMP fiber/PP film laminates.

4.3. Results and Discussion

4.3.1. Effects of the Plasma Barrier on the Tensile Strength Properties

Figure 4.2 shows the secondary O_2 plasma field effect on the tensile strength properties of TPL. The plasma barrier provided O_2 plasma overflow from the primary to the secondary region on the surface of the samples. The barrier minimized thermal damages on the surface of the TMP fiber handsheets and PP films. The barrier also provided 55% increased tensile strength over control samples and also resulted in a 20% increase compared to samples treated without the plasma barrier plate. The TMP fiber handsheets and PP films could not be treated for 5 minutes due to extreme thermal damage. Therefore, the plasma barrier plate was used to prevent thermal transfer from the electrode to the surface of the TMP fiber handsheets and PP films.

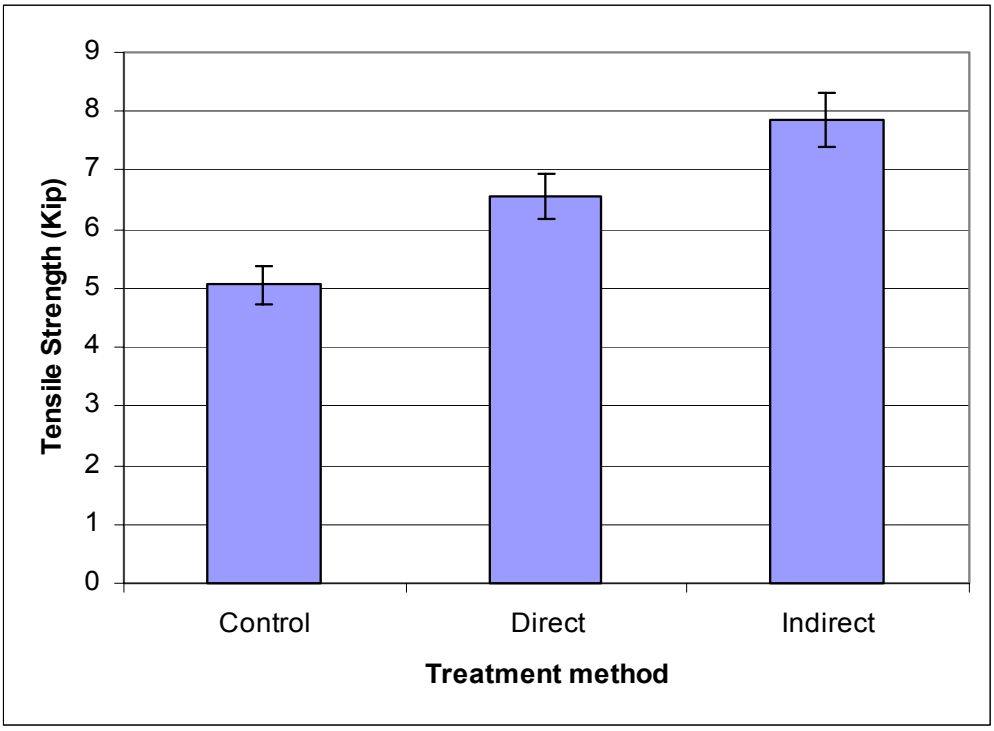

Figure 4.2. Effects of O_2 plasma treatment methods on the tensile strength properties of thermomechanical pulp fiber handsheet and polypropylene laminates (The error bars represent one standard deviation).

4.3.2. Effects of the Plasma Sources on the Tensile Strength Properties

Figure 4.3 shows the effect of Ar- and O_2-plasma sources on tensile strength of TMP fiber handsheet and PP film laminates as a function of surface exposure time. The tensile strength properties of treated laminates increased 60 to 85% with O_2-plasma and 50 to 78% for Ar-plasma treatment. The optimum plasma effect was obtained in the 30 to 60 second range of treatment times. The plasma enhanced process showed a couple of limitations of material conditions of a complex geometry as wood-based lignocellulosic materials. These related to low vacuum used and to thermal damage. There was a strong interaction between the two plasma treatments used in the experiment and treatment time on increased tensile strength of TPL as seen in Figure 4.4.

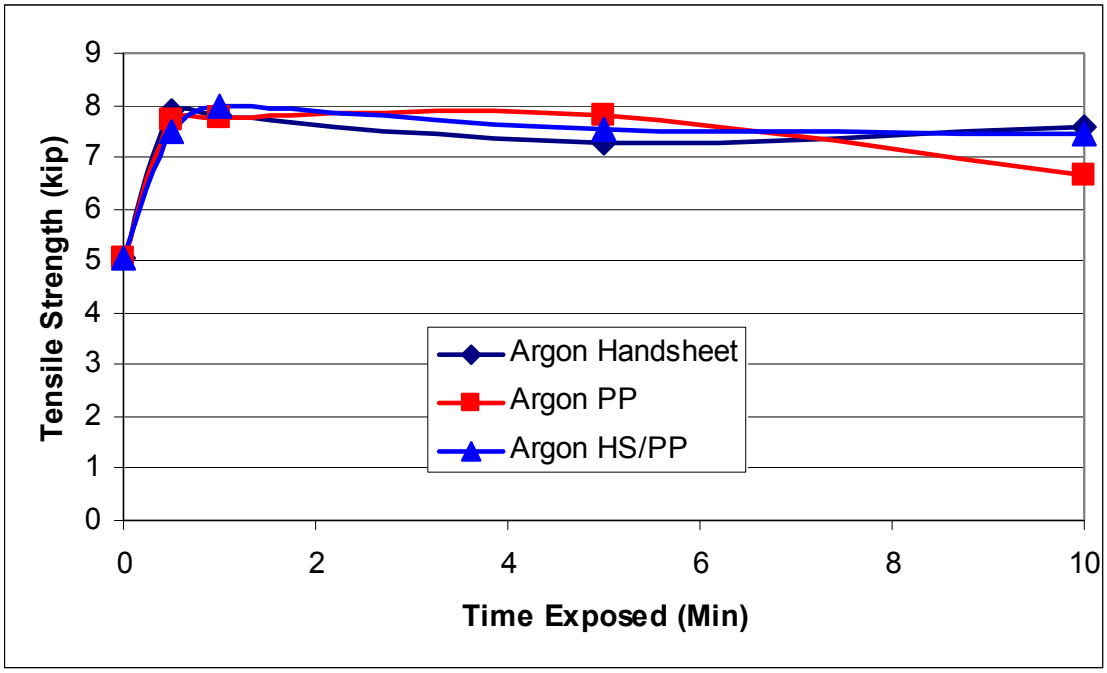

(a)

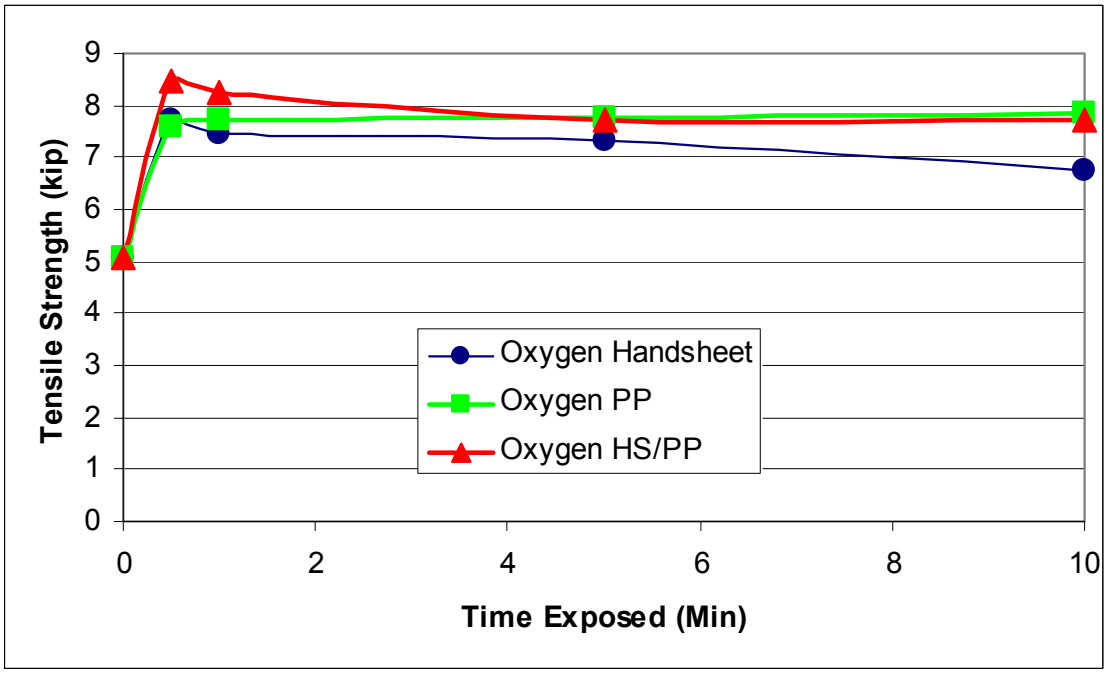

(b)

Figure 4.3. Effect of (a) Ar- and (b) O_2 -plasma sources on tensile strength as a function of surface exposal time to plasma under 100 mtorr pressure.

4.3.3. O_2-plasma Treatment on Three Different Fiber Surfaces

Figure 4.4 shows the effect of the O_2-plasma treatment on tensile strength properties of three levels of lignin content. The fibers were controlled with different lignin contents in the chemical composition of each fiber type. TMP fibers consisted of 25.4% lignin, and the lignin content decreased under 6.8% with macerated TMP fibers and lignin-free filter paper (contains less than 0.02% lignin content). The filter paper fiber handsheet and PP film laminates showed a two fold increase in tensile strength compared to the TMP fiber-based handsheet laminates due to the higher cellulose content of the former. However, TPL were the most effective O_2-plasma treatment for tensile strength. Thirty second treatment on the TMP fiber handsheet increased the strength properties by 80% while other fiber types led to an increase of 17 to 18%. It should be noted that 30 second O_2-plasma treatment on the TMP fiber handsheets, containing 25.4% lignin, showed better tensile properties than O_2-plasma treatment of the PP film only.

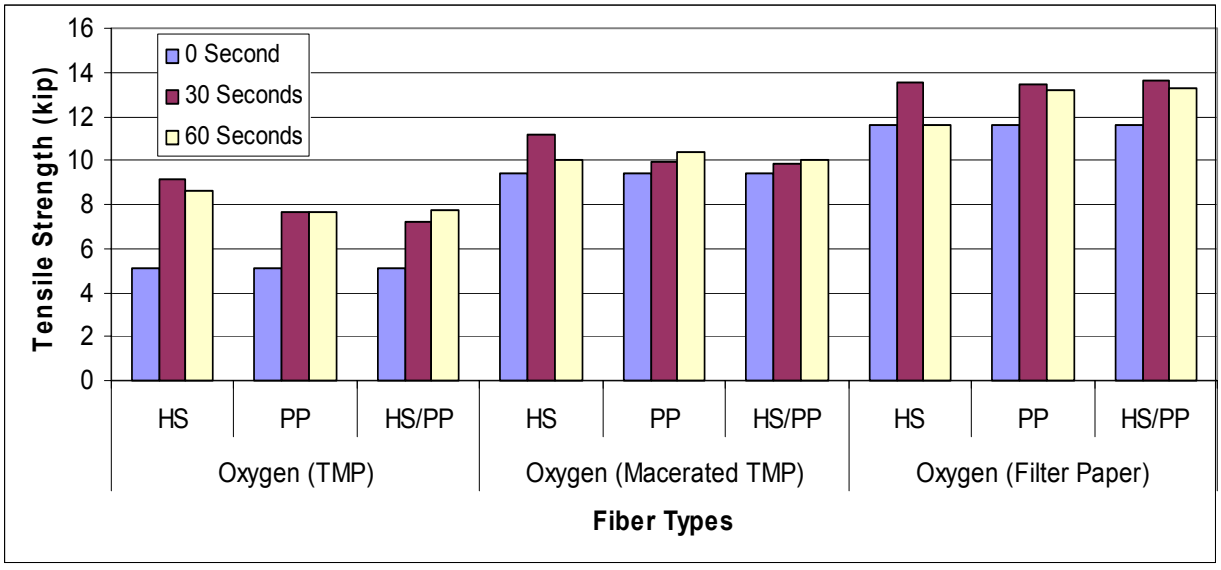

Figure 4.4. The effects of O_2 plasma sources at 200 mtorr pressure as a function of three different fiber types, three plasma treated surfaces, and three treatment times on tensile properties of thermomechanical pulp fiber handsheet and polypropylene film laminates. (HS = Handsheet and PP = Polypropylene)

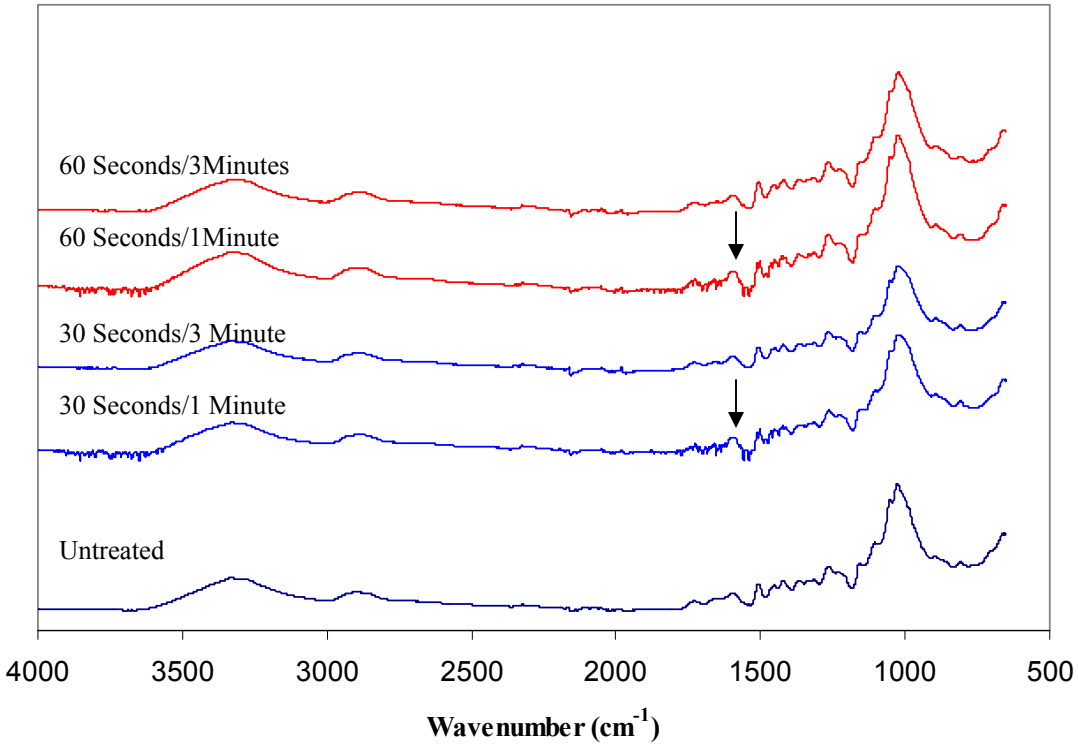

(a)

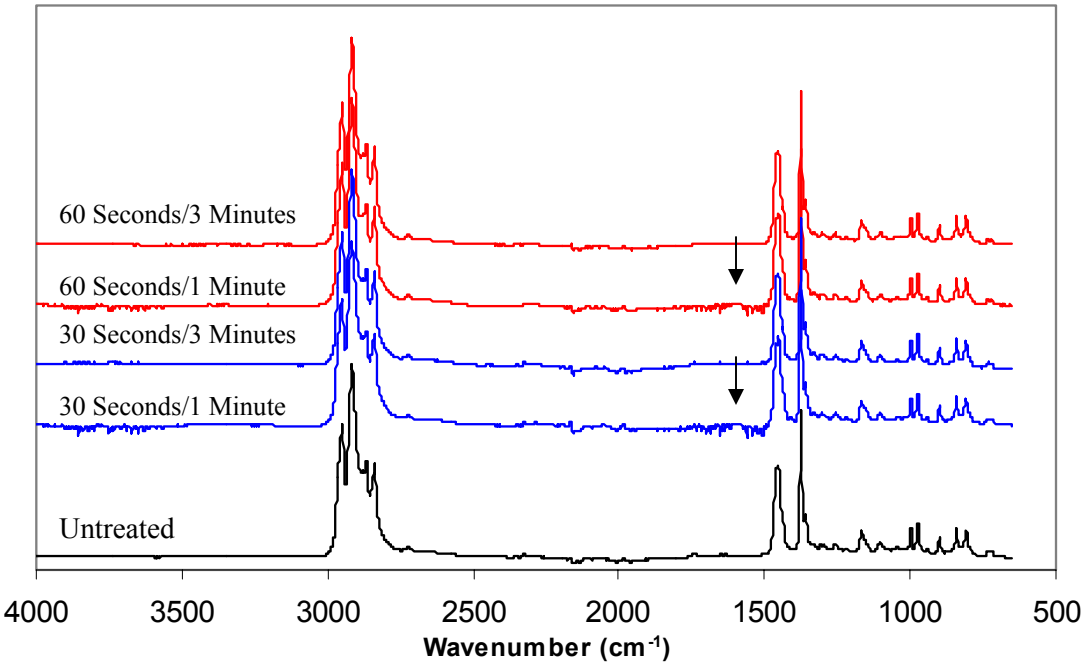

(b)

Figure 4.5. Fourier-transform infrared spectroscopy spectra of O_2-plasma treated (a) thermomechanical pulp fiber handsheet and (b) polypropylene film with one and three minutes exposal to atmospheric conditions after 0, 30, and 60-second treatment time.

4.3.4. Fourier-transform Infrared Spectroscopy (FTIR)

FTIR absorbance spectra of oxygen-plasma treated TMP fiber handsheets and PP film is shown in Figure 4.5. The intensified peaks represented chemical skeletons of the TMP fibers and PP structures. Figure 4.5a showed FTIR bends of TMP fiber such as 3348cm^{-1} assigned as an alcoholic hydroxyl group, C-O stretching at 1300 - 100 cm^{-1}, and CH_2 at 2908 cm^{-1}. Figure 4.5b showed PP skeletons of symmetric and anti-symmetric CH_2 and CH_3 stretching vibration at the bend range of 3000 - 2800 cm^{-1} as well as deformation vibration at 1500 - 1350 cm^{-1}. The noises from bend ranges of 3900 - 3500 cm^{-1} and 1500 - 2000 cm^{-1} appeared with the oxygen plasma treatment. However, after three minutes of exposure to atmospheric conditions the spectra appeared to have less noise after air was introduced into the plasma chamber before the FTIR scan. The spectra represented were matched with untreated FTIR spectra. The noise may be caused by either ionized oxygen activation or a magnetic field effect in contact of a material surface. The noise regions from the FTIR spectra are nebulous to assign as a certain bond due to the lack of the instrumental sensitivity.

4.3.5. Thermodynamic Characteristics

Table 4.1 shows thermal characteristics of wood fiber handsheet and PP laminates fabricated with O_2 based DC-plasma treated handsheets and PP films. In general, the thermal quantities were reduced due to the 30 second treatment and then slightly increased with 60 seconds of treatment as determined from both the endothermic and exothermic curves. The PP crystallinity (X_C) decreased to 30's and glass transition temperatures (T_g) increased with the TMP fibers. The crystallinities are lower than for 100% PP film scan. The decreased melting point (T_m) with TMP fibers may be influenced by introducing an ion implanted surface which also may reduce crystallinity (Bai et al. 1999, Ali et al. 2005). Addition of the wood fibers as

filler and ion implantation may reduce the T_m and X_C. This result indicates that thermal behavior of PP with O_2-plasma treatment positively influenced the interfacial strength enhancement.

Table 4.1. Thermodynamic quantities of O_2 based direct current (DC)-plasma treated wood fiber handsheet and polypropylene laminates.*

Fiber Sources, Processing Conditions and Time		Density	Endothermic Curve				Exothermic Curve			
			T_g	T_O	T_m	ΔH	T_O	T_C	ΔH	X_C
		(g cm^{-3})	(°C)	(°C)	(°C)	(J/g)	(°C)	(°C)	(J/g)	(%)
PP film		---	-21.1	156.9	161.7	69.6	121.4	117.3	95.0	46
TMP	0	1.05	-12.5	152.7	163.1	56.1	120.9	116.2	82.2	40
Handsheet	30	1.13	-14.0	149.8	162.9	48.2	121.1	116.9	74.2	36
	60	1.17	-14.0	150.4	162.8	38.8	121.1	116.4	63.2	31
PP	30	1.06	-22.6	153.0	162.9	41.9	121.0	116.3	71.2	34
	60	1.08	-18.2	151.8	162.8	51.6	121.2	116.7	77.8	38
Both	30	1.06	-22.4	151.5	163.0	46.4	121.2	116.8	75.2	36
	60	1.06	-21.8	149.9	162.3	43.0	121.3	116.6	68.2	33
Macerated TMP	0	1.18	-20.9	149.9	162.7	40.1	121.2	116.9	64.5	31
Handsheet	30	1.17	-22.7	149.7	162.8	41.1	121.3	117.1	68.5	33
	60	1.15	-22.3	150.0	162.5	41.7	121.5	117.3	66.7	32
PP	30	1.16	-21.6	154.4	163.4	41.6	121.2	116.7	64.5	31
	60	1.17	-21.5	155.1	162.3	34.1	121.2	116.8	60.9	29
Both	30	1.22	-22.9	150.2	162.4	37.1	121.0	116.8	63.9	31
	60	1.09	-22.7	149.4	162.6	44.8	121.4	117.3	71.8	35
Filter Paper	0	1.10	-20.7	149.7	160.9	38.7	126.0	120.4	68.4	33
Handsheet	30	1.17	-22.8	150.9	160.0	39.7	126.4	120.5	65.0	31
	60	1.15	-22.7	150.4	160.1	44.5	126.3	122.7	70.0	34
PP	30	1.11	-22.3	149.9	160.6	39.9	126.3	120.1	68.3	33
	60	1.07	-22.3	150.6	161.4	47.3	125.8	120.3	80.5	39
Both	30	1.12	-22.6	150.4	159.6	37.7	126.0	122.6	62.9	30
	60	1.13	-22.1	150.6	160.2	38.9	125.8	122.0	71.5	35

* Each value represents an average of three specimens.

4.3.6. Surface Topography and Roughness

The PP film surfaces that had been treated with oxygen plasma using different exposure times and applying DC power are shown in Figure 4.6. Three dimensional AFM images of 24 plasma treated handsheets and PP film samples were generated. The AFM images show that increased plasma treatment time on the film surface created small spherical nodule structures.

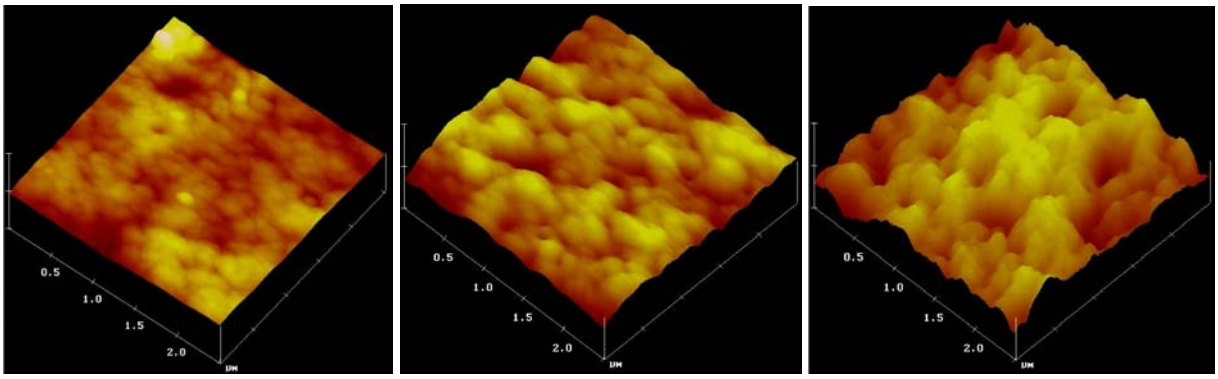

(a) (b) (c)

Figure 4.6. O_2 plasma modification of the surface of polypropylene film. (a) Untreated; Z=353.5 nm and 10.9 Hz, (b) 30 seconds; Z=94.6 nm and 1.2 Hz, and (c) 60 seconds surface treatment; Z=35.8 nm and 1.3 Hz.

The AFM images appeared to have rough surfaces without Z scales. However, a closer look on a nano-scale reveals a distinct difference among the three surfaces. In this study, untreated surfaces consisted of small irregular structures while the treated surface appeared with nodule structures forming a layer on the PP film surfaces. The PP film surface was nearly smooth and completely covered with small spherical nodules and resulted in a reduction in surface roughness. The PP surface treated with plasma for 60 seconds is covered with nodules which are about twice in size of those on samples exposed for 30 seconds.

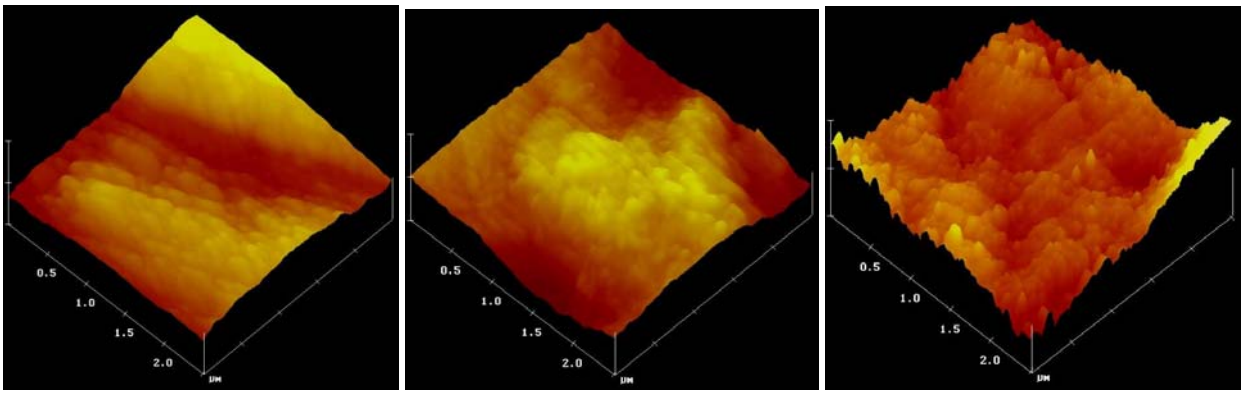

(a) (b) (c)

Figure 4.7. O_2 plasma modification on the surface of thermomechanical pulp fiber handsheets. (a) Untreated; Z=188.5 nm and 1.3 Hz, (b) 30 seconds; Z=209.5 nm and 0.84 Hz, and (c) 60 seconds surface treatment; Z=67.5 nm and 0.84 Hz.

Three dimensional AFM scan images of O_2-plasma treated TMP fiber handsheets are presented in Figure 4.7. The AFM images of handsheet surfaces were more difficult to scan than those made with macerated TMP fiber and filter paper due to the surfaces of coarse and fractured fibers. Plasma treated handsheet surfaces also showed nodule structures while the special structures were rarely formed on the untreated TMP fiber surface in the scanning size of 6.25 um^2 and 1 um^2. The plasma-treated TMP fiber surface may be covered with ionized oxygen and electromagnetic fields which could influence surface structure changes. The TMP fiber surface is relatively smooth and the size of the nodules increased when the surface was treated for 60 seconds as seen on PP film surface. The nodule structures were not typically observed on the untreated wood fiber surface. The nodular coverage similar to macerated TMP and filter paper fibers was found in the flat areas.

Table 4.2 shows quantitative RMS measurements from AFM with four material sources, three plasma treatment times, and two scan sizes. The RMS roughness yielded very similar

Table 4.2. Quantitative root mean squire (RMS) from atomic force microscopy.

Sample types	Treat Time	Scan Size		
		2.5 μm* (nm)	PSD Equ.** (nm)	1 μm* (nm)
Polypropylene	0 Sec.	14.9	17.9	7.7
	30 Sec.	8.4	9.2	6.4
	60 Sec.	9.99	11.4	7.1
TMP Fiber	0 Sec.	121.5	139.98	37.5
	30 Sec.	65.4	82.9	36.0
	60 Sec.	77.0	91.6	36.3
Macerated TMP Fiber	0 Sec.	52.5	49.0	17.4
	30 Sec.	48.4	54.9	19.5
	60 Sec.	63.5	71.2	30.4
Filter Paper	0 Sec.	44.4	50.7	22.1
	30 Sec.	41.8	46.4	17.4
	60 Sec.	52.7	66.5	17.6

* The values are an average of 10 scan for the 2.5 μm scan size and 30 scans for the 1 μm scan size.
** PSD Equ.; Power spectral density equivalent RMS (Root mean square).

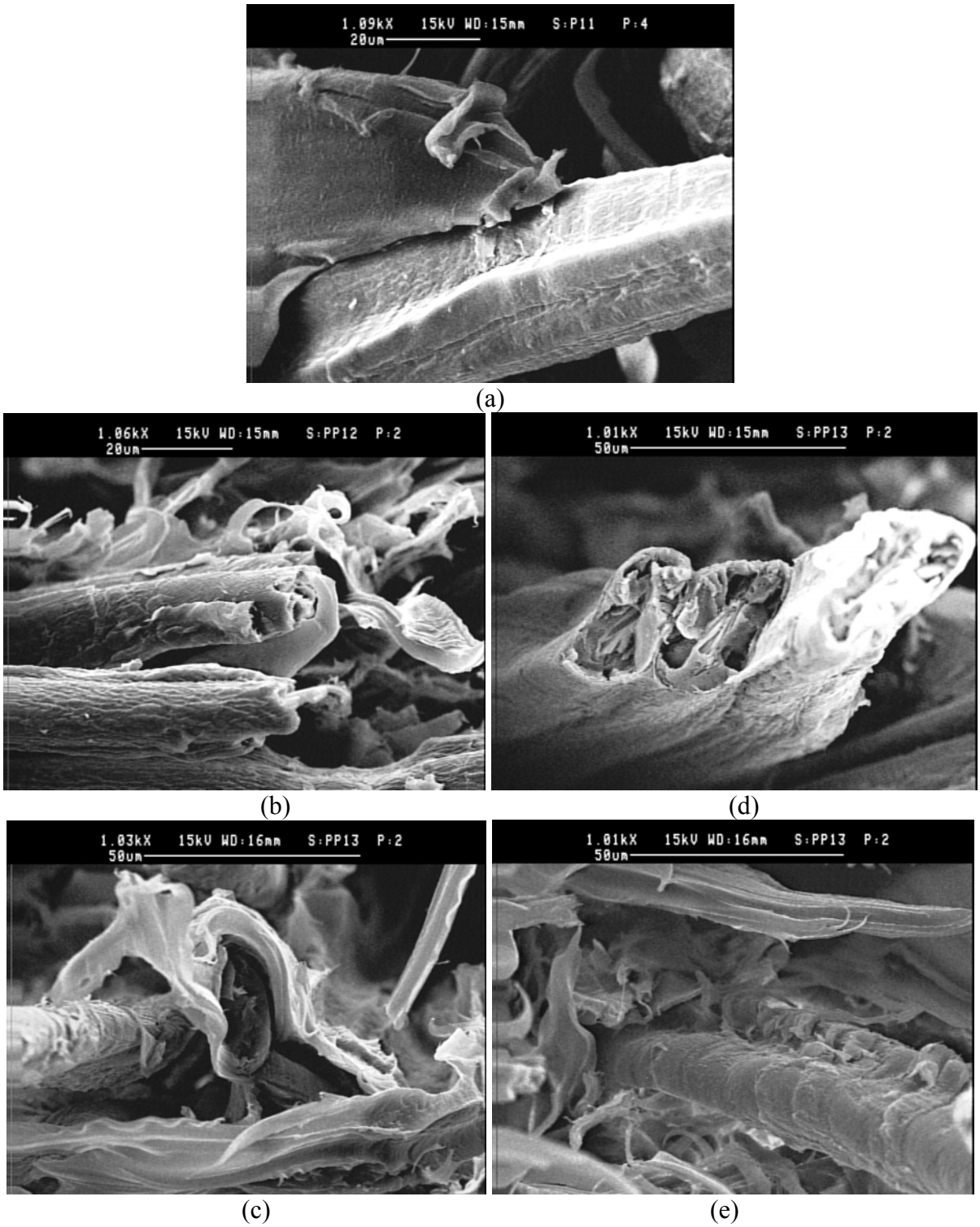

Figure 4.8. Scanning electron microscopy (SEM) micrographs of fracture surfaces of thermomechanical pulp fiber handsheets and polypropylene laminates. (a) Untreated, (b) 30 sec. on the handsheet, (c) 60 sec. on the handsheet, (d) 30 sec. on polypropylene film, and (e) 60 sec. on polypropylene film.

results as thermal characteristics of T_g and X_C from DSC. The RMS roughness of the four material surfaces was lower with 30 second plasma treatment and slightly higher with 60 seconds of treatment. It seems likely that the DC-based O_2-plasma is responsible for the change in surface roughness of both fiber and PP film. The modification may generate ionized oxygen and an electron rich donor surface from electromagnetic field generation. Power spectral density (PSD) Equivalent RMS was generated using light intensity and provided the highest surface roughness compared to 2.5 and 1 um scan sizes.

4.3.7. Fracture Surface Morphology

Fracture surface morphology of tensile failures is shown in Figure 4.8. A poor interfacial interaction between TMP fibers and PP was observed with control samples (Figure 4.8a). TMP fiber failure rarely occurred and fibers pulled out from the PP matrix without surface damage. Thirty second O_2-plasma treatments showed thermoplastic and TMP fiber failure instead of failure at the wood fiber and thermoplastic interface. Figure 4.8b and d show a distinctive thermoplastic failure. Handsheets exposed for 30 seconds under O_2-plasma showed many stretched PP fibers around TMP fibers. The findings were not observed with 30 second PP treatment. Sixty seconds exposure under the O_2-plasma provided similar results as 30 second handsheet treatment except some of the interfacial failure at the TMP fiber and thermoplastic interface.

CHAPTER 5

TMP FIBER SURFACE MODIFICATION FOR ENHANCING THE INTERFACIAL ADHESION WITH POLYPROPYLENE

5.1 Introduction

The potential use of thermomechanical pulp (TMP) fibers as a reinforcing component for thermoplastics opens up further possibilities for use of low-cost lignocellulosic fiber resources. Researchers have shown an increasing interest in natural fiber-reinforced polymer composites due to the inherent properties of bio-based fibers, such as low density, relatively high toughness, high strength and stiffness, and good thermal properties and biodegradability (Rowell and Clemons 1992, Rezai and Warner 1997, Wu et al. 2000, Joseph et al. 2003). However, a main disadvantage of natural fibers is their poor compatibility with hydrophobic thermoplastics. Therefore, chemical modifications are necessary to increase interfacial adhesion at the wood fiber and semicrystalline polymer interphase.

Surface modification with multifunctional monomers increases interfacial adhesion by modifying surface chemistry, surface roughness, and surface free energy of the wood fibers (Gray 1974, Liu et al. 1994, Wang and Hwang 1996a,b). Anhydrides as a coupling agent have received a great amount of interest (Maldas et al. 1989a, Maldas and Kokta 1991b, Khan and Idriss Ali 1993, Bamford and Al-Lamee 1994, Lu and Chung 1998, Hill and Cetin 2000, Li et al. 2001). Anhydride groups react chemically with the hydroxyl groups of wood fiber to form ester bonds. These bonds between the treated wood fiber and PP provide a good interfacial adhesion for wood fiber and thermoplastic composites (WPC). Maleic anhydride (MA), polymethylene polyphenyl isocyanate (PMPPIC), and maleic anhydride polypropylene (MAPP) are recognized as well known coupling agents in WPC (Lu et al. 2000). MA and MAPP have been shown to be relatively effective in improving both physical and mechanical properties of TMP fiber and PP

composites. Both the chemical structure and the modification procedure improved mechanical properties of WPC through their coupling actions at the interface. The reaction rate and the number of anhydride groups reacted with the lignocellulosic fibers differenced from those of MA due to differences in their chemical structure which affected their reactivity (Clemons et al.1992, Felix and Gatenholm 1993, Grell 2001, Lu 2002).

Benzoyl peroxide (BPO) and dicumyl peroxide (DCP) were commonly used as initiators for the modification of wood fibers and thermoplastics to graft MA onto the wood fiber surfaces (Raj et al. 1990, Keener et al. 2004, Demir et al. 2005, Denac et al. 2005a, Denac et al. 2005b, Minisini 2005). Initiators have been used to improve interfacial adhesion by adding them directly to the fiber-plastic mixture (Cousin et al. 1989, Sapieha et al. 1990). However, the BPO impregnation was much less effective than the direct blending process with an exception of some improvement in the yield stress of LDPE composites (Raj et al. 1990). The lower effectiveness of the impregnation method was caused by fiber surface adsorption which reduced the amount of peroxide available when the fibers were treated with MA (Bataille et al 1990). A small amount of BPO or DCP sharply increased the yield stress of PE composites. The BPO or DCP concentration, defined as a peroxide weight fraction at which the yield stress reaches 95% of its maximum, depended on the fiber content (Sapieha et al. 1990, Gassan and Bledzki 1997). DCP was more effective than BPO at low levels of peroxide addition due to the lower decomposition rate at high temperatures ensuring a better dispersion in the polymer. However, thermodynamic mechanical properties of polyvinyl chloride (PVC) based composites increased 20% by using 4.12 % MAPP (Raj et al. 1990, Raj and Kokta 1995, Matuana et al. 1998, Lu et al. 2004).

The MA has two different functional groups, an unsaturated carbon-carbon double bond

and an anhydride group (Figure 1.1). Both groups attack wood fiber surfaces and build crosslinking reactions via hydroxyl groups. This characteristic makes MA an attractive coupling agent in WPC. Esterification reactions between wood fiber and MAPP also proved to be beneficial in increasing strength properties (Marcovich et al. 2001). The esterification reaction can be optimized by using catalysts, sodium hypophosphite hydrate, for esterification between the MA and the bleached wood fibers (Kazayawoko et al. 1997a). However, little effect on the esterification of chemical-thermomechanical pulp (CTMP) fibers was reported. Tensile strength properties of PP based composites were improved with 2-5% MA addition (Mohanakrishnan et al. 1993, Wu et al. 2000).

With regard to mechanical properties of WPC, interfacial property enhancement is important at the TMP fiber-thermoplastic interface. The maleation of the wood fiber surfaces provided a high variation on the mechanical properties of WPC depending on the wood or plastic materials, copolymer types, and processing conditions. Therefore, this study was conducted to evaluate the effects of MA grafted TMP fiber surfaces in contact with PP melts. It also evaluated the porosity of TMP fiber handsheets and number of fibers exposed on the fracture surfaces to determine its relationship to tensile strength properties of TMP fiber handsheets and PP laminates (TPL).

5.2 Materials and Methods

5.2.1. Materials

Wood fiber samples used in this study were loblolly pine chips (*Pinus taeda* L.) converted to thermomechanical pulp fibers at 8 bar steam pressure conditions and 8.2% moisture content (Lee 2002). Maleic anhydride (Huntman Chemical Co., Chesterfield, MO) was used as a modifying agent with a purity > 99 % and a melting point of 52ºC. Benzoyl peroxide (BPO;

Benox® A-80; NORAC, Inc. Azusa, CA) was used as an additive component to initiate MA reaction on the TMP fiber surface. It contained 20% water and 5.1% active oxygen. Toluene (Fisher Scientific Inc., Pittsburgh, PA) was used as a reagent. A PP film (Plastic Suppliers, Inc., Columbus, OH) was used to fabricate TPL.

5.2.2. Thermomechanical Pulp Fiber Modification

Table 5.1 shows the conditions of the TMP fiber surface modification. The modification with MA was carried out by soaking the fibers in an MA/BPO solution. Treatment solutions were formulated based on the weight fraction of MA (12.5, 25, and 50 grams)/BPO (12.5 grams) in toluene (1 L) which was heated to 100 °C. The final total solution was 2 L. Fifty-eight grams of TMP fiber were soaked for 10 minutes. The treated fibers were removed from the treatment solution and excess chemicals on the surface of the TMP fibers were washed out with distilled water. The fibers were ovendried at 60 °C for 38 hours.

Table 5.1. Maleic anhydride grafting conditions for the thermomechanical pulp fiber surface modification.

TMP Fibers	7.5 grams (each load)
MA and BPO ratios	0:0, 1:1, 2:1, and 4:1
Reagent Chemicals	Toluene
Reaction Temperature	100 °C
Treatment Time	10 minutes

5.2.3. Fabrication of Handsheet and Polypropylene Film Laminates

A total of 36 handsheets were formed with 2 grams (OD wt.) of treated TMP fibers and were press-dried at 25 °C and 60 °C with 50 psi pressure to evaluate the effect of drying conditions on the handsheet porosity and tensile strength properties of TPL. Handsheets were stored in a vacuum dessicator until laminates were fabricated. The TPL (50/50% weight fraction) were pressed under 100 psi pressures for three minutes at 400 ºF.

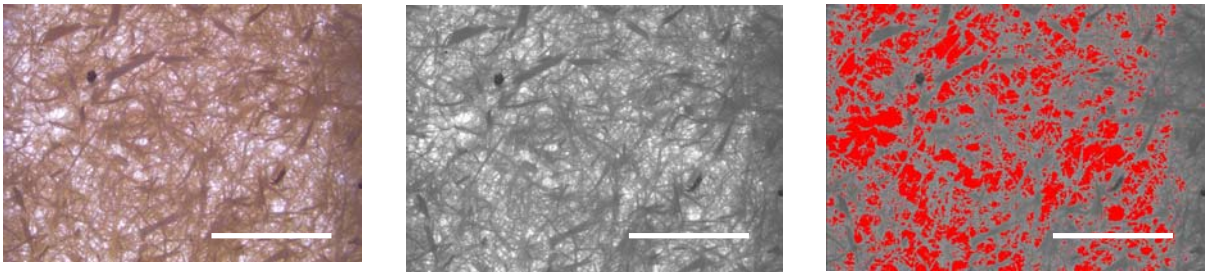

(a) (b) (c)

Figure 5.1. Porosity of wood fiber handsheet and polypropylene laminates using image analysis; (a) Stage I. Original Images, (b) Stage II. Gray Transformation, and (a) Stage III. Intensity Range Selection. (16 x 11 mm^2). (Scale bar on each image represents 5 mm)

5.2.4. Image Analysis

A SPOT RT Color "F" mounted digital camera (Diagnostic Instruments Inc., 1520 x 1080 resolution and Spot Adventure – Ver. 3,2,4) was employed for microphotographing handsheet porosity and number of fiber measurements. The images for the handsheets were transformed into gray scale images and data were collected using light intensity selection with 146 to 255 intensity range (Figure 5.1). Measurement of the number of TMP fibers in the tension break, using the fracture mode images (Figure 5.2), was performed with image transformation. The images were transformed using an edge finder function. For the image analysis and data collection, Image-Pro® plus software (Media Cybernetics – Ver. 5,0) was used

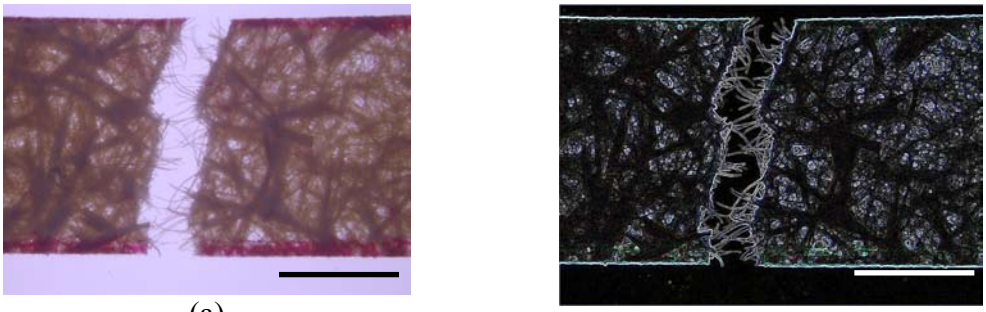

(a) (b)

Figure 5.2. Photomicrographs of handsheet and fibers from failure section of the tensile strength test (a) Stage I. Original fracture image, and (b) Stage II. Image transformation. (Scale bar on each image represents 5 mm)

to collect quantitative measurements of porosity, porous (%), and number of fibers in the tensile failure section of the dog-bone samples.

5.2.5. Tensile Strength

Two hundred and sixteen dog-bone tensile samples were cut in a nominal dimension of 5 × 0.8 × 0.01-inch with a neck width of 0.35-inch. Tensile strength properties were tested using an Instron 4465 mechanical testing machine at a crosshead speed of 0.05 in. min.$^{-1}$ according to ASTM D638-03 (ASTM 2003). At least 21 specimens were tested for each set of samples and the mean values as well as the standard deviations were calculated.

5.2.6. Thermal Characteristics

A DSC (Perkin-Elmer DSC 7) system was used to evaluate and confirm thermal characteristics of surface modified TMP fiber and PP laminates at levels of MA fraction. Thermal characteristics of glass transition (T_g), onset (T_{om} and T_{oc}), and peak temperature (T_m and T_c) were determined by exothermic curves during the polymer melt and crystallization process based on ASTM E793-01 and E794-01 (ASTM 2001). The X_C (Eq. 5.1) with PP and 4 levels of MA treated fiber combinations was used to calculate parameters of interest. A heating rate of 5 °C min^{-1} from -30 °C to 200 °C and a cooling rate of 5 °C min^{-1} from 200 °C to 50 °C for DSC samples were applied for this study.

$$X_C = \left(\frac{\Delta H_f}{w \Delta H_f^0} \right) \times 100 \tag{5.1}$$

Where: X_c = % of crystallinity
ΔH_f = Heat of fusion from DSC
ΔH_f^0 = 100% Crystalline PP
w = Mass fraction of PP

5.2.7. Fracture Surface

Scanning electron microscopy (SEM: Hitachi S-3600N) observations of the fracture surfaces of MA-grafted TMP fiber handsheet and PP film laminates was used to study the MA treatment effect at the treated fiber and PP interfaces. Mounted fibers were coated with an approximately 15-nanometer thin gold layer using an ion sputter (Technics Hummer V). Morphological characteristics were analyzed from photomicrographic images to study the fiber surface conditions. Images were generated at 15 kV and 1,000x.

5.3. Results and Discussion

5.3.1. Porosity of Thermomechanical Pulp Fiber Handsheet

Figure 5.3 shows the influence of a handsheet porosity and porous percentage on tensile strength properties. Prepressing conditions for the TMP fiber handsheets were 50 psi pressure at

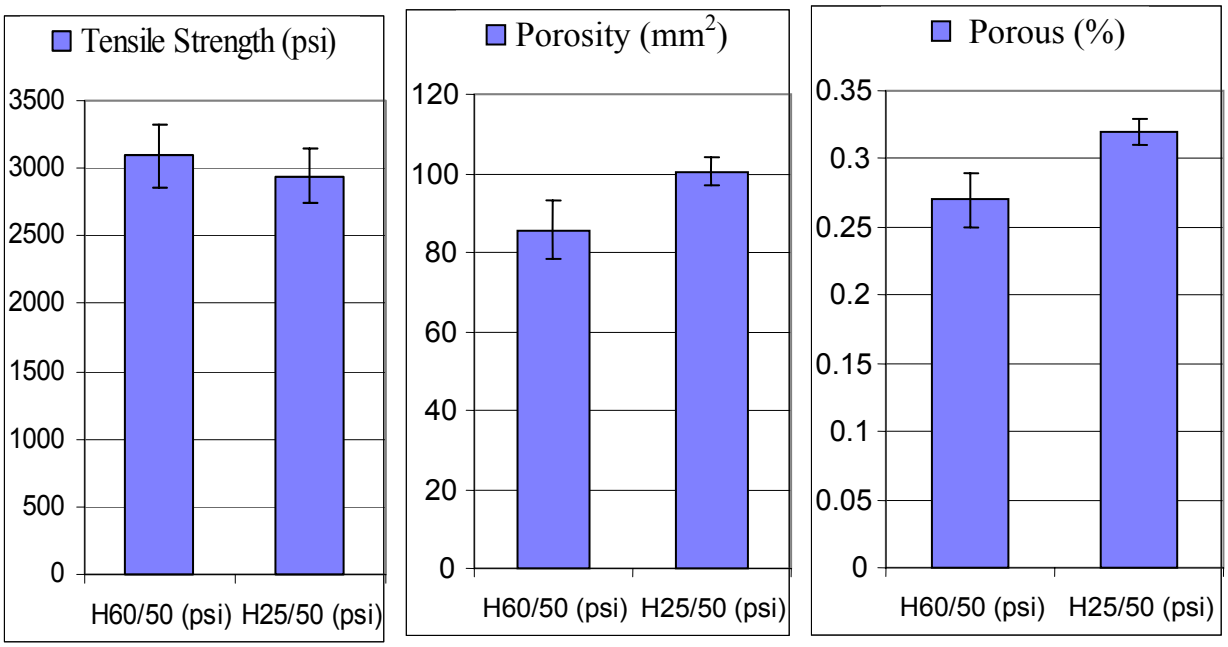

(a) (b) (c)

Figure 5.3. Test sample laminate conditions on the (a) tensile strength, (b) porosity, and (c) porous (The error bars represent one standard deviation). H60/50 (psi)=50 psi pressure at 60 °C and H25/50 (psi)=50 psi pressure at 25 °C. (21 samples per each condition)

25 °C and 60 °C. The handsheet porosity and porous percentage between the two temperature pressing conditions were statistically significant to each other. The higher porosity and porous percentage lowered the tensile strength property of laminates. However, the tensile strength properties of TPL poorly correlated to porosity and porous percentage. The strength property pressed at 60 °C showed slightly higher mean values. This result shows that the porosity effect was eliminated because the handsheets pressed at 100 psi were smoother and denser.

5.3.2. Number of Fibers at the Fracture Surface

Figure 5.4 shows the tensile strength properties of treated TMP fiber handsheets (MA and BPO ratio=2:1) and PP film laminates as a function of the number of fibers exposed on the fracture surface. Prepressing handsheets at 60 °C provided a better correlation with the number of fibers and tensile strength properties (R^2=0.92) while 25 °C prepressing condition yielded 0.90. This result shows the density and fiber to fiber stress transfer effects. In general, the tensile strength of WPC decreases with an increasing percentage of non-fibrous wood materials,

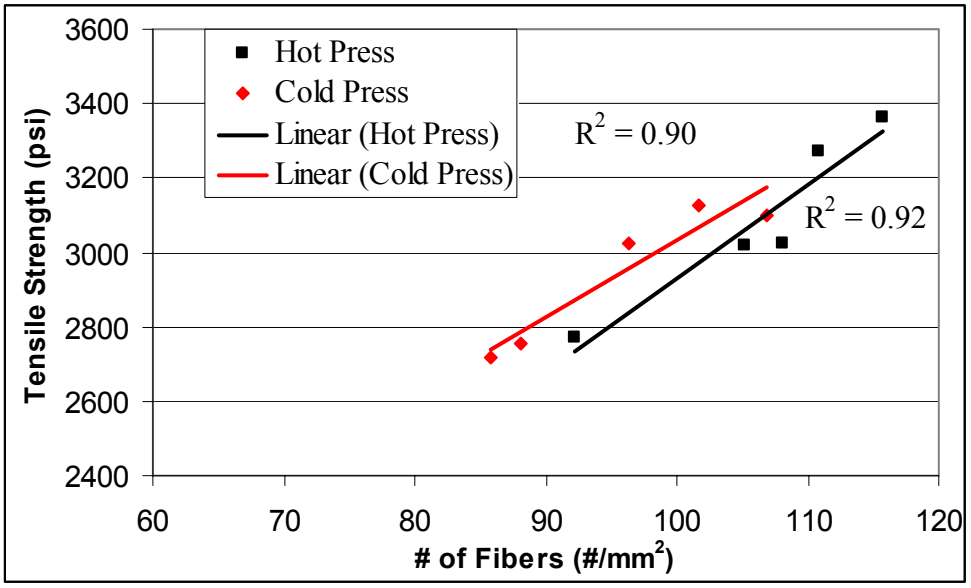

Figure 5.4. Tensile strength of sample laminates as a function of the number of fibers exposed on the fracture surface.

due to the poor stress transfer at the material interface. However, TMP fiber handsheet characteristic and fiber geometries such as fiber width, length, structure, and number of fibers contributed to the tensile strength enhancement of TPL (Michell et al. 1978, Thwe 2002, Bledzki and Faruk 2003, 2005).

5.3.3. Effects of the Maleic Anhydride and Benzoyl Peroxide Ratios

The effect of MA and BPO ratios on tensile strength properties of TMP fiber handsheet and PP laminates is shown in Figure 5.5. TMP fibers treated with MA and BPO ratio 2:1 yielded the highest tensile strength properties. Treatment effects of ratios 1:1 and 4:1 were less effective on the strength property enhancement than ratio 2:1. The result clearly shows that the MA and BPO ratio 2:1 is an optimum condition for the TMP fiber treatment used in this experiment. It showed 52% tensile strength property enhancement over untreated laminates.

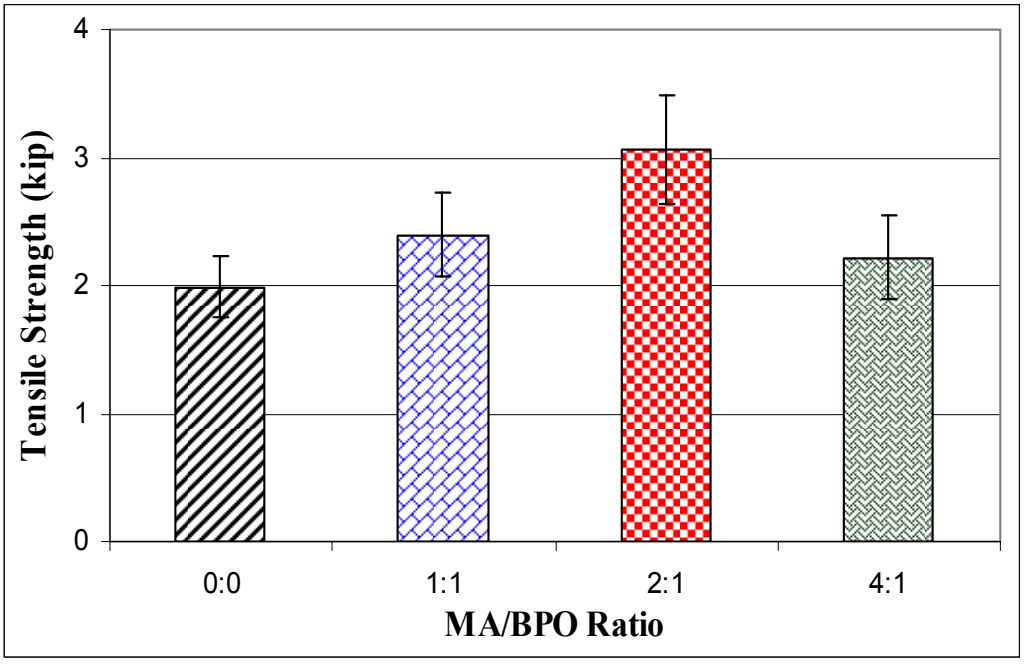

Figure 5.5. Effect of weight fractions between maleic anhydride (MA) and benzoyl peroxide (BPO) in toluene on tensile strength properties of thermomechanical pulp fiber handsheet and polypropylene film laminates. (The error bars represent one standard deviation)

5.3.4. Thermal Analysis

The treatment effect of four levels of MA and BPO ratios on the thermal behavior is presented in Table 5.2. The thermodynamic behavior of MA treated TMP fiber handsheets and PP film laminates on glass transition (T_g), onset (T_O), and melting and crystallization peaks (T_m, T_C) from the endothermic and exothermic curve did not influence behavior except for heat flow (ΔH) and PP crystallinity (X_C). The ΔH and X_C decreased with increased MA and BPO ratios. The ratio 4:1 showed slightly different thermal quantities and resulted in poor strength performance due to the excessive copolymer loading effects. In general, this result indicates that introducing TMP fiber to the PP matrix improves the semicrystalline polymer nucleation and crystallization and appears to confirm the work of Joseph et al. (2003) and Lee et al. (2006).

Table 5.2. Thermodynamic quantities of maleic anhydride treated thermomechanical pulp fiber handsheets laminated with polypropylene film.

MA/BPO Ratio	Density (g cm^{-3})	Endothermic Curve				Exothermic Curve			
		T_g (°C)	T_O (°C)	T_m (°C)	ΔH (J g^{-1})	T_O (°C)	T_C (°C)	ΔH (J g^{-1})	X_C (%)
0:0	0.89	-21.5	153	162	62.4	121	117	103.5	50.0
1:1	0.95	-21.8	153	162	61.7	121	117	98.6	47.6
2:1	1.00	-21.6	153	162	55.9	121	118	91.1	44.0
4:1	0.72	-22.4	152	161	56.4	122	118	94.9	45.8

Note: MA=Maleic anhydride, BPO=Benzoyl peroxide.

5.3.5. Scanning Electron Microscopy

Fracture surfaces of MA treated TMP fiber handsheets and PP film laminates show the effectiveness of MA loading at the TMP fibers and PP interface (Figure 5.6). The failure mode of MA loading levels under tension differed substantially from each other. Untreated samples show that the fiber was pulled out without surface damage and the brittle wood fiber failure mode was hardly observed in the tensile tests. The PP matrix showed evidence of interfacial isolation between the TMP fiber and PP. However, improved interfacial adhesion in the case of

MA treated laminates also evidenced apparent TMP fiber and PP matrix failure. TMP fibers failed in a brittle mode, and the PP matrix remained on the TMP fiber surface. The PP failure also indicates that the properties of PP may have changed due to the MA treatment on the TMP fiber surface. The improved interfacial interaction is due to the coupling agent acting as a true bridge polymer at the interface and led to additional fiber interlocking from the melting and flowing characteristics of the thermoplastics on the surface of TMP fibers.

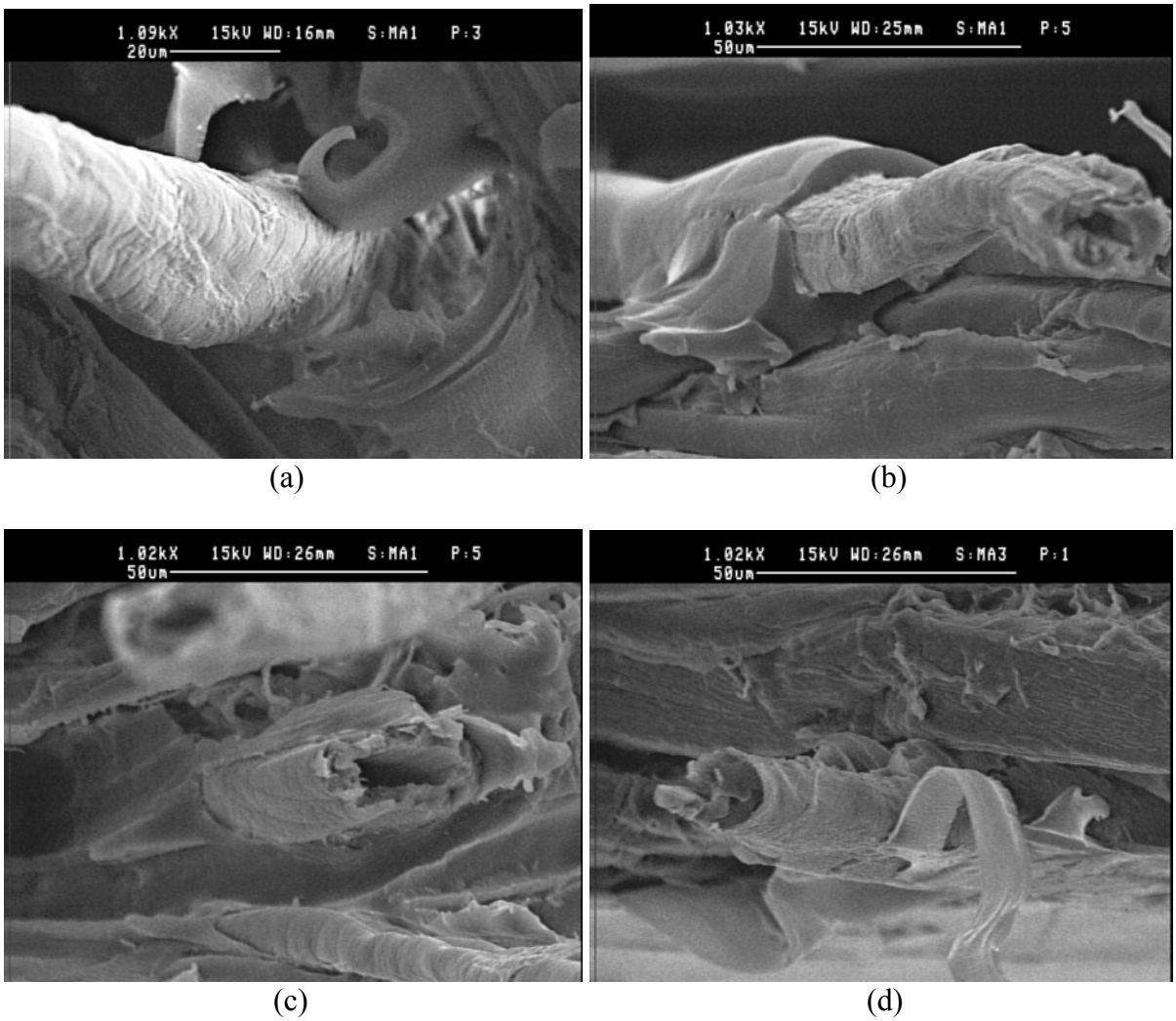

Figure 5.6. Scanning electron microscopy micrographs of fracture surfaces of wood fiber handsheet and polypropylene laminates; maleic anhydride grafted thermomechanical pulp fiber handsheets. (a) Untreated, (b) MA:BPO = 1:1, (c) MA:BPO = 2:1, and (d) MA:BPO = 4:1.

CHAPTER 6

MALEATED POLYPROPYLENE FILM AND WOOD FIBER HANDSHEET LAMINATES

6.1. Introduction

Anhydride-based compatibilizers at the hydrophilic wood fiber and hydrophobic PP interface are of growing interest to increase interfacial adhesion. Anhydride compounds can react with wood fibers to form ester linkages with the hydroxyl groups of the wood fiber, thus providing the fiber surfaces a certain degree of hydrophobicity, depending on the composition of the anhydrides (Oever and Peijs 1998, Simonsen et al. 1998, Dale Ellis and O'Dell 1999). Among anhydride coupling agents, maleic anhydride (MA) as a copolymer has improved the mechanical properties of wood fiber-thermoplastic composites (WPC) (Maldas and Kokta 1991a, Lia et al. 2001, Machadoa et al. 2001, Keener et al. 2004). Considerable research has been directed toward promoting interfacial interactions between polymer matrixes and wood fiber surfaces (Bledzki et al. 1998, Sain and Kokta 1994, Felix and Gatenholm 1993, Maldas and Kokta 1993, Gauthier et al 1995, Lu et al. 2004). However, the treatment effects on the interfacial strength properties of WPC varied with the different fiber sources and polymer types.

The use of MA to graft the surface of wood fiber and polyolefins was explored as a technique to improve the physicochemical properties of thermoplastics (polypropylene; PP, polyethylene; PE, polystyrene; PS and polyvinylchloride; PVC) (Trivedi and Culbertson 1982, Bratawinjaja and Gitopadmoyo 1989). The grafting of MA on plastics can be carried out under a variety of conditions. The most frequently used technique for WPC is free radical initiation reactions (Minisini and Tsobnang 2005). When the MA reacts with the thermoplastic polymers,

the C=C bond may break and new C-C bond or bonds are formed between the MA residue and the backbone of the plastics. The reaction scheme is shown in Figure 1.2.

The concentration of MA and the initiators type and amount have a great influence on the efficiency of MA-polymer treatment of PP and fibers. Initiators, such as benzoyl peroxide (BPO; Maldas and Kokta 1990a, Lu et al. 1998, Lu et al. 2004), dicumyl peroxide (DCP; Collier et al. 1996), tert-butyl peroxy benzonate (TBPB; Takase and Shiraishi 1989), have been used as an initiator for MA grafting on the polymer backbone. The DCP was more effective than BPO to treat wood fibers with MA-polymer (PS or HDPE) (Maldas and Kokta 1991a). The properties improved along with the rise in concentration of MA and initiators up to 3% MA and 0.5% initiators, and then decreased at higher concentrations (Maldas and Kokta 1991a, b). The extent of improvement also depended on the type of polymer matrixes.

The mechanical properties of these plastics generally decrease after MA grafting (Takase and Shiraishi 1989, Collier et al. 1996) due to the chain scission during the maleation process that results in decreased average molecular weight (Mohanakrishnan et al. 1993), the presence of non-reacting MA (Maldas and Kokta 1990a), and the decrease in crystallization degree in the case of crystalizable polymers. However, the mechanical properties of composites with the modified plastics were enhanced as the matrix or part of the matrix, owing to the improvement of interfacial adhesion (Fernanda et al. 1997, Caulfield et al. 1999). Tensile strength of WPC was improved 20-30% over the untreated PP-based composites (Mohannakrishnan et al. 1993). However, tensile modulus decreased 20-30%. Further increase in mechanical properties of WPC was also obtained using MA modified PP (Takase and Shiraishi 1989).

The MA grafted on the backbone of synthetic polymers such as PE and PP has been proven to form either covalent ester or hydrogen bonds when reacting with hydroxyl groups at

the cellulose surface. The presence of anhydride groups was confirmed by IR spectrum. The formation of ester bonds between cellulose backbone and MA grafted polyolefins has been confirmed by fourier-transform infrared (FTIR) spectroscopy with the appearance or increase in the intensity of the absorption bands near 1720 cm^{-1}, which is characteristic of ester bonds (Clemons et al.1992, Kazayawoko et al. 1997a, Pandey 1999, Chun et al.2002). Incompatibility between the wood fiber surface and PP interface resulted in lower interfacial strength. Interfacial failure occurred as the PP matrix began to draw, which produced voids and cracks (Beshay and Hoa 1990, Angles et al. 1999, Alexy et al. 2000, Amash and Zugenmaier 2000, Bledzki et al. 2005).

In light of the aforementioned research, this study was conducted to elucidate the interfacial interaction between maleated PP film and wood fiber handsheet laminates. Using TMP fibers, the effect of MA concentrations and grafted levels of MA and BPO on PP film on fracture characteristics, thermal behavior, and mechanical properties of TMP fiber handsheet and PP film laminates (TPL) was studied. Quantitative techniques were developed for measuring the effect of interfacial bonding by microscopic examination of tensile tests of the laminates.

6.2. Materials and Methods

6.2.1. Materials

Thermomechanical pulp (TMP) fibers used were loblolly pine (*Pinus taeda* L.) chips which were converted into coarse TMP at the Bio Composites center, University of Wales, Bangor, Wales, UK at a steam pressure of 8 bars. Some of the TMP fibers were used for previous experiments (Lee 2002). The moisture content for the fibers used for this study was 8.2%. Maleic anhydride (Huntman Chemical Co., Chesterfield, MO) used as a modifying agent had a purity of > 99 % and a melting point of 52ºC. Benzoyl peroxide (Benox® A-80; NORAC,

Inc., Azusa, CA), as an initiate for MA reaction on the PP film surface, contained 20% water and 5.1% active oxygen. Toluene (Fisher Scientific Inc., Pittsburgh, PA) was used as a reagent. A PP film (Plastic Suppliers, Inc., Columbus, OH) was used to make TPL.

6.2.2. Polypropylene Film Modification and Laminate Fabrication

The PP film modification with MA was accomplished by a soaking method involving the 7 × 12 inch^2 film sheets in a MA/BPO solution diluted in toluene. Treatment solutions were formulated based on the weight fraction of MA/BPO in toluene. Toluene (1L) was heated to 100 °C and 12.5, 25, and 50 grams of MA and 12.5 grams BPO were dilution ratios. PP films were soaked in 2L of solution for 5 minutes. The treated PP films removed from the solution and dried at room temperature.

A total of 22 handsheets measuring 12 × 12 inch^2 were made with 10 grams (OD wt.) of TMP fibers and press-dried at 60 °C with 50 psi pressure. Handsheets were cut into 6 × 7 inches of 34 sheets and stored in a vacuum dessicator. Thus, two experiment designs of 2 (dry conditions) × 3 (film locations) × 4 (replications) to characterize the effect of fibers in the web and 3 (MA treatment conditions) × 3 (replications) for the ratio effect were used. The TPL (50/50% weight fraction of TMP/PP) were pressed between hot plates at 100 psi pressures for three minutes and 400 ºF to reach the flow point of the PP film. Tensile strengths were measured for pressing conditions which were measured for pressing conditions of PP film on bothsides, the top side only and the bottom side only.

6.2.3. Tensile Strength Properties and Image Analysis

Two hundred-sixteen dog-bone tensile samples were cut with nominal dimension of 5 × 0.8 × 0.01-inch^3 with a neck width of 0.35 inch. Tensile properties were tested using an Instron 4465 mechanical testing machine at a crosshead speed of 0.05in min^{-1} according to ASTM

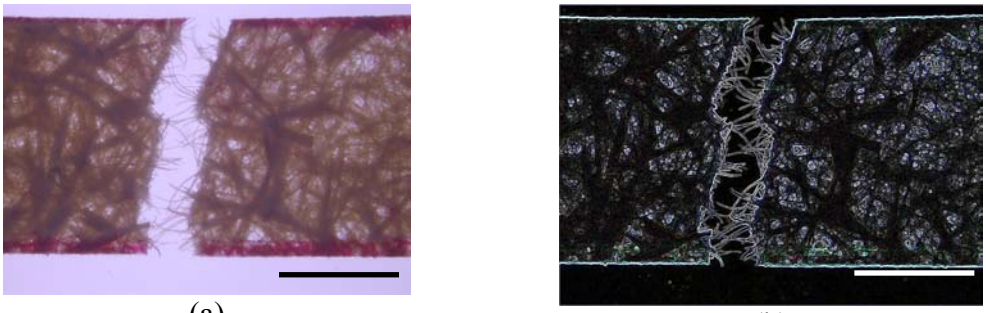

(a) (b)

Figure 6.1. Photomicrographs of failure sections from the tensile strength test (a) Stage I. Original fracture image, and (b) Stage II. Image transformation. (Scale bar on each image represents 5 mm).

D638-03 (ASTM 2003). At least 7 specimens were tested for each TPL and the means and the standard deviations were calculated. Failure sections of the dog-bone samples were viewed using light microscopy to generate failure section images using a Spot RT camera. The images were further processed using Image Pro Plus software (V 4.5) with a simple intensity range to count the number of TMP fibers at the fracture surface of the tensile test samples. In short, the data collection process included (1) generating original fracture images, (2) transforming images using "Edge Finder Function" to make the edges clear, and (3) collecting the number of fibers of exposed fibers (Figure 6.1).

6.2.4. Analysis for Grafting Effects

A confirmation of MA interaction between the TMP fiber and MA grafted PP matrix was determined by use of the FTIR (NEXUS^{TM} 670 FTIR E.S.P.; Thermo Nicolet). The FTIR is equipped with "Smart Golden Gate" and mid- range (4000- 650cm^{-1}) capabilities. The data acquisition software was OMNIC 5.2. Treated PP films were scanned at the mid-IR range to study the multi-functional monomer retention on the surface of PP films. Most of the grafted MA on the films showed a cyclic form with a peak from 1690 to 1760 cm^{-1}, which should be assigned

to the carboxylic acid of cyclic anhydride with broad band width. The benzoyl peroxide peak was expected to appear from 675 to 760 cm^{-1}.

Thermal characteristics of the surface-polymer interphase were evaluated using a DSC (Perkin-Elmer DSC 7) system to confirm PP melt flow and crystallization parameters in the presence of different levels of MA treatment. Thermal characteristics of T_o and T_c were determined by exothermic curves during the polymer crystallization process from the melt, based on ASTM E793-01 and E794-01 (ASTM 2001). A heating rate of 5 °C min^{-1}. from -30 °C to 200 °C and a cooling rate of 5 °C min^{-1}. from 200 °C to 50 °C for DSC samples were used for this study. The X_C (Eq. 6.1) with levels of MA treatment on PP surface and TMP fiber combinations was also calculated with the following equation.

$$X_C = \left(\frac{\Delta H_f}{w \Delta H_f^0} \right) \times 100 \tag{6.1}$$

Where: X_c = % of crystallinity
ΔH_f = Heat of fusion from DSC
ΔH_f^0 = 100% Crystalline PP
w = Mass fraction of PP

Morphological observations on the fracture surfaces of the tensile test specimens were sputtered coated with gold and observed using a scanning electron microscope (SEM: Hitachi S-3600N) at 15 kV and 1,000x. The fracture surfaces of the TMP fiber handsheets and MA grafted PP film laminates were studied to confirm the MA treatment effect at the TMP fiber and MA grafted PP interface. Mounted fracture sections were coated with an approximately 15-nm thin gold layer using an ion sputter (Technics Hummer V) apparatus.

6.3 Results and Remarks

6.3.1. Number of Fibers at Fracture Surface

Figure 6.2 shows tensile strength of TPL as a function of the number of fibers exposed at the fracture surface of the tensile test specimens for each experimental condition of PP film loading and handsheet drying. The PP film loading conditions were on the top, bottom, and both sides of the TMP fiber handsheets with its 50% weight. The two handsheet drying conditions were air dried at 22 °C and oven dried at 60 °C with 50 psi press loading. The laminates were fabricated using treated PP film sheets with a MA and BPO ratio of 2:1. The PP film sheets loaded on both sides provided an uniform and greater volume of PP melt flow into the TMP handsheets compared to the other two pressing conditions. The uniform melt flow resulted in higher correlation between the number of fibers in the web and tensile strength. This result was observed for both handsheet drying conditions. The R^2 values for loading on both sides were 0.95 for air-dry and 0.94 from oven-dry. This result shows that the greater volume of melt flow characteristics of the thermoplastic matrix resulted in a better fiber reinforced composite materials than the other two hot pressing conditions. Further, it shows the effect of gravity (PP film on the top side) improves the melt flow of PP. Additionally, the results show that the technique of counting the numbers of TMP fibers at the tension failure provides a sensitive measure of wood fiber-PP interfacial bonding.

6.3.2. Effects of the Maleic Anhydride and Benzoyl Peroxide Ratios

MA and BPO ratios on tensile strength properties of TMP fiber handsheet and MA treated PP film laminates are shown in Figure 6.3. It is obvious that MA is generally an effective modifier in increasing the tensile strength regardless of the levels of MA and BPO ratios used. The highest mean tensile strengths obtained from the PP film treated with the 2:1 ratio, which

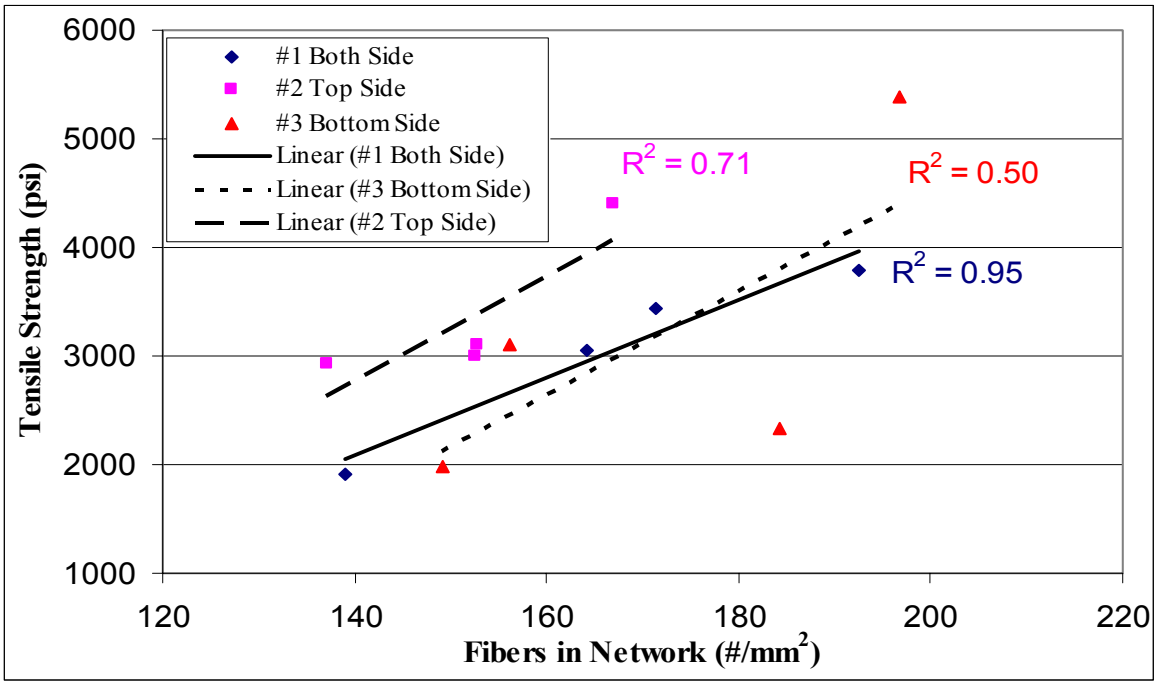

(a)

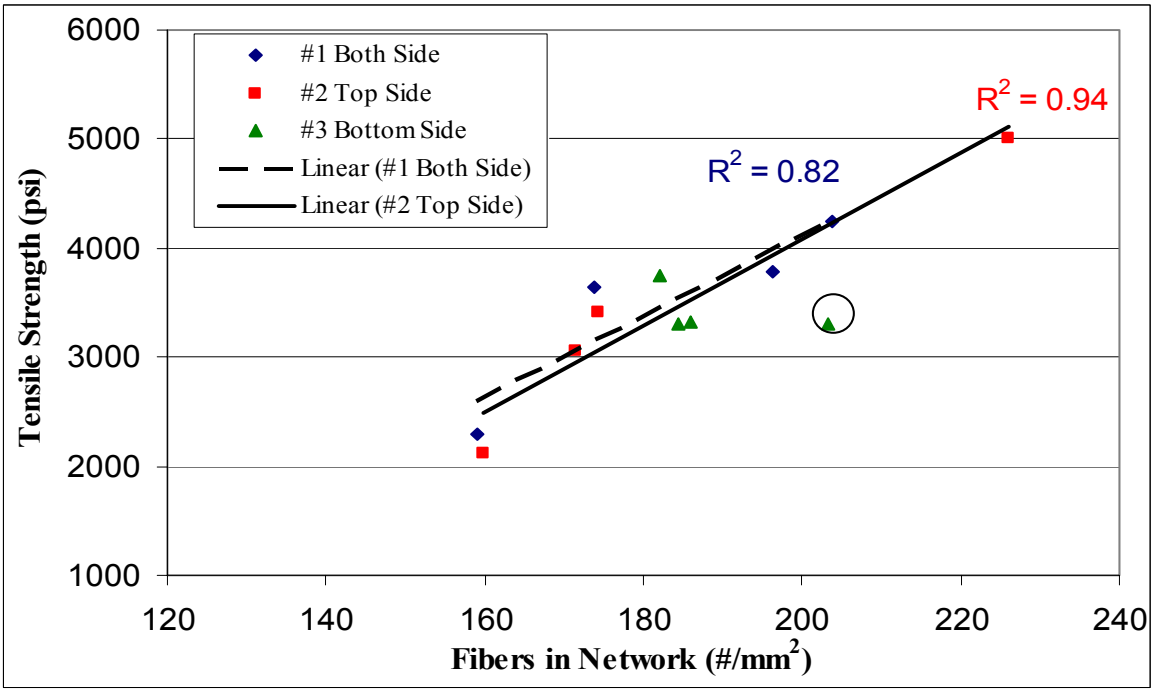

(b)

Figure 6.2. Tensile strength of laminates as a function of the number of fibers shown at the tension break with two handsheet press drying conditions of (a) air-dry at 22 °C and (b) oven-dry at 60 °C. (Each data point represents the average of seven tensile specimens).

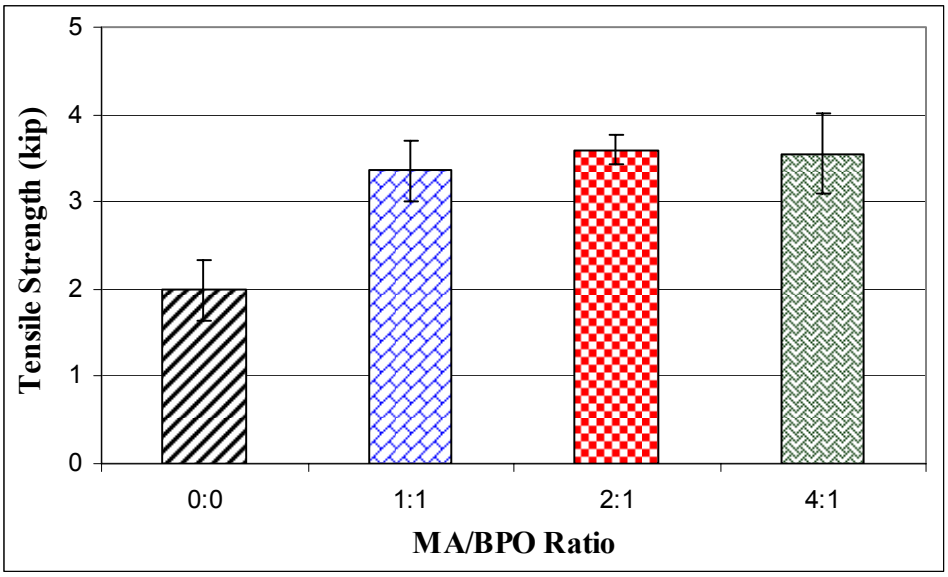

Figure 6.3. Tensile strength properties of maleic anhydride grafted polypropylene film laminated with thermomechanical pulp fiber handsheets. (The error bars represent one standard deviation).

was 76 % greater than the untreated laminates. It is well known that addition of MA to wood fiber and PP composites increases the tensile properties of the composites (Sain et al. 1994, Wua et al. 2001a, b, Thwe and Liao 2002). Although all treatments were significantly better than no treatment, there was no statistically significant difference among the tensile test samples of the MA loadings on the tensile strength of TPL witch proved that counting the number of fibers at the tensile break is a better method of measuring the effect of MA grafting at the TMP fiber and PP interface.

6.3.3. Fourier-Transform Infrared Spectroscopy (FTIR)

Absorbance of FTIR spectra from the MA modified PP film with BPO as a catalyzer is shown in Figure 6.4. In the cases of the MA grafted PP, absorption bands at 1714 and 702 cm^{-1} were observed, which can be assigned to the absorption of the carboxylic acid (C=O) of anhydride in a cyclic form. The absorptions from 2850 to 2970 cm^{-1} and from 1350 to 1480 cm^{-1} represent the characteristic absorption of the PP skeleton. The absorption band at 702 cm^{-1} also

indicates evidence of BPO on the PP film. Therefore, the absorption bands at 1714 and 702 cm^{-1} were assigned MA loading on the wood fiber and PP film. When using MA, BPO, and toluene to treat PP film, the MA and BPO ratios of two-to-one appeared to be an optimum ratio with an evidence of a strong, sharp, and well-defined absorption band near 1714 cm^{-1} from the digital subtraction spectra of the treated and untreated PP films. The number of anhydride groups reacted with PP may differ greatly due to the difference in chemical ratios.

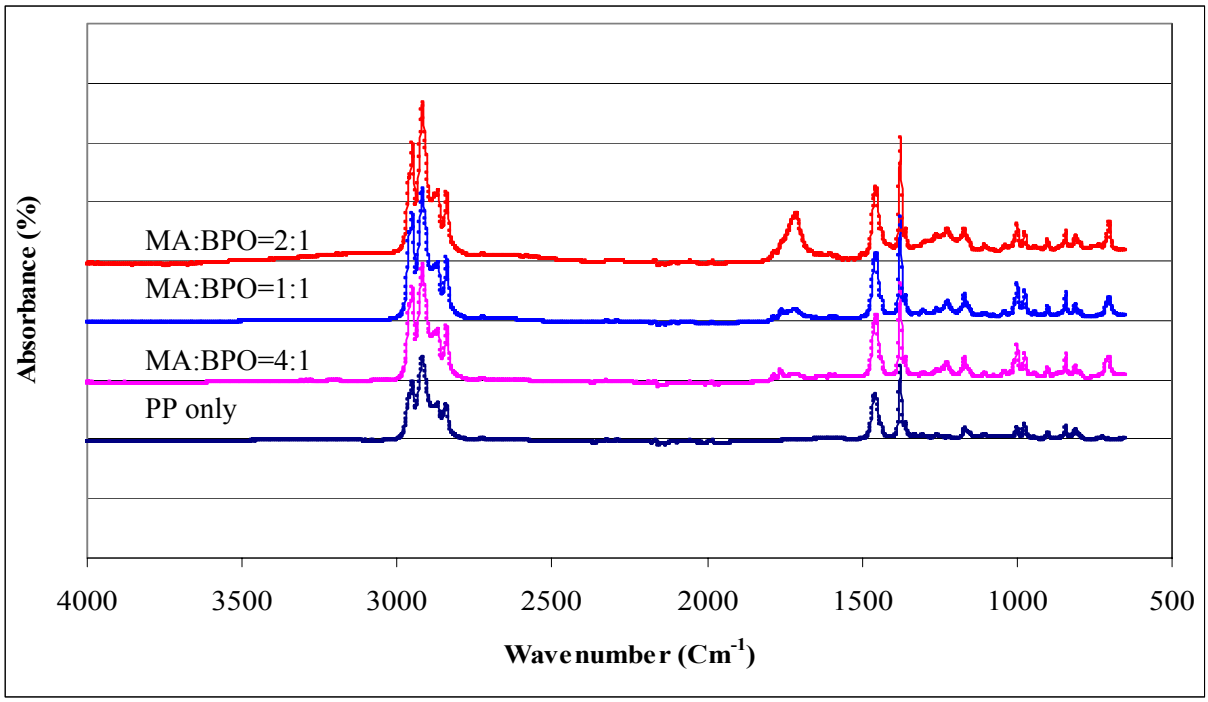

Figure 6.4. Absorbance of fourier-transform infrared spectroscopy spectra from maleic anhydride modified polypropylene film with benzoyl peroxide as a catalyzer. (MA=Maleic anhydride, BPO=Benzoyl peroxide).

6.3.4. Thermal Analysis

Table 6.1 shows the treatment effect of four levels of MA and BPO on the thermal behavior of MA treated PP film surfaces. The thermodynamic behaviors of TMP fiber handsheet and MA treated PP film laminates on glass transition (T_g), onset (T_O), heat flow (ΔH), melting

and crystallization peaks (T_m, T_C) and crystallinity (X_C) from the endothermic and exothermic curve are presented. The thermal quantities of T_g, T_O, and T_m from the endothermic curve generally decreased with increased MA and BPO ratios. The ratio 4:1 showed an initial increase although the thermal quantity was lower than untreated PP films. In contrast, the quantities of T_O and T_m decreased in the endothermic curve but increased in the exothermic curve. This result indicates that introducing MA into the PP matrix may alter the PP nucleation ability and lead to a decrease in the thermal quantities. The ΔH and X_C of the treated PP films also decreased with MA treatment ratios of 1:1 and 4:1. The table shows that the ratio 2:1 may be the optimum treatment condition used in this experiment, but no definite conclusions can be drawn.

Table 6.1. Thermodynamic quantities of maleic anhydride treated polypropylene films laminated with wood fiber handsheets.

MA/BPO Ratio	Density	Endothermic Curve				Exothermic Curve			
		T_g	T_O	T_m	ΔH	T_O	T_C	ΔH	X_C
	(g/cm^3)	(°C)	(°C)	(°C)	(J/g)	(°C)	(°C)	(J/g)	(%)
0:0	0.89	-21.5	153	162	62.4	121	117	103.5	50.0
1:1	0.88	-22.1	150	157	48.6	130	122	91.7	44.3
2:1	0.76	-22.5	150	157	64.4	123	118	106.1	51.2
4:1	0.79	-22.3	152	160	57.4	126	120	93.1	44.9

Note: MA=Maleic anhydride, BPO=Benzoyl peroxide.

6.3.5. Fracture Surface

Fracture mode differences from tensile samples of TMP fiber handsheets and MA treated PP film laminates are presented in Figure 6.5. The figure compares the untreated and MA and BPO (2:1) treated dog-bone samples. Untreated samples showed that the TMP fiber pulled out from the PP matrix due to the weak interfacial interaction at the TMP fiber and PP interface. This result led to poor tensile strength performance. However, the fibers in the treated samples

were broken and fewer fibers were pulled out from the PP matrix. The broken fibers indicate that there was a strong interaction at the TMP fiber and PP interface resulting from MA loading on the PP film surface. There was no difference found in the fracture mode of the modified laminates from the images generated from an edge finder function of the image analysis system.

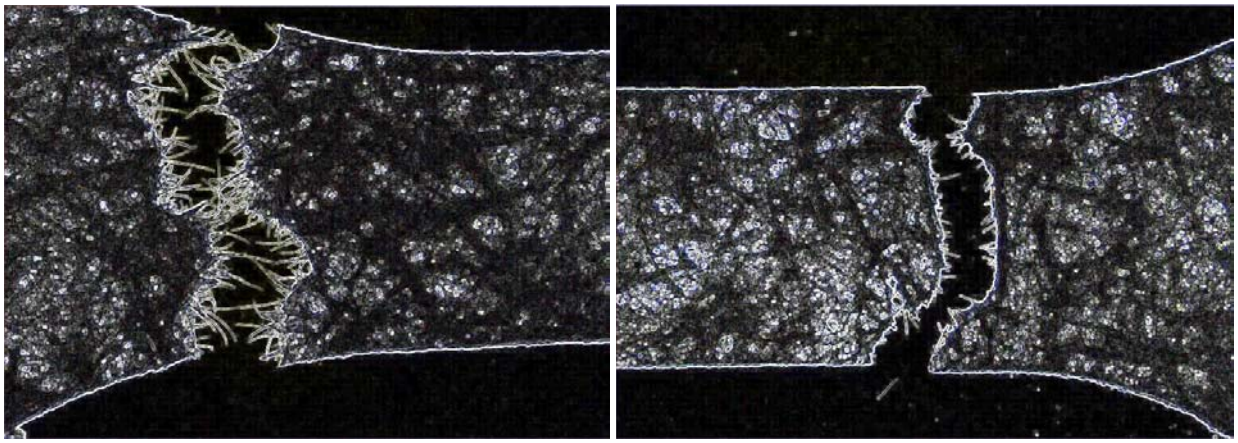

(a) (b)

Figure 6.5. Fracture surface from tensile strength test of thermomechanical pulp fiber handsheet and maleic anhydride treated polypropylene film laminates. (a) Untreated and (b) MA:BPO = 2:1.

SEM micrographs of the fracture surfaces of TMP fiber handsheet and MA treated PP film laminates showed the effectiveness of MA loading on the PP film surface (Figure 6.6). The failure mode of MA loading levels under tension load slightly differed from each other. Untreated samples showed evidence of interfacial isolation between TMP fiber and the PP matrix. It was also observed that the fibers pulled out without surface damage and the samples failed in a brittle wood fiber failure mode due to the possible thermal degradation of the cellulose in the fibers. However, improved interfacial adhesion of MA treated PP laminates was observed in the micrographs. The PP matrix held the TMP fiber surface without interfacial failure. The failure of both TMP fiber and the PP matrix was in a brittle mode due to the improved interfacial interaction at the TMP fiber and PP interface. Therefore, the interfacial bond between the PP

and TMP fiber surface was strong and resulted in fracture of the TMP fibers rather than being pulled out of the matrix. Additionally, it should be noted that the PP melt flow into the lumen structure of the TMP fibers was observed in only a few specimens.

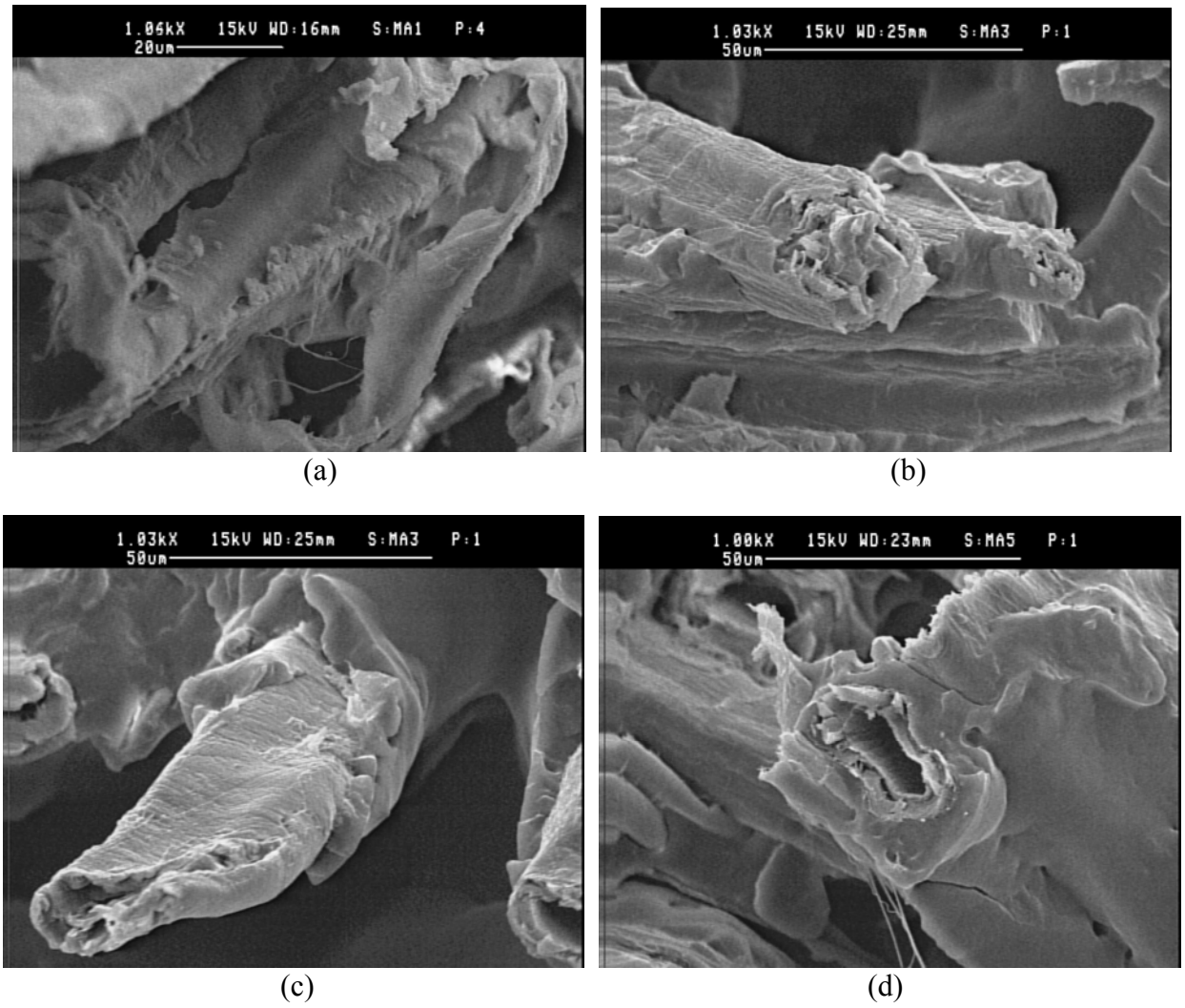

Figure 6.6. Scanning electron microscopy micrographs of fracture surfaces of wood fiber handsheet and polypropylene laminates; polypropylene film grafted with maleic anhydride. (a) Untreated, (b) MA:BPO = 1:1, (c) MA:BPO = 2:1, and (d) MA:BPO = 4:1.

CHAPTER 7

THERMOSETS AS COMPATIBILIZERS AT THE POLYPROPYLENE FILM AND THERMOMECHANICAL PULP FIBER INTERFACE

7.1. Introduction

Thermosets have a wide range of applications for the bio-based composites with extensive compatibility with hydrophilic substrates. Due to the lack of polar groups in the polypropylene (PP), thermoset compatibility to thermoplastics resins generally is very poor and has resulted in few applications in the field of wood fiber-plastic composites (WPC). Yet the selective addition of thermosets to wood and wood fiber can yield a wide variation in the mechanical and physical properties of WPC regardless of limitations due to the inherent incompatibility at the interface and differences in the thermal histories (Bliznakov et al. 2000, Marcovich et al. 2001). Therefore, most investigations have focused on the thermoset application at the wood fiber and thermoplastic interface (Frontini et al. 1993, Park et al. 1998).

Relatively few studies have been made to combine PP with thermosets such as UF (urea formaldehyde) (Khan and Idriss Ali 1992, Bliznakov et al. 2000), PF (phenol formaldehyde) (Chiang et al. 1994, Larson Børve et al. 2000), epoxy resin (Sain and Kokta 1993, Colombini et al.1999), polyester (Marcovich et al. 2001), and isocyanate (Parida et al. 1995, Neff et al. 1998, Pittman Jr. et al. 2000, Chiou and Schoen 2002). The thermosets can be used as compatibilizers to coat the surface of wood fibers and increase interfacial adhesion at the wood fiber and polyolefin interphase, but they may be less effective to enhance WPC properties (Queiroz and Pinho 2002). However, the thermosets combined with heat conditioning and ionomer treatment have been shown to enhance interfacial strength properties due to the increased interaction

between the two materials (Spirkova et al. 1993, Chuang and Maciel 1994, Teo et al. 1997, Dale-Ellis and O'Dell 1999, Sakai et al. 1999).

The extrusion originally was used to produce WPC in a continuous process from a material inlet to the cooling system (Clemons 2002). When the thermosets are applied into the process, the process faces various problems due to the cure of the thermosets before the thermoplastic reaches its melting point. However, it is proposed that this problem does virtually not exist when wood fiber handsheets are laminated with PP film. The thermoset loading can also add strength to the handsheet and improve tensile strength properties of TMP fiber handsheets and PP film laminates (TPL). In this study, investigation focused on the loading effects of thermosets such as UF and PF on the tensile strength properties of TPL as well as factors related to handsheet preparation and evaluation technologies for quantizing the improvements in strength properties for the laminates.

7.2 Materials and Methods

7.2.1. Materials

Thermomechanical pulp (TMP) fibers of loblolly pine (*Pinus taeda* L.) were processed at 8 bar pressure and contained 8.2% moisture content. A PP film (Plastic Suppliers, Inc., Columbus, OH) was used for TPL. Two thermosets - urea formaldehyde (UF; Dynea Inc., Chembond® YTT-063-02, 60% solid content) and phenol formaldehyde (PF: Dynea 13B410, 100 cps, Sp. Gr.: 1.202, 52% solid content)- were used as compatibilizers.

7.2.2. Experimental

A total of 27 handsheets was formed in 12 x 12 inch with 10 grams (OD wt.) TMP fibers and dried at 60 °C with 50 psi pressure for 72 hours. Handsheets were cut into 5 x 6 inch and stored in a vacuum dessicator. UF and PF were sprayed on the surface of the TMP fiber

handsheets at three weight fraction levels of 1%, 3%, and 5%. The PF or UF loaded TPL (50/50% weight fraction) were pressed at 100 psi for three minutes with 350 and 400 ºF.

Tensile strength properties were tested using an Instron 4465 mechanical testing machine at a crosshead speed of 0.05 in. min.$^{-1}$ according to ASTM D638-03 (ASTM 2003). Two hundred-sixteen dog-bone tensile samples were cut in a nominal dimension of 5 × 0.8 × 0.01-inch with a neck width of 0.35 inch. At least 21 specimens were tested for each set of samples and the mean values as well as the standard deviations were calculated.

A DSC (Perkin-Elmer DSC 7) system was used to evaluate and confirm thermal characteristics of UF and PF-loaded TPL. Thermal characteristics of glass transition (T_g), onset (T_{om} and T_{oc}), and peak temperature (T_m and T_c) were determined by exothermic and endothermic curves during the polymer melt and crystallization process based on ASTM E793-01 and E794-01 (ASTM 2001). Percentages of crystallinity ($X_C = \left(\frac{\Delta H_f}{w \Delta H_f^0} \right) \times 100$) with three levels of UF and PF loaded fiber combinations were used to calculate X_C. The ΔH_f is the heat of fusion from DSC and ΔH_f^0 (= 207.14 J g^{-1}) is 100% pure crystalline PP. The mass fraction of PP from the laminates is w. A heating rate of 5 °C min^{-1} from -30 °C to 200 °C and a cooling rate of 5 °C min^{-1} from 200 °C to 50 °C for DSC samples were applied for this study.

Morphological characteristics of the fracture surfaces of UF and PF loaded TPL were observed by using scanning electron microscopy (SEM; S-3600N) to confirm the loading effect at the TMP fiber and PP interface. Mounted laminates were coated with an approximately 15-nanometer thin gold layer using an ion sputter apparatus (Technics Hummer V). Images were generated at 15 kV and 1,000x.

7.3. Results and Discussion

7.3.1. Tensile Strength Properties

The effect of the method used for thermoset loading and the two pressing conditions on the tensile strength of PF loaded TPL is shown in Figure 7.1. Phenol formaldehyde resin was loaded on the TMP fiber surface in two ways in the wet and dry fiber conditions. Five percent PF (solid basis) was added to the TMP fiber slurry for the wet loading. For the dry loading, an equal amount of PF was sprayed on the surface of TMP fiber handsheets. In general, the dry condition increased the strength properties regardless of the pressing temperatures of 350 ºF for PF resin and 400 ºF for PP melt flow. PF sprayed on the dry handsheet and pressed at 400 ºF resulted in the highest tensile strength properties of laminates due to PP melt flow on the fiber surface. The tensile strength was increased by 63% over the control samples. This result clearly related to the penetration of low-molecular weight fractions of the PF resin into the wood fiber structure as well as to the gross capillary openings in the fiber mat, leaving less PF on the surface than was sprayed on the dried surface.

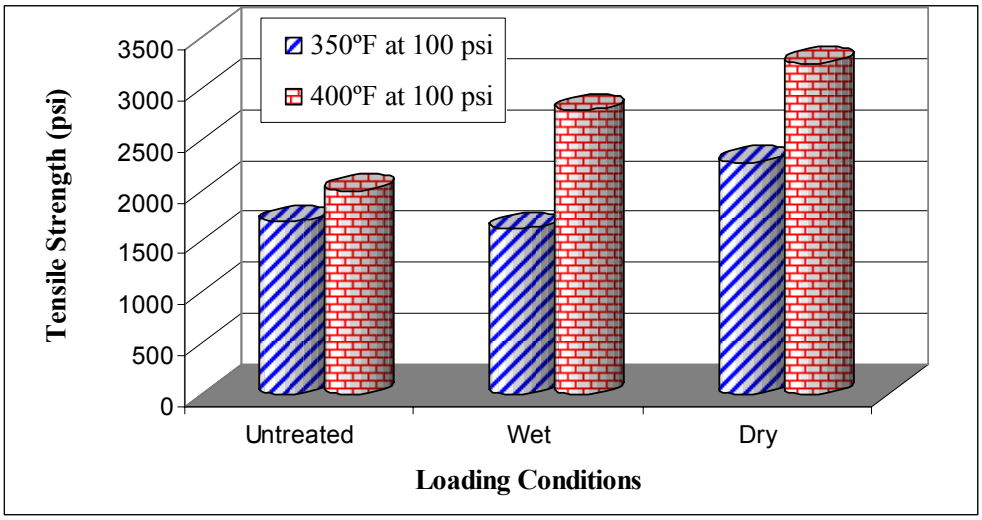

Figure 7.1. Tensile strength of phenol-formaldehyde resin as a compatibilizer at the thermomechanical pulp fiber and polypropylene interface as a function of phenol-formaldehyde loading conditions and pressing temperatures at 100 psi.

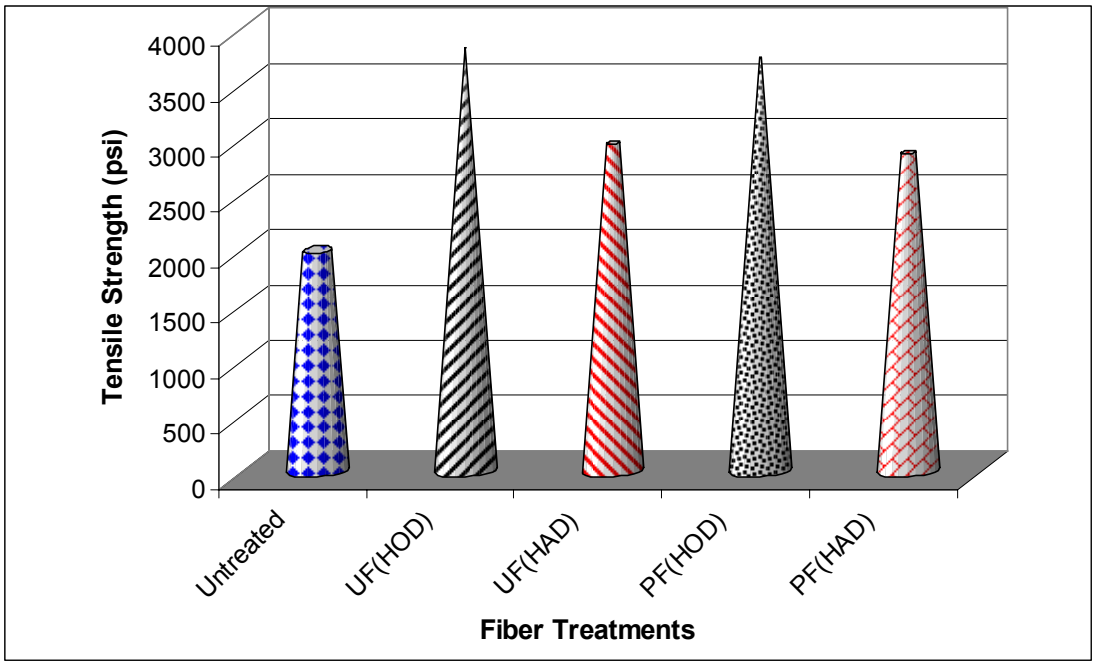

Figure 7.2. Preconditioning effect of handsheets on the tensile strength of laminates with sprayed thermosets as compatibilizers. UF=Urea-formaldehyde, PF= Phenol-formaldehyde, HOD=Handsheet with oven-dry, and HAD=Handsheet with air-dry.

The handsheet drying conditions also influenced the strength properties of laminates (Figure 7.2). Applying the thermoset on the surface of TMP fiber handsheets, tensile strength properties were increased 92% with UF and 88% with PF for the oven dried conditions over oven-dried untreated samples. In both cases, the result reflects the fact that the OD handsheets absorbed more water from the resins than did the air-dried specimens because the molecular weight and viscosity of UF which were relatively higher than PF. Thus, moisture content of the handsheet influenced the tensile strength of TPL, when the UF and PF resin used in this study were promoted to enhance interfacial bonding with PP film laminates.

Figure 7.3 shows tensile strength properties of laminates when 5% UF and PF were applied to one side of the TMP fiber handsheets or PP film as compatibilizers. The data collected from UF and PF applied on the PP film was compared with resins applied on the TMP fiber

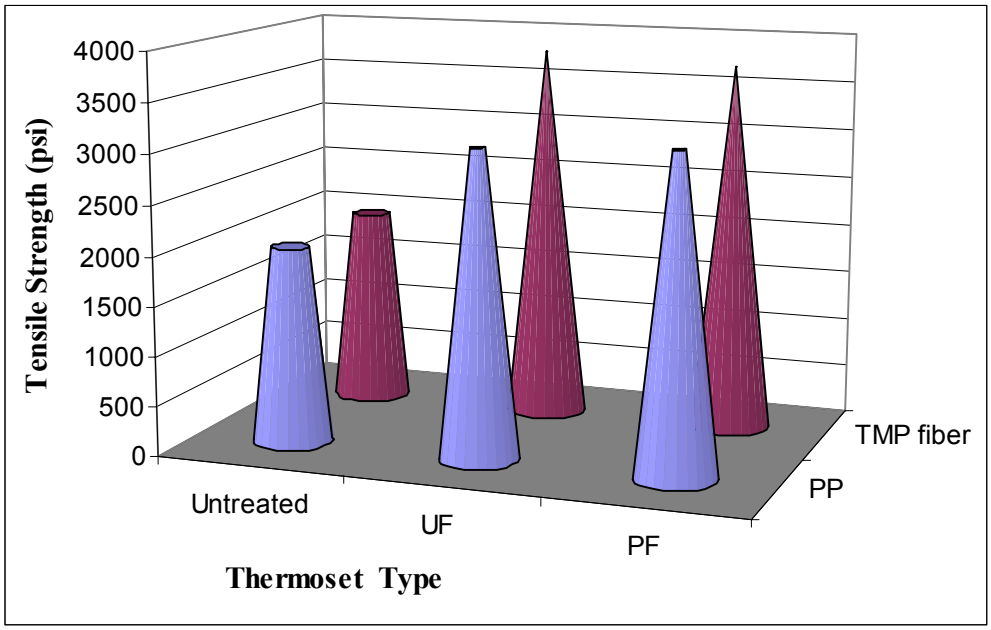

Figure 7.3. The effect on tensile strength of 5% thermosets when applied on a single side of thermomechanical pulp fiber handsheets or polypropylene film. UF=Urea-formaldehyde and PF=Phenol-formaldehyde.

handsheet. Confirming the results shown in Figure 7.2, the UF applied on the handsheet surfaces yielded slightly higher tensile strength properties than PF resin. The strength property enhancement (92% over untreated) significantly differed to the PF and UF applied on the PP film surface. But the tensile strength values between resin types were not statistically significant. This result indicates that the PF penetrated relatively faster into the handsheets than UF and provided a relatively lower holding strength to the TMP fiber handsheet (Hwang 1998). Thermoset loading on the handsheet surfaces provided strength enhancement for TLP. Furthermore, the tensile strength properties of UF and PF loaded laminates were significantly different compared with unloaded laminates.

The effect of the levels of application of UF and PF resin to TMP fiber handsheets is shown in Figure 7.4. It shows how three levels (1, 3, and 5%) of thermoset adhesives used as compatibilizers at the TMP fiber and PP interface improved tensile strength properties of the

laminates compared with the untreated specimens. The investigation showed that the strength properties of both resin types improved with increased resin content on the surface of the handsheets with the PF resin being more influenced by the treatment level than the UF. Thus, UF generally was more compatible at the TMP fiber and PP interface, confirming the observation made earlier. It is obvious that both thermosets positively influenced the tensile strength properties of TPL.

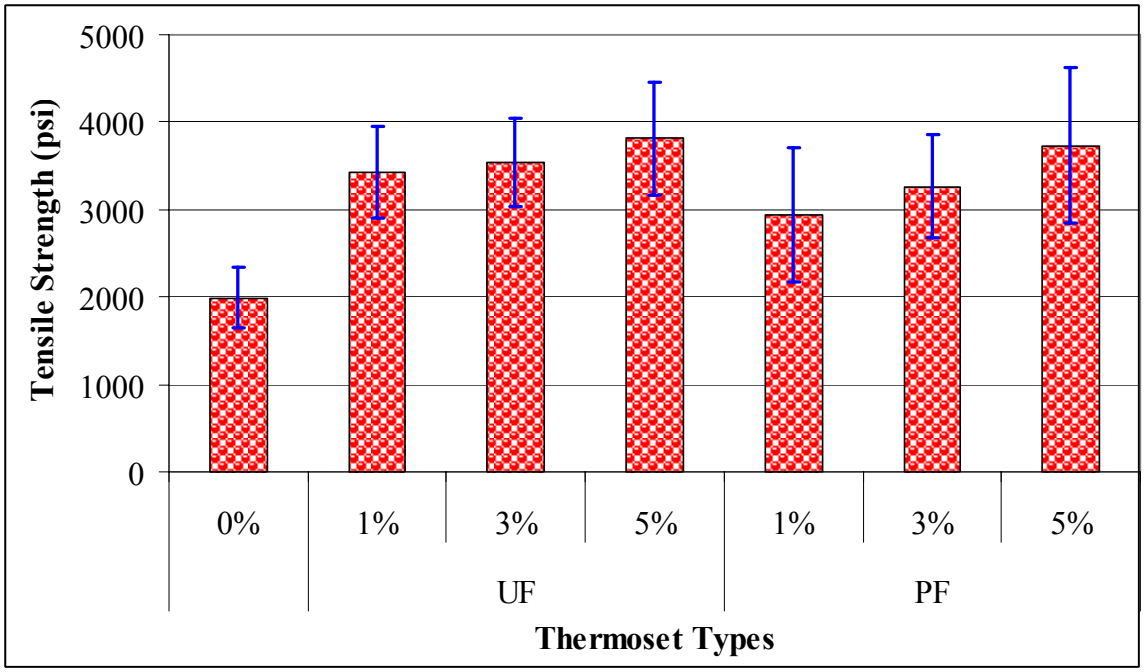

Figure 7.4. The effect of thermoset levels on tensile strength at the thermomechanical pulp fiber and polypropylene interface. UF=Urea-formaldehyde and PF=Phenol-formaldehyde. (The error bars represent one standard deviation).

7.3.2. Thermal Analysis

The thermodynamic quantities of the resins sprayed on the TMP fiber handsheets laminated with PP film are summarized in Table 7.1. Treatment effect at three levels of each thermoset resin on the thermal behavior was pronounced with percentages of PP crystallinity (X_C). The X_C of both resin types, generally, increased the tensile strength with the exception

Table 7.1. Thermodynamic quantities of urea-formaldehyde and phenol-formaldehyde sprayed on thermomechanical pulp fiber handsheets laminated with polypropylene film.

Resin Type		Density	Endothermic Curve				Exothermic Curve			
			T_g	T_O	T_m	ΔH	T_O	T_C	ΔH	X_C
		(g/cm^3)	(°C)	(°C)	(°C)	(J/g)	(°C)	(°C)	(J/g)	(%)
Control		0.89	-21.5	153	162	62.4	121	117	103	50.0
UF	1%	1.05	-23.8	154	163	61.8	122	118	106	51.2
	3%	1.09	-24.4	154	163	63.6	122	118	111	53.7
	5%	1.10	-24.4	154	163	64.4	122	118	108	52.1
PF	1%	1.01	-24.4	154	163	58.9	122	118	100	48.1
	3%	1.09	-24.5	154	163	60.7	122	118	110	53.1
	5%	1.08	-24.6	153	163	71.2	122	118	111	53.8

Note : UF=Urea-formaldehyde, PF=Phenol-formaldehyde.

of 1 % PF loading which had a high standard deviation (Figure 7.4). This result is conclusively confirmed by the heat flow (ΔH) from both the endothermic and exothermic curves. It shows that higher levels of resin application improved resin penetration into the fiber network. Thus, the reinforced fiber network obtained the inherent tensile properties of the fibers which improved the tensile strength properties of the laminates. The thermodynamic quantities of thermoset loaded laminates showed that onset (T_O), melting (T_m) and crystallization peaks (T_C) from the endothermic and exothermic curves were increased with additional thermoset put into the handsheets compared to pure PP. However, the glass transition (T_g) was decreased with an increased in resin content. This result indicates that the thermoset may provide interfacial interaction at the TMP fiber surface and PP matrix and yield increased PP crystallinity.

7.3.3. Fracture Surface

Figure 7.5 shows SEM micrographs of the fracture surface of TPL which were loaded with UF and PF. The fracture surface of unloaded laminates showed that TMP fibers were pulled out without surface damage and fiber failure and could not improve significantly in tensile strength of TPL. However, when thermosets were applied on the surfaces, fiber and PP bonding

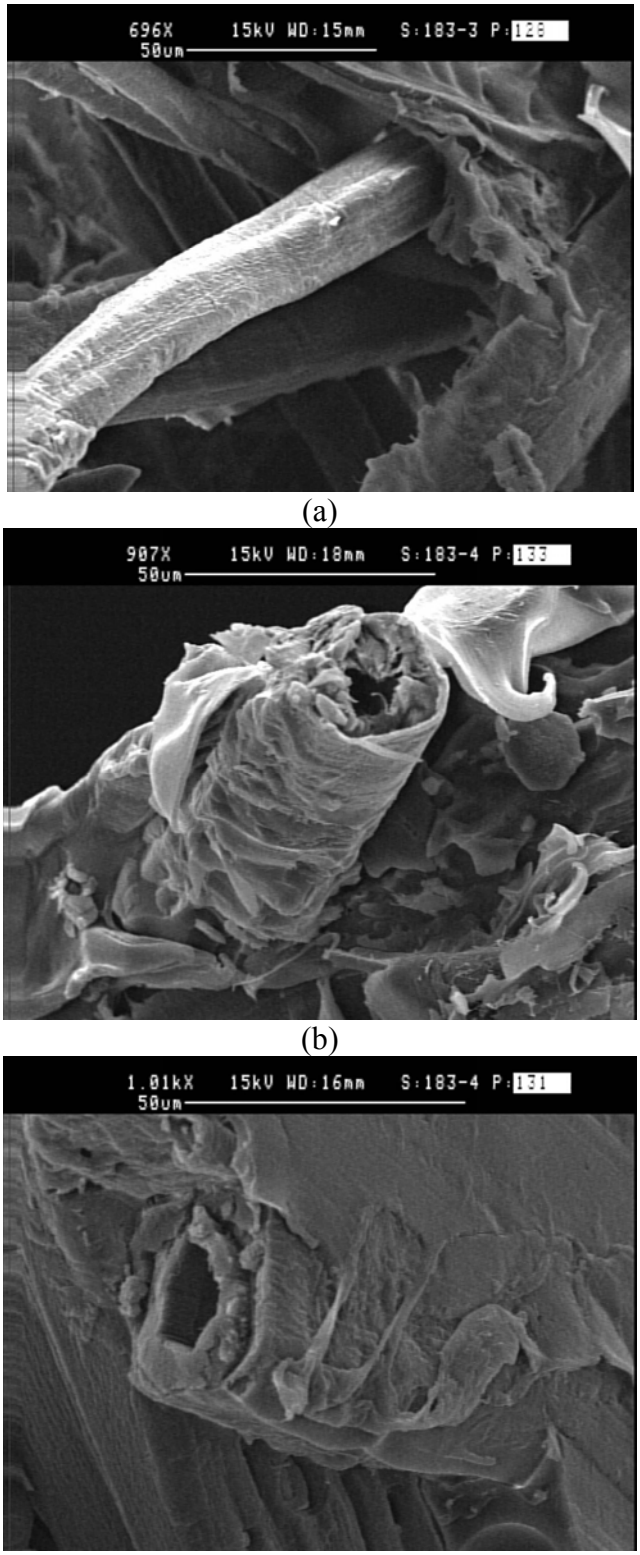

(a)

(b)

(C)

Figure 7.5. Scanning electron microscopy micrographs of fracture surfaces of phenol-formaldehyde (PF) and urea-formaldehyde (UF) sprayed on wood fiber handsheets and polypropylene laminates; (a) Untreated, (b) PF sprayed, and (c) UF sprayed.

improved as indicated by the brittle failure of the laminates. The PP matrix also covered fiber surfaces in both resin micrographs (Figure 7.5b and c). This result clearly shows that the thermoset adhesive provided interaction at the fiber surface and PP interface as well as added handsheet strength. Additionally, there were slight differences on the PP failure between applied resins. The PF loading micrograph (Figure 7.5b) showed that PP failure was mixed with brittle and stretching modes while only a brittle mode was represented with UF loaded surfaces (Figure 7.5c).

CHAPTER 8

HETEROGENEOUS NUCLEATION OF A SEMICRYSTALLINE POLYMER ON THE SURFACE OF WOOD FIBERS

8.1. Introduction

The occurrence of an extended source of nuclei confined on the wood fiber surface is known as crystallization. Various aspects of transcrystallinity have been examined on the mechanical properties of fiber-reinforced semicrystalline polymer composites, which were affected by transcrystallinity more than by crystal growth in the bulk (Sharples 1966, Chang 1977, Hsiao and Chen 1990, Quillin et al. 1993, Ebengou 1997, Lin and Du 1999). However, the current detailed understanding of the nucleation mechanism on the wood fiber surface remains uncertain and is insufficient to explain material functionality on the interfacial phenomenon of matrix materials.

Previous researchers have proposed concepts for increasing nucleation efficiency by modifying or controlling the polymer matrix and surface characteristics such as copolymers, additives, chemical composition, surface roughness, and surface free energy (Gray 1974, Liu et al. 1994, Lee 2002). However, increased surface free energy was unlikely to influence nucleation and affect the ability to induce transcrystallization on the fiber surface because the transcrystalline layer (TCL) was generated on the fiber surface regardless of whether or not the surface free energy was changed by the surface modification (Westerlind 1988, Hsiao and Chen 1990, Mahlberg et al. 1998). Wang and Hwang (1996a, b) found that a thicker TCL formed at higher temperatures, and larger residual stresses at the interface indicate an important role on the mechanical strength. Yin et al. (1999) found that the nucleation density with addition of MAPP up to 10 % was significantly increased, and a sufficient amount of nuclei on a single wood fiber

induced transcrystallization around the wood fiber. The nucleation ability of semicrystalline polymers was also related to chemical containment and topography of the fiber surface during the nucleation process of thermoplastic polymers (Wang and Harrison 1994). Furthermore, transcrystallization was easily induced on the exposed surfaces of the pure cellulose surfaces of cotton and purified wood fibers (Gray 1974).

In the acid-base theory, hydrogen bonding is the main form of bonding at a polymer interface with hydroxyl group rich surfaces. The theory is based upon interaction energies that are dependent on the acidity of the hydrogen donor and the hydrogen acceptor. Acid-base interactions cover any interaction that involves the sharing of an electron pair, particularly hydrogen bonding. In the case of cellulose, the acid-base interactions can be described as predominantly hydrogen bonding with surfaces dominated by hydroxyl groups. Interfacial energy and internal bond measurements indicate a strong correlation between the hydroxyl-rich (acid-base) interface and good adhesive properties (Jensen 1978, Pizzi 1994). Fowkes (1987) showed that the advantage of interfacial acid-base bonding is the predictable enhancement of interfacial interactions.

Attractive forces are usually insufficient for strong bonding when the molecules are small, but the attractive forces become stronger with larger molecules. The strong bonding forces exist between molecules when their distance of separation is closer than 9Å (Chung 1991). The classical theory of polymer nucleation is based on changes in the overall excess free energy (ΔG) between particles on a foreign body and semicrystalline matrix. Gibbs free energy is also influenced by intimate molecular contact, volume of the matrix, and size of the nucleus. However, most of the nucleation is heterogeneously induced by particles on the surface of

materials rather than by a spontaneously induction of nucleation known as homogeneous nucleation (Mullin 1993).

$$\Delta G = \Delta G_S + \Delta G_V = 4\pi r^2 \gamma + \frac{4}{3}\pi r^3 \Delta G_\upsilon \tag{8.1}$$

ΔG (Equation 8.1) is generally combined with two quantities of positive (Surface free energy; ΔG_S) and negative (Volume free energy; ΔG_V). In the Gibbs free energy equation, the γ_C is known as critical free energy (ΔG_{Crit}). Set $d\Delta G/dr = 0$ for the differential calculation of Eq. 8.1;

$$\frac{d\Delta G}{dr} = 8\pi r\gamma + 4\pi r^2 \Delta G_\upsilon = 0 \tag{8.2}$$

therefore, the radius of a critical nucleus is given by

$$r_c = \frac{-2\gamma}{\Delta G_\upsilon} = \frac{-2\gamma T^*}{\Delta H_f \Delta T} \tag{8.3}$$

where ΔG_υ is the volume free energy ($\Delta G_\upsilon = \frac{\Delta H_f \Delta T}{T^*}$), T^* is solid liquid equilibrium temperature, ΔH_f is the latent heat of fusion and $\Delta T = T^* - T$ is supercooling. The Gibbs free energy at the γ_C is called a critical free energy (ΔG_{Crit}). However, the heterogeneous nucleation on the wood surface differs from the homogeneous nucleation because of differences in nucleus sizes (γ_C). The differences are also associated with the critical free energy (ΔG_{Crit}). Therefore, the heterogeneous nucleation has less unity than homogeneous nucleation. The unity can be expressed with a correlation between two ΔGs (Eq. 8.4).

$$\Delta G'_{Crit} = \phi \Delta G_{Crit} \tag{8.4}$$

This factor highly correlates with interfacial tensions at the boundaries of crystalline deposit, amorphous region, and foreign surface. The contact angle (θ) between a crystalline deposit and a wood fiber surface can be generated to calculate the unity factor. The factor equation is:

$$\phi = \frac{\Delta G'_{Crit}}{\Delta G_{Crit}} = \frac{(2 + Cos\theta)(1 - Cos\theta)^2}{4} \quad (0 < \theta < 180) \tag{8.5}$$

Thus, the objectives for this study were to determine interaction mechanisms at nucleation sites on fiber surfaces and investigate the effect of increased hydrophobicity of the fiber surface on the PP matrix. This study also provides factors from the quantitative measurements of crystalline deposit angles and h/E ratios of the crystal deposit system on the fiber surface. Accordingly, six fiber types and three surface treatment conditions were used for a set of the two factor experimental design with a thermoplastic type.

8.2. Materials and Methods

8.2.1. Materials and Surface Conditioning

A total of six fiber types [8 bar thermomechanical pulp; TMP, refined mechanical pulp; RMP, commercial thermomechanical pulp; TMP (C), bleached Kraft pulp; BKP, unbleached Kraft pulp; UNP, and carbon fibers; CF) were used to evaluate the influence of surface morphology and hydrophobicity on the surface induced heterogeneous nucleation phenomenon. Three different fiber conditions (control, extracted, and water soaked) were used.

Extraction was performed with dichloromethane (CH_2Cl_2) on 8 bar TMP fibers, which were produced from juvenile portions in a continuous, pressurized, single-disc refiner (80 μm refiner plate gaps). Soxhlet extraction was performed in accordance with TAPPI standard T 204 om-88 (Tappi 1988). All of the fiber materials were washed out with distilled water at room

temperature after 24 hours of water soaking. Morphological changes were observed on the wood fiber surfaces due to removal of extractives.

Polypropylene (PP; Escorene PD7292N E7, Exxon Mobil Chemical Co. Houston, TX) was used for the evaluation of heterogeneous nucleation phenomena at the interface of the fiber surface and the semicrystalline polymer at an isothermal temperature of 140 ± 0.1 ºC.

8.2.2. Instruments for Monitoring the Interfacial Phenomena

To determine the number of nuclei, h/E ratios, and crystalline deposit angles during the PP crystallization process on the TMP fibers, a polarizing light microscope (PLM; Leica DM LB 30TL implemented with a HCS302-STC200 cold/heating stage) was used. Isothermal PLM observations characterized each crystallization process related to the different surfaces of the wood/non-wood fibers with PP. The PLM photomicrographic images were provided h/E ratios and crystalline deposit angles to calculate unity factors (ϕ) using Eq. 8.5, on the linear fiber surface (Figure 8.1). A Spot RT digital camera (Diagnostic Instruments Inc., Model #3,1,0 with 1600 x 1200 resolution) was used for developing images as a function of observation time. Image-Pro® Plus software was used to conduct the image analysis and collect quantitative measurements of h/E ratios and crystalline deposit angles.

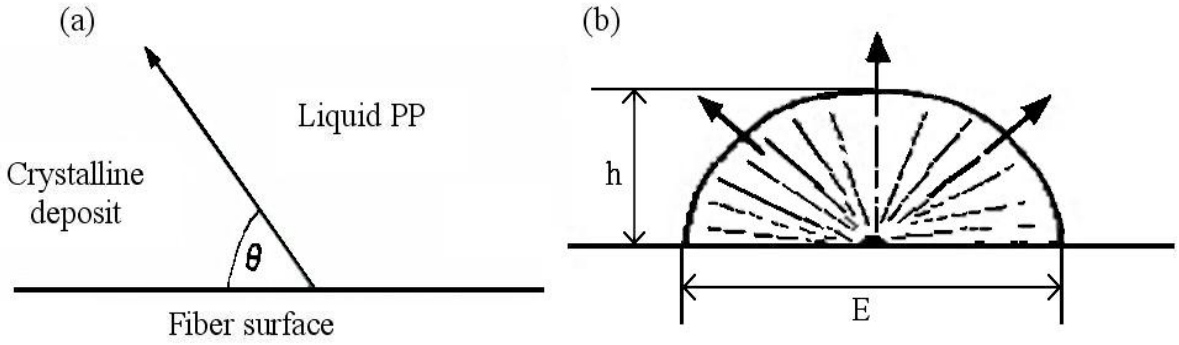

Figure 8.1. Measurements for crystalline deposit angles and ratios of lamella deposit between the fiber surface and the bulk area; (a) $Cos\theta$ and (b) h/E ratios.

Morphological characteristics of the wood and non-wood fibers were studied with a scanning electron microscope (SEM: Hitachi S-3600N). Fibers, which were coated with a thin layer (approximately 15-nanometers) of gold, were observed. The morphological characteristics and surface conditions were analyzed from photomicrographic images with image generation conditions of 20 Kv and 1,500x.

Particle Size Analysis (PSA) was achieved using a particle size analyzer and micrographic image analysis to obtain quantitative particle distributions on the fiber surfaces. The quantitative measurement addressed possible PP nucleation caused by relatively small particles on the fiber surface. Accusizer™ 770A SIS-Syringe Injection Sampler with a wide dynamic range sensor (LE400-0.5; covers 0.5 - 400 μm of particle radius) was used to analyze particle sizes on the fiber surfaces. The number of nuclei, particle size and distribution were generated from PLM and SEM images. Quantitative evaluation of PP nucleation on the fiber surface from 200x micrographs as a function of unit surface area were determined with a mounted digital camera equipped with Image-Pro® Plus software.

Data for the PLM result of unity factors and lamella deposit ratios were analyzed using SAS version 9.1e (SAS 2004). Analysis of variance with general linear model (GLM) was employed for the preliminary evaluation of differences among the three levels of the treatments and six different fiber types. Tukey's multiple comparison procedure was conducted to determine which levels of treatments and fiber types differed from the rest.

8.3. Results and Discussion

8.3.1. General Characteristics of Fiber Materials

Table 8.1 shows general fiber characteristics based on the pulping process, species, producers, and process conditions. It was expected that the fibers provided differentiated surface

Table 8.1. General characteristics of sample fibers.

Pulping Process	Thermomechanical		Kraft		Mechanical	HT Batch[1]
Fiber[2]	8barJ	TMP (C)	UKP	BKP	RMP	CF
Species	Loblolly pine (*Pinus taeda*)	Ponderosa pine (*Pinus ponderosa*) Western hemlock (*Tsuga heterophylla*) Western White Pine (*Pinus monticola*)	Western hemlock (*Tsuga heterophylla*)		N/A	N/A
Producer[3]	BCCUW	Plum Creek MDF, Inc.	Potlatch Co. Lewiston, ID		Inland Empire Paper Co.	Zoltek Companies, Inc.
Properties	175 ºC Preheating	163 ºC Preheating	5-7% Lignin	99.5% Cellulose	N/A	> 99.5% Carbon
Moisture Content	5.6 %	10.5 %	5.6 %	5.2 %	11.8 %	0.03 % %
Extractives	3.2 %	3.9 %	0.78 %	0.36 %	1.2 %	0.08 %

[1]HT Batch; High temperature batch.
[2]8barJ = 8 bar Juvenile (TMP), TMP (C) = Commercial TMP Fibers, UKP = Unbleached Kraft Pulp, BKP = Bleached Kraft Pulp, RMP = Refined Mechanical Pulp, CF= Carbon Fiber.
[3]BCCUW; Bio Composites center, University of Wales.

chemistry due to the extended removal of extractives and other extractable materials from wood fiber cell wall layers such as primary wall, S_1, S_2, S_3, and the middle lamella (Smook 1992, Sundholm 1999). The carbon and Kraft fibers also provide extreme surface characteristics between hydrophobicity and hydrophilicity with less extractives. The RMP, produced under a lignin glass transition point of 140 ºC, had lower extractable materials compared to the TMP fibers. Therefore, there was no lignin redeposit after the defibrillation process with the RMP fiber surface, which represented a higher surface roughness with wood fractions.

8.3.2. Unity Factor and Crystalline Deposit

Figure 8.2 shows unity factor (ϕ) and crystalline deposit ratio changes as functions of three levels of fiber treatments and fiber types. In general, untreated fibers provided lower mean unity factors (Figure 8.2a). The unity factors increased with additional treatment on the fiber

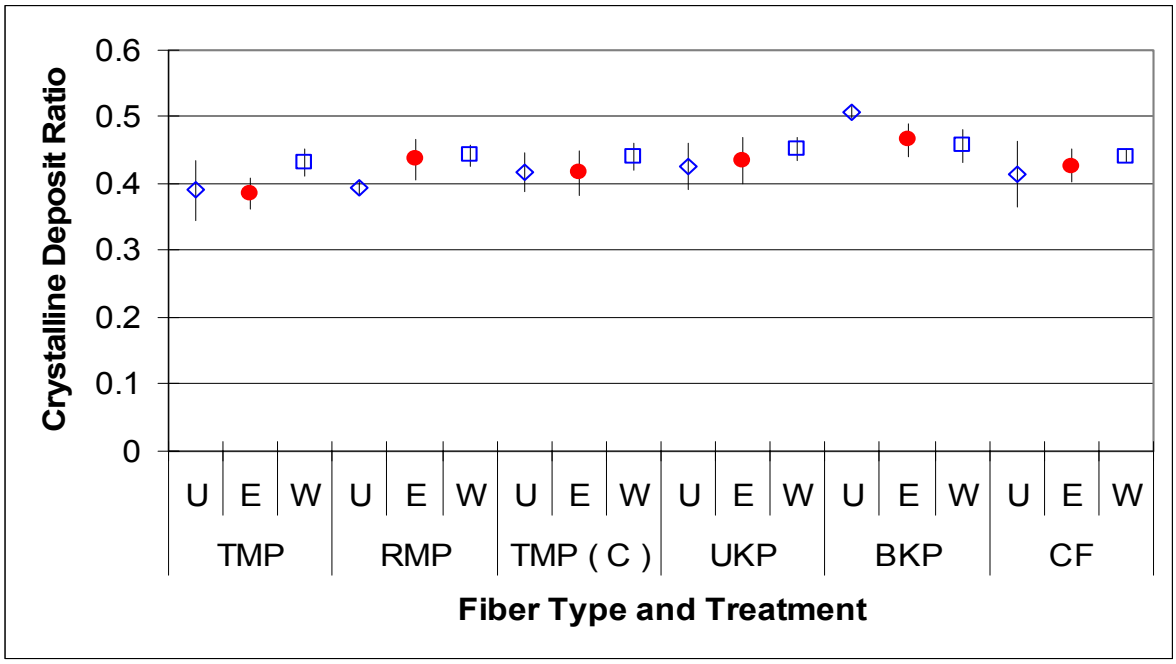

(a)

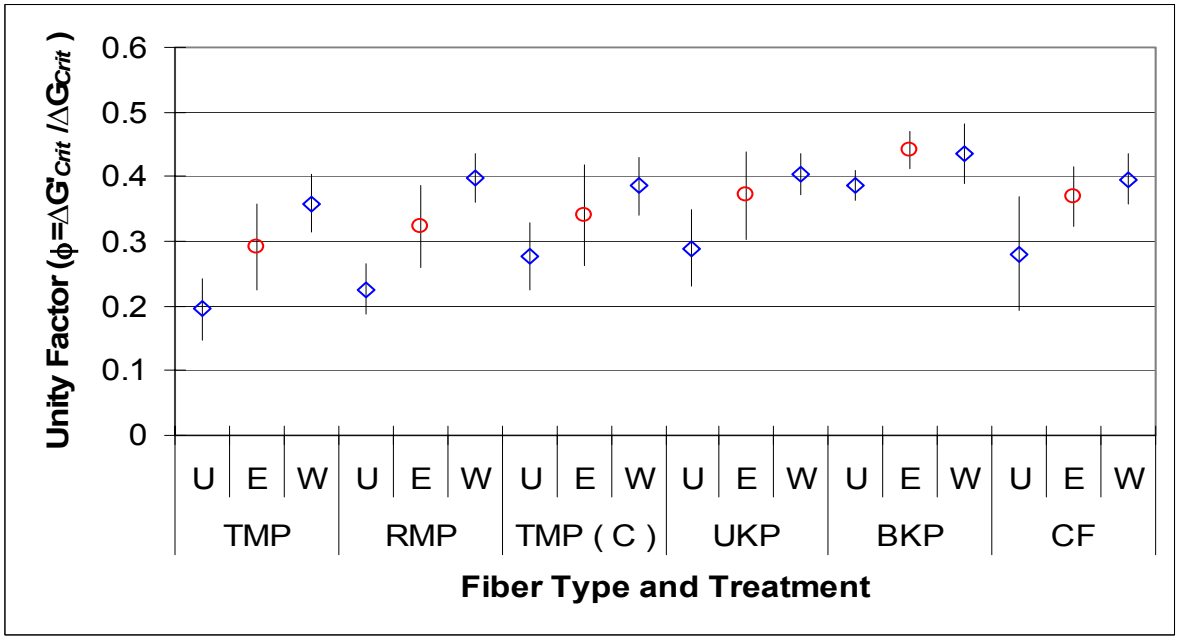

(b)

Figure 8.2. Unity factor (ϕ) and crystalline deposit ratio changes with the three levels of fiber treatments on the different fiber types (U=Untreated, E=H_2O_2 Extracted, W=H_2O Washed, TMP=Thermomechanical Pulp, TMP(C)=Commercial Thermomechanical Pulp Fibers, UKP=Unbleached Kraft Pulp, BKP=Bleached Kraft Pulp, RMP=Refined Mechanical Pulp, and CF=Carbon Fiber).

surface such as extraction and cleaning regardless of the fiber types. Mechanical pulp fibers (TMP, RMP, and commercial TMP) were significant differences at each level of treatment, while the chemical pulp (UKP and BKP) and carbon fibers were not statistically significant different between the extractions and surface treatment. This indicates that each treatment altered the fiber surfaces by increasing hydrophobicity which was caused by the removed or dislocated deposits on the fiber surfaces. The lignocellulosic nature of wood fibers generated from mechanical and chemical processing improved interaction with the molten PP. Thus, lignin contains surface and redeposited extractives on the fiber surfaces during the mechanical pulping process when heated above lignin glass transition temperature apparently had a beneficial effect on the nucleation of the molten PP matrix.

The crystalline deposit factor (h/E = 0.5) effect as shown in Figure 8.2a indicates that crystalline growth on the fiber surfaces essentially was not affected either by fiber type or treatment. With respect to the unity factor, however, it is clear that bleach Kraft pulp was the best (Figure 8.2b). Mechanical pulp fiber surfaces showed the least benefit from the fiber extraction on the crystalline deposit.

Table 8.2 shows Tukey's multiple comparison of unity factor and crystalline deposit on the fiber surface at a significant level of 0.05. The removal of surface deposit materials influenced the unity factor. This indicates that altered fiber surfaces were not effective on the surface induced PP nucleation. The extracted fiber surfaces were not significantly differed from untreated surfaces due to the hydrophobic surface conditions. The TMP fiber surfaces provided the best surface for the molten PP behavior due to the hydrophobicity of the lignin rich surface. Refined mechanical pulp (RMP) and carbon fiber (CF) also contained relatively high hydrophobic nature on the surface. However, RMP and CF surfaces were less effective on the

Table 8.2. Tukey's multiple comparison procedure at a significant level of 0.05.

Unity factor (ϕ) (Treatment)	Untreated		Extracted		Washed	
h/E (Treatment)	Untreated		Extracted		Washed	
Unity factor (ϕ) (Fiber Types)	TMP	TMP (C)	RMP	CF	UKP	BKP
h/E (Fiber Types)	TMP	TMP (C)	RMP	CF	UKP	BKP

Note: TMP=Thermomechanical Pulp, TMP (C)=Commercial Thermomechanical Pulp Fibers, UKP=Unbleached Kraft Pulp, BKP=Bleached Kraft Pulp, RMP=Refined Mechanical Pulp, CF=Carbon Fiber. (The bar represents not significantly differ from each other)

fiber surface induced heterogeneous nucleation and crystalline deposit on them. Bleached Kraft fibers showed completely different behaviors and it can be explained by surface hydrophobicity. It also indicates that hydrophilic surfaces are incompatible with a hydrophilic PP matrix. The UKP contained less than 5% chemically modified lignin and extractives showed a significant difference on the unity factor and crystalline deposit factor of molten PP behaviors compared to the BKP.

The general effect of the crystalline deposit ratios on the unity factor (ϕ) determined by polarizing light microscope (PLM) observations is shown in Figure 8.3. Apparently, the surface morphology and chemistry influenced crystal impurities on the fibers surfaces which provided a better nucleation site for the PP matrix. The $\Delta G^{/}_{Crit}$ differences of the fiber surfaces contributed to PP crystalline deposits on the surfaces. The SEM and PLM results correlated to the unity factor using a method of tabular and numerical comparisons among the fibers. The result also

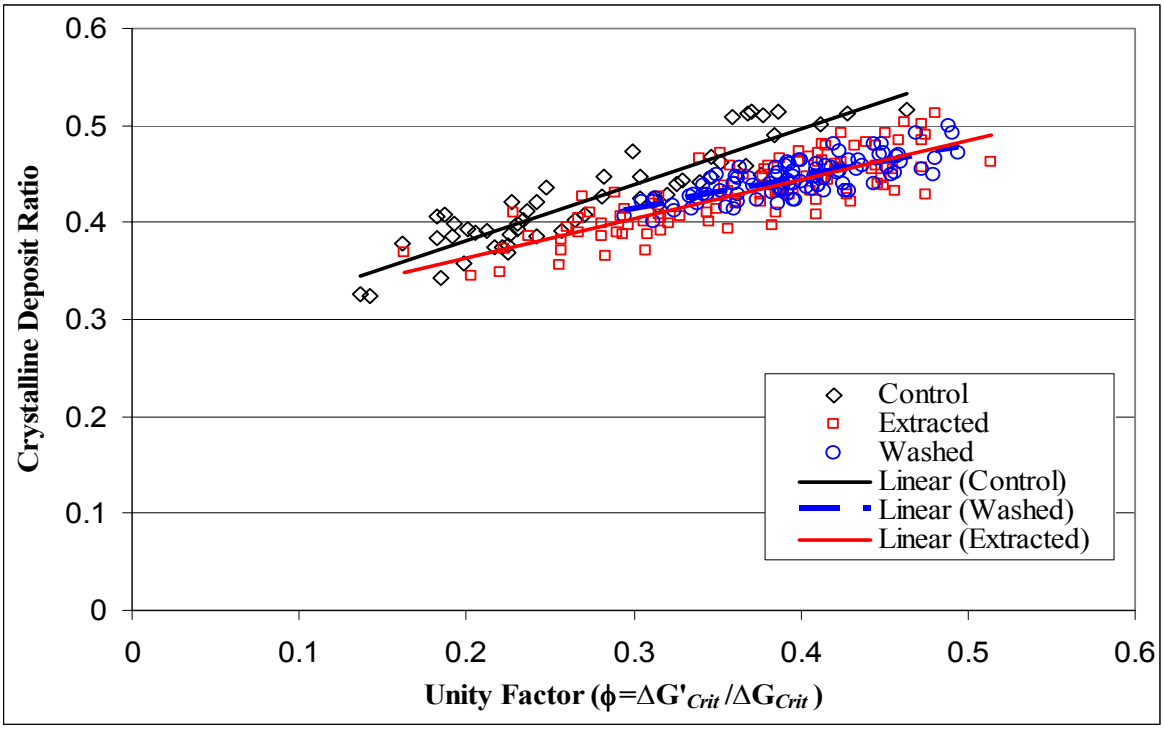

Figure 8.3. Correlation between the crystalline deposit ratio (h/E) and unity factor (ϕ) changes of crystalline deposit angle measurements with the three levels of fiber treatments on the surface of thermomechanical fibers.

shows what kind properties of wood fiber surfaces are effective in inducing heterogeneous nucleation and how surface properties influence the purity changes of $\Delta G^{/}_{Crit}$ on the wood/non-wood surface compared to the bulk area. Some degree of material hydrophobicity on the fiber surface will be beneficial in the promoting computability on the fiber surface and create an intimate contact system between the fiber surface and PP. This might be explained by the development of secondary valence forces (i.e., the role of the Van der Walls forces) that interact with the non-polar surface molecules on the PP.

8.3.3. Nucleation and Surface Morphology

Figure 8.4 shows heterogeneous nucleation phenomena associated with the fiber surface morphology due to the three levels of fiber conditioning. The micrographs illustrate the

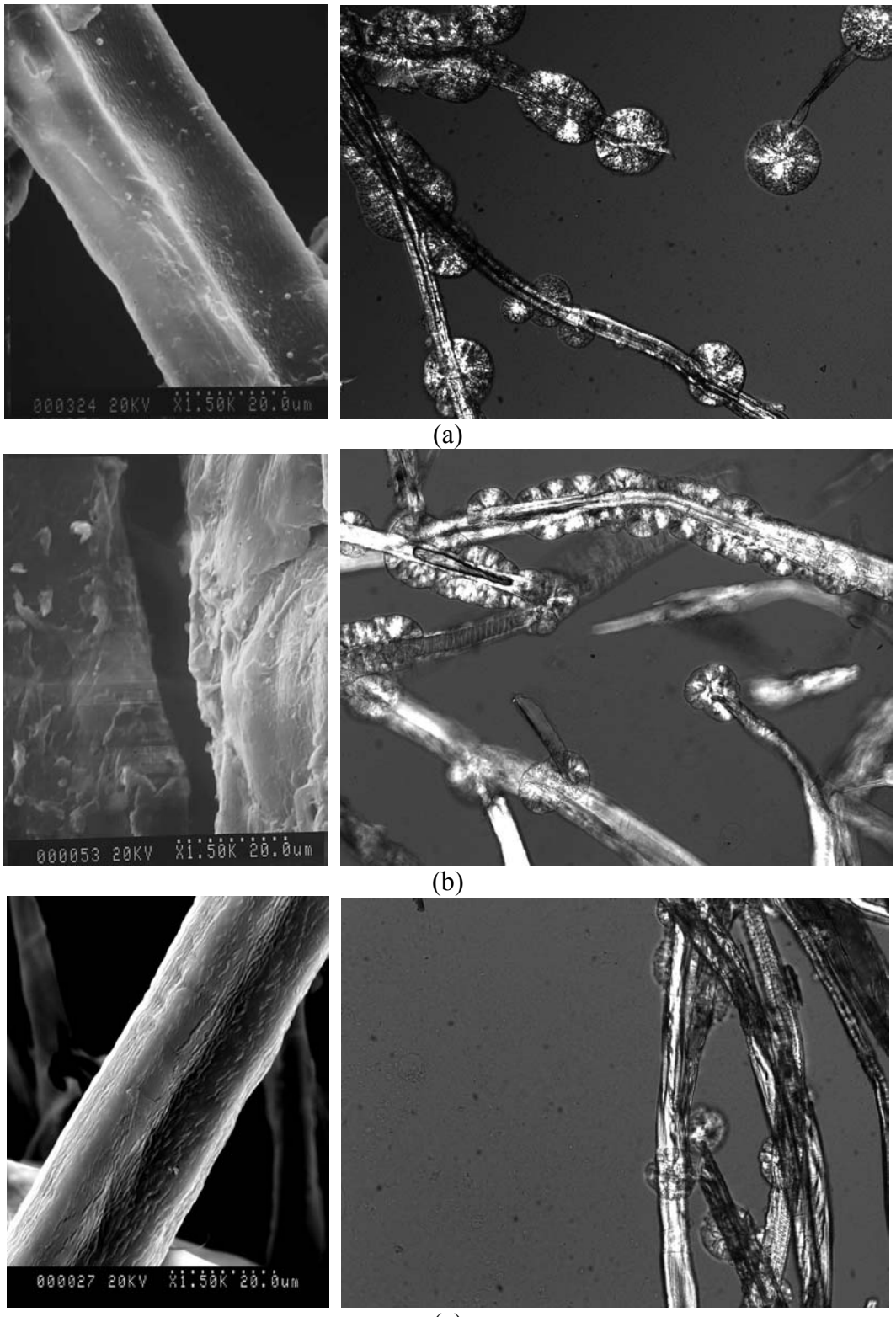

Figure 8.4. Heterogeneous nucleation phenomena (Left) associated with the surface morphology (Right) due to the fiber treatments. (a) Untreated fibers, (b) Extracted fibers, and (c) Washed fibers.

morphological changes among the fiber materials due to each surface treatment. The extraction of the surface did not influence PP nucleation on the extracted fiber surfaces (Figure 8.4b). Surface cracks and particles still remained on the rough surface of extracted fibers. However, the washed surfaces (Figure 8.4c) showed an extreme reduction in heterogeneous nucleation. The surfaces showed surface checks but a clean morphology and fewer particles. Surface roughness could affect the fiber/matrix adhesion and the nucleation ability of semicrystalline polymers (Cai 1997). However, the surface roughness and checks did not correspond directly to PP nucleation. The figure also indicates that water washed fibers gave an increased unity factor and produce poor nucleation. However, they did influence PP nucleation as well as surface chemical composition and surface free energy.

8.3.4. Particles in the Fiber Surface

Figure 8.5 shows that particles located on the fiber surface to induce heterogeneous PP nucleation. Particles of variable sizes can be seen on the surfaces of the wood fibers. Most of the particles are located in surface checks and damaged surfaces. The particles have a relatively

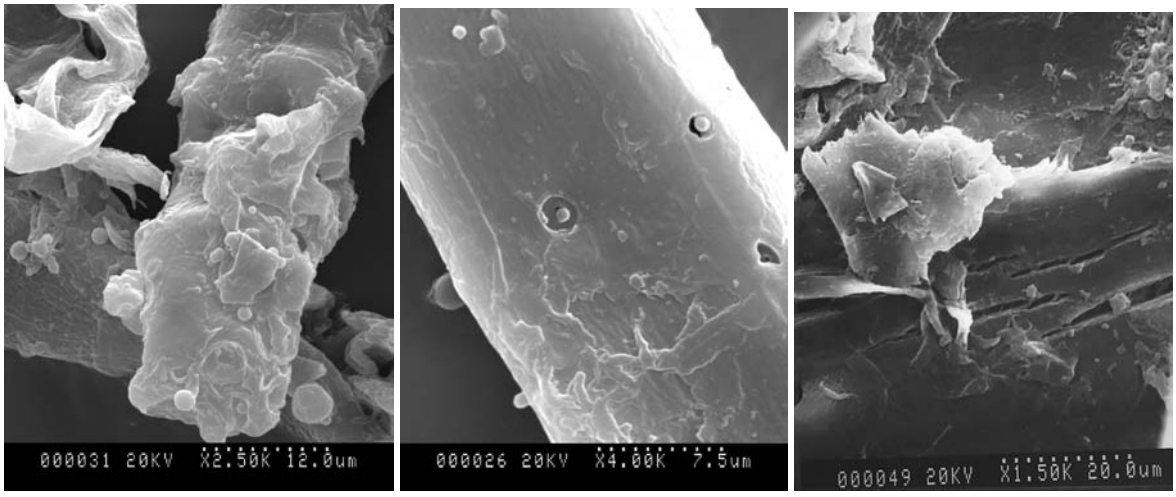

(a) (b) (c)

Figure 8.5. Particles on the fiber surface of (a) rough, (b) smooth, and (c) crack sites to induce nucleation.

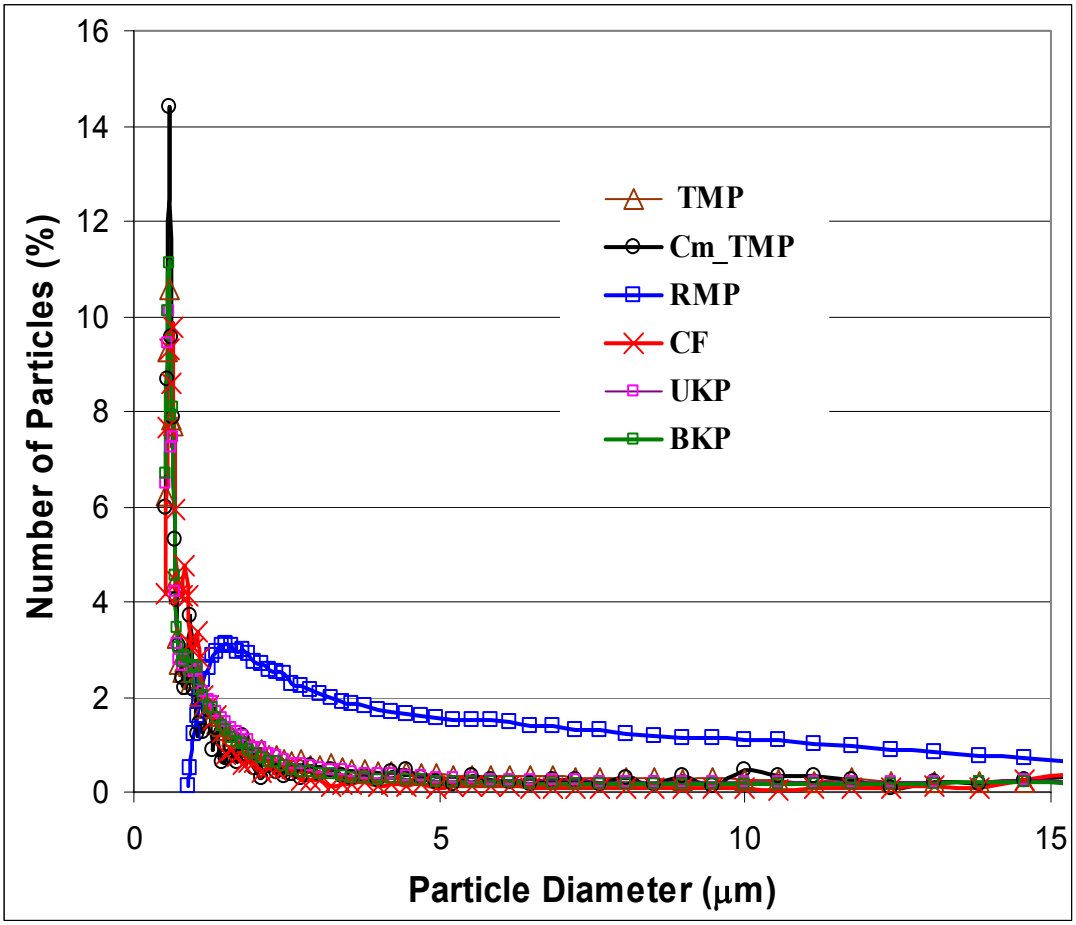

(a)

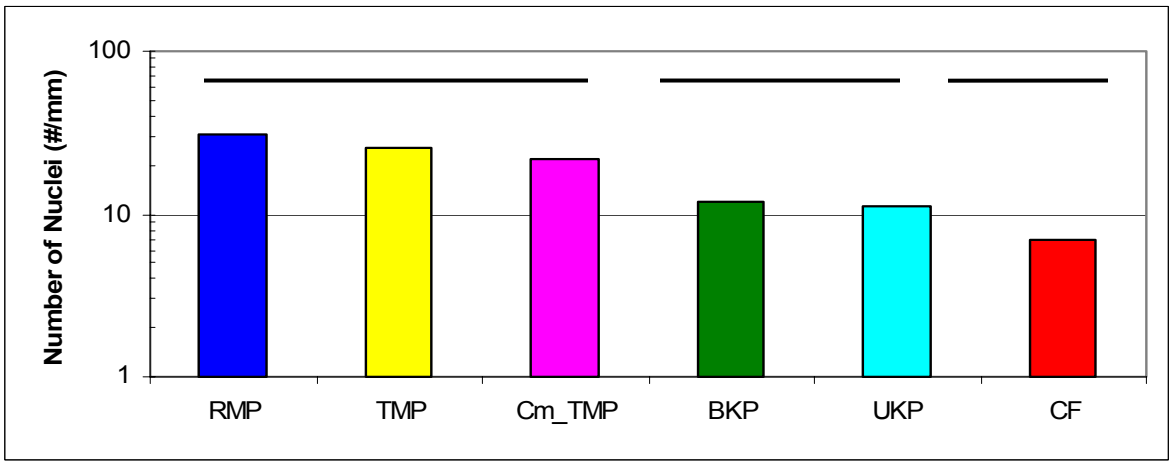

(b)

Figure 8.6. (a) Particle distribution and (b) number of nuclei on the fiber surface. (The bar represents not significantly differ from each other).

smooth and round shapes. Based on the nucleation theory, smooth and round surfaces provide lower surface areas and hence relatively lower the surface free energy, compared with the rough surfaces on molten PP. The function of surface checks and roughness of fibers may be to promote nucleation and hence, compatibility with the small particles on the source of PP nucleation sites.

8.3.5. Particle Distribution and Number of Nuclei

Figure 8.6 shows both particle distribution and number of nuclei on fiber surfaces. Wood fibers produced by the three mechanical pulping processes (RMP, TMP and commercial TMP) showed the highest degree of nucleation. This probably related to the greater surface area in refined fibers compared to unrefined pulp fibers. The median from the particle distributions of each fiber types was 0.64 μm, except for RMP (2.68 μm). Relatively smaller particles (< 0.5μm) on the fiber surface can be important for the heterogeneous nucleation of PP. However, the instrumental limitation with a wide dynamic range sensor - from 0.5 to 400 μm particle radius- suggests that further investigation should be made with an instrument capable of measuring particle sizes smaller than 0.5 μm. The average radius of nucleus was 0.64 μm, and the nuclei radius is much smaller than nucleus.

CHAPTER 9

SUMMARY OF CONCLUSIONS

Thermomechanical pulp (TMP) fiber sheets formed in a standard sheet mold were used to fabricate handsheet/polypropylene (PP) film laminates. The effects of surface treatments and fiber interlocking were evaluated on the properties of wood fiber handsheet/thermoplastic laminates. Enhanced interfacial interaction proved to be important in promoting interfacial adhesion at the hydrophilic wood materials and hydrophobic PP interphase. This provided a basis for designing a series of experiments to study the effect of surface treatments on the properties of the wood fiber handsheet/PP film laminates. The study was also extended to evaluate surface induced interfacial phenomena known as heterogeneous PP nucleation on different fiber surfaces. Details of the summary and conclusions derived from the individual experiments are as follows.

Macro- and micro-size resin droplets were applied to the microtomed surface of solid wood and contact angles were measured. There were small differences between the sessile droplet and the atomic force microscopy (AFM) scanning method in heterogeneous wetting characteristics. The sessile droplet shape changed from spherical to hemispherical and finally to a complete enclosed hemispherical geometry within 30 seconds. Thus, the droplet behavior and volume changes cannot be expressed with a single equation. The combination of two-force balanced equations provided a more accurate means to determine sessile droplet volume. Regarding the dispersing behavior of urea-formaldehyde (UF) and Phenol-formaldehyde (PF) droplets, dispersion was always greater in the fiber direction than across the grain on the earlywood surfaces due to differences in wood anatomy as well as surface roughness.

Differential wetting due to the structural variation on the material surface also accounted for some of the shear strength differences between the resin types. Micro-droplets also were more sensitive with UF resin applied to latewood surfaces than sessile droplets and resulted in a mean shear strength of 244 psi, which was 53% greater than when 1% UF microdroplets were applied to the earlywood surfaces. However, shear strengths of PF resin treatment were not sensitive to droplet sizes.

DC-based plasma treatment using argon and oxygen as ion sources on TMP fiber handsheet and PP film surfaces improved interfacial adhesion at the TMP fiber and PP interface. The plasma barrier between electrodes prevented thermal damages of the TMP fiber handsheets and PP film and allowed treatment of more than 5 minutes. O_2-plasma treatment provided better surface activation on the TMP fiber and PP film than Argon-plasma treatment. Treatment effects of O_2-based plasma on tensile strength were measured from thirty to sixty seconds surface exposure. The treatment resulted in 43 to 80% tensile strength enhancement over the non-treated samples. Treatment longer than sixty seconds led to slightly reduced tensile strength. O_2-plasma treatment changed the topography of the wood fiber and PP to a nodular structure found in the flat areas. The size of the nodules increased as the treatment time increased. Root mean square (RMS) roughness measurement yielded very similar results as the thermal characteristics of T_g and X_C obtained by using the differential scanning calorimetry (DSC). The RMS roughness and thermal quantities were lower with 30-second plasma treatment but slightly recovered with 60-second treatment. Finally, this study found that the mechanical interlocking of a PP matrix and fibers with ion implantations resulted in fiber reinforcement and interfacial strength enhancement at the TMP fiber and PP interface.

Chemical coupling on both the TMP fiber and PP film surfaces improved tensile strength of the TMP fiber handsheet and PP film laminates. For the maleic anhydride (MA) with benzoyl peroxide (BPO) as an initiator, tensile strength increased 52% for the TMP fiber treatment and 76% with PP film over untreated laminates. The optimum strength properties were obtained with a MA and BPO ratio of 2:1 regardless of material type. Scanning electron microscopy (SEM) images also showed the effectiveness of MA loading on the surface of TMP fibers due to increased fiber failure without fiber pullout from the PP matrixes. Crystallinity and heat flow from DSC, as expected, decreased with the addition of MA on the TMP fiber surface. These results were also in accordance with the morphological observations at the fracture surface, fourier-transform infrared spectroscopy (FTIR) spectra, and thermal analysis. However, MA treatment on the surface of PP film was more effective in promoting a compatible strength enhancement and has the added benefit of reduced fiber drying expenses in an industrial setting. Based on the high correlation between tensile strength and the number of fibers counted at the point of failures, the number of fibers proved to be a sensitive measure of the effectiveness of surface treatment.

The treatment of handsheets with two thermoset resins, PF and UF, resulted in statistically significant improvement in tensile strength of laminates with PP films. The effects of the resins as interfacial compatibilizers between the TMP fibers and PP film interfaces were pronounced. Tensile strengths were increased 92% over untreated samples. The X_C of both resin types was increased as evidenced by the increased tensile strength. It should be noted that preconditioning of the TMP handsheets and a pressing temperature of 400 °F led to the highest tensile strength of TMP fiber handsheet and PP film laminates. However, the brittle failure surface showed the effect of some heat degradation of the fibers.

Relatively high nucleation density was obtained on the surface of mechanical pulp fibers. Smooth and hydrophobic fiber surfaces appeared to be beneficial in measuring the crystalline deposit angles, unity factor (ϕ) changes, and h/E ratios. A higher ϕ group was obtained with surfaces cleaned with water but resulted in the poor nucleation ability of the semicrystalline polymer. Rough and fracture surfaces acted as a natural particle holding device. Isolated materials from the fiber surface influenced material impurity of the fibers and created polymer nucleation sites. The particles and materials extracted from the fiber surfaces may play an important role with regard to heterogeneous nucleation and crystalline deposits.

Finally, it was concluded that ion implantations, thermoset resin, and chemical modification of fiber and PP surfaces resulted in interfacial strength enhancement at the wood fiber and PP interface. If both of the fibers and the PP film were chemically treated, the best increase in tensile strengths of the laminates occurred. Electron interaction combined with mechanical interlocking within the fiber handsheet to promoted interfacial interaction between the hydrophilic and hydrophobic interfaces. Additionally, this research should be useful in furthering the fundamental understanding of wood fiber-polymer interactions.

LITERATURE CITED

Alexy, P., B. Košíkováb, and G. Podstránskab. 2000. The effect of blending lignin with polyethylene and polypropylene on physical properties. Polymer. 41:4901-4908.

Ali, Z.I., H.A. Youssef, H.M. Said, and H.H. Saleh. 2005. Thermal stability of LDPE, iPP and their blends. Thermochimica Acta. 438:70-75.

American Society for Testing and Materials (ASTM). 1994. Standard practice forclassifying failure modes in fiber-reinforced-plastic joints. Vol. 15.06. ASTM D5573-94. West Conshohocken, PA.

American Society for Testing and Materials (ASTM). 2001a. Standard test method for enthalpies of fusion and crystallization by differential scanning calorimetry. ASTM E793-01. West Conshohocken, PA.

American Society for Testing and Materials (ASTM). 2001b. Standard test method for enthalpies of fusion and crystallization by differential scanning calorimetry. ASTM E794-01. West Conshohocken, PA.

American Society for Testing and Materials (ASTM). 2003. Standard test method for enthalpies of fusion and crystallization by differential scanning calorimetry. ASTM D638-03. West Conshohocken, PA.

Amash, A. and P. Zugenmaier. 2000. Morphology and properties of isotropic and oriented samples of cellulose fibre–polypropylene composites. Polymer. 41:1589-1596.

Anglès, M.N., J. Salvadó, and A. Dufrensne. 1999. Steam-exploded residual softwood-filled polypropylene composites. J. Appl. Polym. Sci. 74:1962–1977.

Avella, M., L. Casale, R. Dell'erba, B. Focher, E. Martuscelli and A. Marzetti. 1998. Broom fibers as reinforcing materials for polypropylene-based composites. J. Appl. Polym. Sci. 68: 1077-1089.

Badey, J.P., E. Espuchet, D. Sage, B. Chabert, Y. Jugnet, C. Batier, and T.M. Duc. 1996. A comparative study of the effects of ammonia and hydrogen plasma downstream treatment on the surface modification of polytetrafluoroethylene. Polymer. 37(8):1377-1386.

Bai, F., F. Li, B.H. Calhoun, R.P. Quirk, and S.Z.D. Cheng, 1999, Physical constants of poly (propylene) in Polymer Handbook. John Wiley & Sons, Inc. pp. v21-24.

Bamford, C.H. and K.G. Al-Lamee. 1994. Polymer surface functionalisation and grafting by a simple and inexpensive method. Macromol. Rapid. Commun. 15:379-384.

Barry, A.O., and Z. Koran. 1990. Surface analysis by ESCA of sulfite post-treated CTMP. J. Appl. Polym. Sci. 39:31-42.

Bataille P., P. Allard, P. Cousin, and S. Sapieha. 1990. Interfacial phenomena in cellulose/ polyethylene composites. Polym. Composites. 11(5):301-304.

Belgacem, M.N., P. Bataille, and S. Sapieha. . 1994. Effect of Corona modification on the mechanical properties of polypropylene/cellulose composites. J. Appl. Polym. Sci. 53: 379-385.

Bente, M., G. Avramidis, S. Förster, E.G. Rohwer, and W. Viöl. 2004. Wood surface modification in dielectric barrier discharges at atmospheric pressure for creating water repellent characteristics. Holz als Roh-und Werkstoff. 62(3):157-163.

Beshay, A. D. 1989. Reinforced Polymer composites with wood fibers grafted with silanes-Grafting of celluloses or lignocelluloses with silanes to reinforce the polymer composites. US Patent 4,820,749.

Beshay, A. and S.V. Hoa. 1990. Improved interface bonding between cellulosic fibers and thermoplastics. Proc. 35th Internl. SAMPE Symp. Exhib.-Advanced materials: the challenge for the next decade. Part 1. 35:571-578.

Biermann, C. 1996. Handbook for pulping and papermaking. 2nd Ed. Academic Press. Inc. 753 p.

Bledzki, A. K., S. Reihmane and J. Gassan. 1998. Thermoplastics reinforced with wood fillers: A literature review. Polym.-Plastics Tech. Engin. 37(4): 451-468.

Bledzki, A.K. and J. Gassan. 1999. Composites reinforced with cellulose based fibres. Prog. Polym. Sci. 24:221-274.

Bledzki, A.K. and O. Faruk. 2003. Wood fiber reinforced polypropylene composites: Effect of fiber geometry and coupling agent on physico-mechanical properties. Appl. Composite Mats. 10(6):365-379.

Bledzki, A.K. and O. Faruk. 2005. Effects of the chemical foaming agents, injection parameters, and melt-flow index on the microstructure and mechanical properties of microcellular injection-molded wood-fiber/polypropylene composites. J. Appl. Polym. Sci. 97(3):1090-1096.

Bledzki, A.K., M. Letman, A. Viksne, and L. Rence. 2005. A comparison of compounding processes and wood type for wood fibre-PP composites. Composites. Part A. 36(6):789-797.

Bliznakov, E.D., C.C. White, and M.T. Shaw. 2000. Mechanical properties of blends of HDPE and recycled urea-formaldehyde resin. J. Appl. Poly. Sci. 77:3220–3227.

Boras, L. and P. Gatenholm. 1999. Surface composition and morphology of CTMP Fibers. Holzforschung. 53:188-190.

Bratawinjaja, A.S. and I. Gitopadmoyo. 1989. Adheson property of polypropylene modified with maleic anhydride by extrution molding. J. Appl. Polym. Sci. 37:1141-1145.

Brown, J.R. and Z. Mathys. 1997. Plasma surface modification of advanced organic fibres Part V: Effects on the mechanical properties of aramid/phenolic composites. J. Mats. Sci. 32:2599-2604.

Bryant, B.S. 1966. The chemical modification of wood; From the point of view of wood science and economics. Forest Prod. J. 16(2):20-27.

Bryant, B.S., C.Y. Hse, B.G. Lee, S.Y. Lee, and T.H. Lin. 2003. Properties of fiber-reinforced composites made with natural fibers. In: Better utilization of wood for human, earth and future. Eds. Lee and Jang, Intl. Conf. Forest Prods. Korean Soc. Wood Sci. Tech. Apr. 2003. Daejeon, Korea. 1: 346-352.

Cai Y., J. Petermann, and H. Wittich. 1997. Transcrystallization in fiber-reinforced isotactic polypropylene composites in a temperature gradient. J. Appl. Polym. Sci. 65:71-74.

Caldwell, D.L. 1993. Interfacial analysis. In Handbook of composite reinforcements. Ed. Lee, S.M. VCH Publishers. pp.283-298.

Cangelosi, F. and M.T. Shaw. 1983. A review of hydrogen bonding in solid polymers: Structural relationships, analysis, and importance. Polym.-Plast. Tech. Eng. 21(1):13-98.

Casilla, R.C., S. Chow, and P.R. Steiner. 1981. An immersior technique for studying wood wettability. Wood Sci. Tech. 15:31-43.

Caulfield, D.F., D. Feng, S. Prabawa, R.A. Young, and A.R. Sanadi. 1999. Interphase effects on the mechanical and physical aspects of natural fiber composites. Die Angewandte Makromolekulare Chemie. 272:57-64.

Cazabat, A.M. 1992. Wetting from macroscopic to microscopic scale. Adv. Coll. Interf. Sci. 42:65-67.

Chang, E.P. 1977. Crystallization studies on fire-retardant polypropylene. J. Appl. Polymer Sci. 21:937-942.

Chaoting, Y., S. Gao, and O. Mu. 1993. Effect of low-temperature plasma surface treatment on the adhesion of ultra-high-molecular-weight-polyethylene fibers. J. Mats. Sci. 28(18):4883-4891.

Chatterjee, J. 2002a. Shape analysis based critical Eotvos numbers for buoyancy induced partial detachment of oil drops from hydrophilic surfaces. Adv. Colloid Int. Sci. 99:163–179.

Chatterjee, J. 2002b. Critical Eotvos numbers for buoyancy-induced oil drop detachment based on shape analysis. Adv. Colloid Int. Sci. 98:265-283.

Chen, M. and J. Meister. 1995. Surface alternation of wood by grafting. In Wood fiber/polymer composites: fundamental concepts, process, and material options. Eds. Caulfield et al. pp118-131.

Chen, M., J. Meister, D.W. Gunnells, and D.J. Gardner. 1995. A process for coupling wood to thermoplastic using graft copolymers. Adv. Polym. Tech. 14(2):97-109.

Chiang, W.Y., W.C. Wu, and B. Pukanszky. 1994. Modification of polypropylene, blending with resole type phenol-formaldehyde resins. Eur. Polym. J. 30(5):573-580.

Chibowski, E. and R. Perea-Carpio. 2002. Problems of contact angle and solid surface free energy determination. Adv. Colloid Interf. Sci. 98:245-264.

Chiou, B. and P.E. Schoen. 2002. Effects of crosslinking on thermal and mechanical properties of polyurethanes. J. Appl. Polym. Sci. 83:212-223.

Chuang, I.S. and G.E. Maciel. 1994. NMR study of the stabilities of urea-formaldehyde resin components toward hydrolytic treatments. J. Appl. Polym. Sci. 52:1637-1652.

Chun, B.C., S.H. Cha, Y.C. Chung, and J.W. Cho. 2002. Enhanced dynamic mechanical and shape-memory properties of a poly(ethylene terephthalate)-poly(ethylene glycol) copolymer crosslinked by maleic anhydride. J. Appl. Polym. Sci. 38:27-37.

Chung F. 1991. Unified theory and guidelines on adhesion. J. Appl. Polym. Sci. 42:1319-1331.

Clemons, C., R.A. Yong, and R.M. Rowell. 1992. Moisture sorption properties of composite boards from esterified aspen fiber. Wood Fiber Sci. 24(3):353-363.

Clemons, C. 2002. Wood-plastic composites in the United States: The interfacing to two industries. Forest Prod. J. 52(6):10-18.

Collier, J.R., M. Lu, M. Fahrurrozi, and B.J. Collier. 1996. Cellulosic reinforcement in reactive composite systems. J. Appl. Polym. Sci. 61:1423-1430.

Colombini, D., G. Merle, J.J. Martinez-Vega, E. Girard-Reydet, J.P. Pascault, and J.F. Gerard. 1999. Effects of thermal treatments on the viscoelastic behavior of the interphase relaxation in a compatibilized thermoset/thermoplastic blend. Polymer 40:935-943.

Cousin, P., P. Bataille, H.P. Schreiber, and S. Sapieha. 1989. Cellulose induced crosslinking of polypropylene. J. Appl. Polym. Sci. 37:3057-3060.

Coutinho, F.M.B., T.H.S. Costa and D.L. Carvalho. 1997. Polypropylene-wood fiber composites: Effect of treatment and mixing conditions on mechanical properties. J. Appl. Polym. Sci. 65:1227-1235.

Dale Ellis, W. and J.L. O'Dell. 1999. Wood–polymer composites made with acrylic monomers, isocyanate, and maleic anhydride. J. Appl. Polym. Sci. 73:2493-2505.

Dalväg H., C. Klason, and H.E. Strömvall. 1985. The efficiency of cellulosic fillers in common thermoplastics. Part II. Filling with processing acids and coupling agents. Intern. J. Polym. Mats. 11:9-38.

Denes, A.R., M. Tshabalala, R. Rowell, F. Denes, and R. Young. 1999. Hexamethyldisiloxane-plasma coating of wood surfaces for creating water repellent characteristics. Holzforschung. 53:318-326.

Denac, M., V. Musil, and I. Šmit. 2005a. Polypropylene/talc/SEBS (SEBS-g-MA) composites. Part 2. Mechanical properties. Composites Part A. 36(9):1282-1290.

Denac, M. I. Šmit and V. Musil. 2005b. Polypropylene/talc/SEBS (SEBS-g-MA) composites. Part 1. Structure. Composites Part A. 36(8):1094-1101.

Demir, H., U. Atikler, D. Balköse, and F. Tıhmınlıoğlu. 2005. The effect of fiber surface treatments on the tensile and water sorption properties of polypropylene-luffa fiber composites. Composites Part A. In Press, Corrected Proof, Available online 21 July, 2006.

Dong, S. and S. Sapieha. 1991. Characterization of interfacial adhesion in cellulose fiber/thermoplastic systems. ANTEC, Proc. 49th Annual Tech. Conf. 37:1154-1156.

Dong, S., S. Sapieha, and Schreiber, H. P. 1993. Mechanical properties of corona-modified cellulose/polyethylene composites. Polym. Engin. Sci. 33(6): 343-346.

Draou, K., N. Bellakhal, J. Brisset, and A. Addou. 1999. Preparation and characterization of thin oxides films formed at a brass surface oxidized by plasma treatment. J. Mats. Sci. 34:5575-5579.

Duvall J., C. Sellitti, C. Myers, A. Hiltner, and E. Bare. 1994. Interfacial effects produced by crystallization of polypropylene with polypropylene-g-maleic anhydride compatibilizers. J. Appl. Polym. Sci. 52:207-215.

Ebengou, R.H. 1997. Adsorption as a mechanism for nucleating activity: A thermodynamic explanation. J. Polym. Sci. Part B: Polym. Phys. 35(9):1333-1338.

Espert, A. and S. Karlsson. 2004. Characterization and comparison of the thermal and mechanical properties of different natural fiber-filled polypropylene composites. In: Proc. 7th Intern. Conf. Woodfiber-Plastic Composites. Forest Products Society. Madison, WI. pp.293-298.

Extrand, C.W. 2003. Contact angles and hysteresis on surfaces with chemically heterogeneous islands. Langmuir. 19:3793-3796.

Felix J.M., and P. Gatenholm. 1991. The nature of adhesion in composites of modified cellulose fibers and polypropylene. J. Appl. Polym. Sci. 42:609-620.

Felix, J. M. and P. Gatenholm. 1993. Formation of Entanglement at brushlike interfaces in cellulose-polymer composites. J. Appl. Polym. Sci. 50:699-708.

Felix, J., P. Gatenholm and H. P. Schreiber. 1993. Controlled interactions in cellulose-polymer composites 1: effect on mechanical properties. Polymer Composites, 14(6): 449-457

Felix J.M. and P. Gatenholm. 1994. Effect of transcrystalline morphology on interfacial adhesion in cellulose/polypropylene composites. J. Mats. sci. 29:3043-3049.

Felix, J., P. Gatenholm, and H.P. Schereiber. 1994. Plasma modification of cellulose fibers: effects on some polymer composite properties. J. Appl. Polym. Sci. 51:285-295.

Fernanda, M., B. Coutinho, T.H.S. Costa, and D.L. Carvalho. 1997. Polypropylene–wood fiber composites: Effect of treatment and mixing conditions on mechanical properties. J. Appl. Polym. Sci. 65:1227-1235.

Forest Products Laboratory (FPL). 1999. Wood Handbook: Wood as an engineering material. Forest Prod. Society, Madision, WI. 463 p.

Fowkes, F. 1980. Donor-acceptor Interaction at interfaces. In Adhesion and adsorption of polymers. L.H. Lee, Ed. Plenum Press, New York. 897 p.

Fowkes F. 1987. Role of acid-base interfacial bonding in adhesion. J. Adh. Sci. Tech. 1(1):7-26.

France, R. and R. Short. 1997. Plasma treatment of polymers: Effects of energy transfer from an argon plasma on the surface chemistry of poly(styrene), low density poly(ethylene), poly (propylene) and poly(ethylene terephthalate). J. Chem. Soc., Faraday Trans. 93(17):3173-3178.

Frontini P.M., M. Rink, and A. Pavan. 1993. Development of polyurethane engineering thermoplastics. I. Preparation and structure. J. Appl. Polym. Sci. 48:2003–2022.

Gardner, D.J., N.C. Generalla, D.W. Gunnells, and M.P. Wolcott. 1991. Dynamic wettability of wood. Langmuir. 7:2498-2502.

Gardner, D.J., M.P. Wolcott, L. Wilson, Y. Huang, and M. Carpenter. 1996. Our understanding of wood surface chemistry in 1995. In: Wood Adhesives. Eds. A.W. Christiansen and A.H. Conner. Forest Products Society. Madison, WI. pp. 29-36.

Gassan, J. and A.K. Bledzki. 1997. The influence of fiber-surface treatment on the mechanical properties of jute-polypropylene composites. Composites Part A. 28(12):1001-1005.

Gasser, U., E.R. Weeks, A. Schofield, P.N. Pusey, and D.A. Weitz1. 2001. Real-space imaging of nucleation and growth in colloidal crystallization. Science. 292:258-262.

Gaur U., G. Desio, and B. Miller. 1989. Interfacial adhesion in fiber reinforced thermoplastic composites. Plastics Engin. 45:43-45.

Gauthier, R., H. Gauthier, and C. Joly. 1999. Compatibilization between lignocellulosic fibers and a polyolefin matrix. Proc. 5th interl. Conf. WPC. Ed. Rowell, R.M. pp. 153-162.

Geoghegan, M. and G. Krausch. 2003. Wetting at polymer surfaces and interfaces. Prog. Polym. Sci. 28:261-302.

Gray D.G. 1974. Polypropylene transcrystallization at the surface of cellulose fibers. Polym. Letters Ed. 12:510-514.

Grell, M. 2001. Kinetics of wood-anhydride reactions: A novel approach. Wood Sci. Tech. 35:529-539.

Han, G.S., S. Saka and N. Shiraishi. 1991. Composites of wood and polypropylene V. Morphological study of composite by TEM-EDXA. Mokuzai Gakkaishi, 37(3):241-246.

Hedenberg, P. and P. Gatenholm. 1995. Conversion of plastic/cellulose waste into composites. I. model of interphase. J. Appl. Polym. Sci. 56:641-651.

Hill, C.A.S. and N.S. Cetin. 2000. Surface activation of wood for graft polymerization. Intern. J. Adhesion Adhesives. 20:71-76.

Holcomb, C.D. and J.A. Zollweg. 1990. Improve calculation techniques for interfacial tensiometers. J. Colloid Inter. Sci. 134:41-50.

Hornof, V., B.V. Kokta and J.L. Valade. 1977. The xanthate method of grafting V. Graftability of mechanical properties. J. Appl. Polym. Sci. 21:477-485.

Hristov, V.N., M. Krumova, S. Vasileva, and G.H. Michler. 2004. Modified polypropylene wood flour composites. II. fracture, deformation, and mechanical properties. J. Appl. Polym. Sci. 92:1286-1292.

Hse, C.Y. 1968. Gluability of southern pine earlywood and latewood. Forest Prod. J. 18(12):32-36.

Hse C.Y., 1971. Properties of phenolic adhesives as related to bond quality in southern pine plywood. Forest Prod. J. 21(1):44-52.

Hse, C.Y. 1972a. Surface tension of phenol-formaldehyde wood adhesives. Holzforschung 26:82-85.

Hse, C.Y. 1972b. Method for computing a roughness factor for veneer surfaces. Wood Sci. 4(4):230-233.

Hse, C.Y. 1972c. Wettability of southern pine veneer by phenol formaldehyde wood adhesives. Forest Prod. J. 22(1):51-56.

Hse, C.Y. and M.L. Kuo. 1988. Influence of extractives on wood gluing and finishing-a review. Forest Prod. J. 38(1):52-56.

Hsiao, B.S. and E.J.H. Chen. 1990. Transcrystalline interphases in advanced polymer composites. Controlled Interphases in Composite materials, Ed. H. Ishida. Elsevier. pp. 613-622.

Hwang, C.Y. 1998. Effect of recycled fiber, compatiblizer and preformed fiber handsheet on the performance of wood-polymer composites. Dissertation. Louisiana State Univ. Baton Rouge, LA. 194 p.

Ihara, T., M. Miyoshi, M. Ando, S. Sugihara, and Y. Iriyama. 2001. Preparation of a visible-light-active TiO_2 photocatalyst by RF plasma treatment. J. Mats. Sci. 36:4201-4207.

Jang, J. and H. Yang. 2000. The effect of surface treatment on the performance improvement of carbon fiber/polybenzoxazine composites. J. Mats. Sci. 35:2297-2303.

Jensen W.B. 1978. The Lewis acid-base definitions: A status report. Chem. Reviews. ACS. 78(1):778-784.

Joseph, P.V., K. Joseph, S. Thomas, C.K.S. Pillai, V.S. Prasad, G. Groeninckx, and M. Sarkissova. 2003. The thermal and crystallisation studies of short sisal fibre reinforced polypropylene composites. Composites Part A. 34(3):253-266.

Karlsson, J.O., J.F. Blachot, A. Peguy and P. Gatenholm. 1996. Improvement of adhesion between polypropylene and regenerated cellulose fibers by surface fibrillation. Polym. Composites. 17(2):300-304.

Kazayawoko, M.J., J. Balatinecz, and R.T. Woodhams. 1997a. Diffuse reflectance Fourier transform infrared spectra of wood fibers treated with maleated polypropylenes. J. Appl. Polym. Sci. 66:1163-1173.

Kazayawoko, M., J.J. Balatinecz, R.T. Woodhams, and S. Law. 1997b. Effects of wood fiber surface chemistry on the mechanical properties of wood fiber-polypropylene composites. Intern. J. Polymeric Mat. 37(3/4):237-261.

Kazayawoko, M., J.J. Balatinecz, and R.N.S. Sodhi. 1999. X-ray photoelectron spectroscopy of maleated polypropylene treated wood fibers in a high-intensity thermokinetic mixer. Wood Sci. Tech. 33:359-372.

Keener, T.J., R.K. Stuart, and T.K. Brown. 2004. Maleated coupling agents for natural fibre composites. Composites Part A. 35(3):357-362.

Khan, M.A., K.M. Idriss Ali, and W. Wang. 1991. Electrical properties and X-ray diffraction of wood and wood plastic composite (WPC). Radiation Physics and Chemistry. 38(3):303-306.

Khan, M.A., and K.M. Idriss Ali. 1992. Effect of urea on the mechanical strength of wood-plastic composites. Radiat. Phys. Chem. 40(1):69-70.

Khan, M.A. and K.M. Idriss Ali. 1993. Wood plastic composite using different monomers in presence of additives. J. Appl. Polym. Sci. 49:1989-2001.

Khan, S., Y.H. Chui, M.H. Schneider, and A.O. Barry. 2004. Wettability of treated flakes of selected species with commercial adhesive resins. J. Instit. Wood Sci. 16(5):258-265.

Kimura, T., H. Ezure, S. Tanaka, and E. Ito. 1998. In situ FTIR spectroscopic study on crystallization process of isotactic polystyrene. J. Polym. Sci. Part B, Polym. Physics. 36(7):1227-1233.

Koch, P. 1972. Utilization of the southern pines. US Government printing office. Washington D.C. Vol. 1. 734p.

Kocurek, M.J. and R.A. Leask. 1997. Mechanical Pulping. Tappi Press. 281p.

Kokta, B.V. and C. Daneault. 1986. Use of grafted aspen fibers in thermoplastic composites: IV. Effect of extreme conditions on mechanical properties of polyethylene composites. Polymer Composites. 7(5):337-348.

Kokta, B. V., D. Maldas, C. Daneault and B. Béland. 1990. Composite of polyvinyl chloride-wood fibers, III: effect of silane as coupling agent. J. Vinyl Tech. 12(3):146-153.

Kokta, B.V. and D. Maladas. 1991. Influence of maleic anhydride as a coupling agent on the performance of wood fiber-polystyrene composites. Polym. Engin. Sci. 31(18):1351-1357.

Kolosik P.C., G.E. Myers, and J.A. Koutsky. 1992. Polypropylene crystallization on maleated polypropylene-treated wood surfaces: effects on interfacial adhesion in wood polypropylene composites. In Materials interactions relevant to recycling of wood-based materials. Mats. Res. Soc. Symp. Proc. 266:137-152.

Kolosik, P.C., G.E. Myers, and J.A. Koutsky. 1993. Bonding mechanisms between polypropylene and wood: coupling agent and crystallinity effects. In Wood Fiber/Polymer Composites: fundamental concepts, process, and material options. Ed. Wolcott, M.P. pp. 15-19.

Kwok, D.Y., T. Gietzelt, K. Grundke, H.J. Jacobasch, and A.W. Neumann. 1997. Contact angle measurement and contact angle interpretation. 1. Contact angle measurement by axisymmetric drop shape analysis and a goniometer sessile drop technique. Langmuir. 13:2880-2894.

Lando, J.L. and H.T. Oakley. 1967. Tabulated correction factors for the drop-weight-volume determination of surface and interfacial tensions. J. Colloid Interf. Sci. 25:526-530.

Larson Børve, K., H.K. Kotlar, and C.G. Gustafson. 2000. Polypropylene–phenol formaldehyde-based compatibilizers. I. Preparation and characterization. J. Appl. Polym. Sci. 75: 347–354.

Lee, S.Y. 2002. Transcrystallization behavior and interfacial strength of a semicrystalline polymer combined with thermomechanical pulp (TMP) fiber. M.S. Thesis. Univ. Idaho, Moscow, ID. 72 p.

Lee, S.Y., J. Lee, and S. Yang. 1999. Preparation of silica-based hybrid materials coated on polypropylene film. J. Mats. Sci. 34:1233-1241.

Lee S.Y., M.P. Wolcott, and T.M. Gorman. 2000. Influence of the surface morphology to the growth of transcrystalline layer (TCL) on the Kraft pulp fibers. Post presentation at the 2000 SWST Annual Meeting. Lake Tahoe. NV.

Lee, S.Y., T.F. Shupe, L.H. Groom, and C.Y. Hse. 2006. Heterogeneous nucleation of a semicrystalline polymer on fiber surfaces. In: Ed. Shupe,T.F. Recent developments in the particleboard, fiberboard, and molded wood products industry. Forest Products Society. Madison, WI. pp. 91-97.

Lennon, P., E. Espuche, D. Sage, H. Gauthier, H. Sautereau, and E. Valot. 2000. Comparison of the wetting behaviour of polyamides presented as particles and films-Influence of a plasma microwave treatment. J. Mats. Sci. 35:49-55.

Li, Y., X.M. Xiea, and B.H. Guoa. 2001. Study on styrene-assisted melt free-radical grafting of maleic anhydride onto polypropylene. Polymer. 42:3419-3425.

Lin, C.W. and Y.C. Du. 1999. Effect of surface topographies of PTEF and polyimide as characterized by atomic force microscopy on the heterogeneous nucleation of isotactic polypropylene. Mats. Chem. Phys. 58:268-275.

Lin, T.H.J. 1986. Some properties of fiber-reinforced, polyester-based composites, made with coir, jute and sisal fiber. Dissertation. Univ. Washington. Seattle, WA. 141 p.

Liu, F.P., M.P. Wolcott, D.J. Gardner, and T.G. Rials. 1994. Characterization of the interface between cellulosic fibers and a thermoplastic matrix. Composite Interfaces. 2(6):419-432.

Liu, F.P., T.G. Rials, and J. Simonsen. 1998. Relationship of wood surface energy to surface composition. Langmuir. 14:536-541.

Lu, B. and T.C. Chung. 1998. Maleic anhydride modified polypropylene with controllable molecular structure: New synthetic route via borane-terminated polypropylene. Macromol**.** 31:5943-5946.

Lu, J.Z., Q. Wu, and H.S. McNabb. 2000. Chemical coupling in wood fiber and polymer composites: A review of coupling agents and treatments. Wood Fib. Sci. 32(1):88-104.

Lu, J.Z., Q. Wu, and I. Negulescu. 2002. Influence of maleation on polymer adsorption and fixation, wood surface wettability, and interfacial bonding strength in wood-PVC composites. Wood Fib. Sci. 34(3):434-459.

Lu, J.Z., Q. Wu, and I. Negulescu. 2004. Surface and interfacial characterization of wood-PVC composites: Thermal and dynamic mechanical properties. Wood Fib. Sci. 36(4):500-510.

Machadoa, A.V., J.A. Covasa, and M. van Duinb. 2001. Effect of polyolefin structure on maleic anhydride grafting. Polymer. 42:3649-3655.

Mahlberg, R., H.E. Niemi, F. Denes, and R.M. Rowell. 1998. Effect of oxygen and hexamethyl-disiloxane plasma on morphology, wettability and adhesion properties of polypropylene and lignocellulosics. Inter. J. Adhe. Adhes. 18:283-297.

Mahlberg, R., L. Paajanen, A. Nurmi, A. Kivistö, K. Koskela, and R. Rowell. 2001. Effect of chemical modification of wood on the mechanical and adhesion properties of wood fiber/poly-propylene fiber and polypropylene/veneer composites. Holz als Roh-und Werkstoff. 59:319-326.

Maldas, D. and B.V. Kokta. 1989. Improving adhesion of wood fiber with polystyrene by the chemical treatment of fiber with a coupling agent and the influence on the mechanical properties of composites. J. Adhesion Sci. Tech. 3(7):529-539.

Maldas, D., B.V. Kokta, and C. Daneault. 1989a. Influence of coupling agents and treatments on the mechanical properties of cellulose fiber-polystyrene composites. J. Appl. Polym. Sci. 37:751-775.

Maldas, D., B.V. Kokta, and C. Daneault. 1989b. Thermoplastic composites of polystyrene: Effect of different wood species on mechanical properties. J. Appl. Polym. Sci. 38(3):413-439.

Maldas, D. and B.V. Kokta. 1990a. Influence of polar monomers on the performance of wood fiber reinforcement polystyrene composites. I. Evaluation of critical conditions. Inter. J. Polym. Mats. 14:165-189.

Maldas, D. and B.V. Kokta. 1990b. Effect of recycling on the mechanical properties of wood fiber-polystyrene composites. I. Chemithermomechanical pulp as a reinforcing filler. Polymer Composites. 11(2):77-83.

Maldas, D. and B.V. Kotka. 1991a. Surface modification of wood fibers using maleic anhydride and isocyanate as coating components and their performance in polystyrene composites. J. Adh. Sci. Tech. 5(9):727-740.

Maldas, D. and B.V. Kokta. 1991b. Influence of organic peroxide on the performance of maleic anhydride coated cellulose fiber-filled thermoplastic composites. Polym. J. 23(10): 1163-1171.

Maldas, D. and B.V. Kokta. 1991c. Performance of treated hybrid fiber-reinforced thermoplastic composites under extreme conditions: part I-Use of mica and wood pulp as hybrid fiber. Polymer Degradation Stability. 31:9-12.

Maldas, D. and B.V. Kokta. 1993. Role of coupling agents and treatments on the performance of wood fiber-thermoplastic composites. Wood fiber/polymer Composites: fundamental concepts, process, and material options. Ed. M.P. Wolcott. Forest Prods. Soc. Madison, WI. pp. 112-120.

Maldas D. 1997. Industrial perspective of cellulosics in thermoplastic composites. In Handbook of engineering and polymeric materials. Ed. Cheremisinoff, N.P. Marcel Dekker Inc. New York. 888 p.

Marcovich, N.E., M.I. Aranguren, and M.M. Reboredo. 2001. Modified woodflour as thermoset fillers Part I. Effect of the chemical modification and percentage of filler on the mechanical properties. Polymer. 42:815–825.

Matuana, L.M., R. Woodhams, C. Park, and J. Balatinecz. 1998a. Effect of surface properties on the adhesion between PVC and wood veneer laminates. Polym. Engi. Sci. 38(5): 765-773.

Matuana, L.M., R.T. Woodhams, C.B. Park, and J.J. Balatinecz. 1998b. Influence of interfacial interactions on the properties of PVC/cellulosic fiber composites. Proc. 56th Annl. Tech. Conf. ANTEC. Part 3. pp. 3313-3318.

Michell, A.J., J.E. Vaughan, and D. Willis. 1978. Wood fiber-synthetic polymer composites. II. Laminates of treated fiber and polyolefins. J. Appl. Polym. Sci. 22:2047-2061.

Minisini, B. and F. Tsobnang. 2005. Molecular dynamics study of specific interactions in grafted polypropylene organomodified clay nanocomposite. Composites Part A. 36(4):539-544.

Minor, J.L., C.T. Scott, and R.H. Atalla. 1993"Restoring Bonding Strength to Recycled Fibers" Proceedings, TAPPI Recycling Symposium, pp.379-385.

Mohanakrishnan, C.K., R. Narayan, and J.D. Nizio. 1993. Reactive extrusion processing of polypropylene-lignocellulosic blend materials. Wood fiber/polymer Composites: fundamental concepts, process, and material options. Ed. M.P. Wolcott. Forest Products Society. Madison, WI. pp. 57-62.

Montes-Morán, M.A., A. Martínez-Alonso, J.M.D. Tascón, and R.J. Young. 2001. Effects of plasma oxidation on the surface and interfacial properties of ultra-high modulus carbon fibres. Composites: Part A. 32:361-371.

Mullin J.W. 1993. Crystallization. 3rd ed. Butterworth-Heinemann Ltd. Burlington. MA. 527 p.

Myers G.E., I.S. Chahyadi, C.A. Coberly, and D.S. Ermer. 1991. Wood flour/polypropylene composites: influence of maleated polypropylene and process and composition variables on mechanical properties. Intl. J. Polym. Mats. 15:21-44.

Myers G.E, C.M. Clemons, J.J. Balatinecz, and R.T. Woodhams. 1992. Effects of composition and polypropylene melt flow on polypropylene–waste newspaper composites. In Proc. Antec '92; May 3–7, 1992. Detroit, MI: Society of Plastic Engineers.

Neff, R., A. Adedeji, C.W. Macosko, and A.J. Ryan. 1998. Urea hard segment morphology in flexible polyurethane foam. J. Polym. Sci. Part B. 36:573-581.

Oever, M. and T. Peijs. 1998. Continuous-glass-fibre-reinforced polypropylene composites II. Influence of maleic-anhydride modified polypropylene on fatigue behaviour. Composites Part A. 29(3):227-239.

Oksman, K. and H. Lindberg. 1998. Influence of thermoplastic elastomers on adhesion in polyethylene-wood flour composites. J. Appl. Polym. Sci. 68(11):1845-1855.

Pandey, K.K. 1999. A Study of Chemical Structure of Soft and Hardwood and Wood Polymers by FTIR Spectroscopy. J. Appl. Polym. Sci. 71:1969-1975.

Parida, D. P. Nayak, D.K. Mishra, S. Lenka, P. L Nayak, S. Mohanty and K.K. Rao. 1995. Polymers from renewable resources. VIII. Thermal properties of the interpenetrating polymer networks derived from castor Oil-isophorone diisocyanate-polyacrylamides. J. Appl. Polym. Sci. 58:1731-1738.

Park, S.H., K.Y. Park, and K.D. Suh. 1998. Compatibilizing effect of isocyanate functional group on polyethylene terephthalate/low density polyethylene blends. J. Polym. Sci. Part B, Polym. Physics. 36:447-453.

Paunov V.N. 2003. Novel method for determining the three-phase contact angle of colloid particles adsorbed at air-water and oil-water interfaces. Langmuir. 19:7970-7976.

Pendleton, D.E., T.A. Hoffard, T. Adcock, B. Woodward, and M.P. Wolcott. 2002. Durability of an extruded HDPE/wood composite. Forest Prod. J. 52(6): 21-27.

Pittman, Jr. C.U., X. Xub, L. Wangb, and H. Toghianib. 2000. Characterizing semi-interpenetrating polymer networks composed of poly(vinyl chloride) and 5–15% of oligomeric MDI isocyanate cross-linked networks. Polym. 41:5405–5413.

Pizzi A. 1994. Advanced wood adhesives technology. Marcel Dekker Inc. New York. 289 p.

Plasma processing and processing science (PPPS). 1995. Commission on physical sciences, mathematics, and applications (CPSMA) National Research Council (NRC). National Academy Press. 36 p.

Poncin-Epaillard, F., J.C. Brosse, and T. Falher. 1997. Cold plasma treatment: surface or bulk modification of polymer films. Macromol. 30:4415-4420.

Porta, G.M., J.D. Rancourt, and L.T. Taylor. 1990. Adhesion of titanium to plasma treated polyester. In: Proc. ACS division of Polymeric materials: Sci. Engin. 63:87-89.

Queiroz, D.P. and M.N. Pinho. 2002. Gas permeability of polypropylene oxide/polybutadiene bi-soft segment urethane/urea membranes. Desalination. 145(1-3):379-383.

Quillin, D.T., D.F. Caulfield, and J. Koutsky. 1993. Crystallinity in the polypropylene/cellulose system (I). Nucleation and crystalline morphology. J. Appl. Polym. Sci. 50(7):1187-1194.

Rabinovich, Y.I., J.J. Adler, M.S. Esayanur, A. Ata1, R.K. Singh, and B.M. Moudgil. 2002. Capillary forces between surfaces with nanoscale roughness. Adv. Colloid Int. Sci. 96:213-230.

Raj R.G., B.V. Kokta, D. Maladas, and C. Daneault. 1988. Use of wood fiber in thermoplastic composites: VI. Isocyanates as bonding agent for polyethylene-wood fiber composites. Polym. Composites. 9(6):404-411.

Raj, R.G., B.V. Kokta. F. Dembele, and B. Sanschagrain. 1989a. Compounding of cellulose fibers with polypropylene: Effect of fiber treatment on dispersion in the polymer matrix. J. Appl. Polym. Sci. 38:1987-1996.

Raj, R.G., B.V. Kokta and C. Daneault. 1989b. Polyethylene-wood fiber composites: Effect of fiber treatment on mechanical properties. Intern. J. Polym. Mat. 12:239-250.

Raj, R.G., B.V. Kokta, and C. Daneault. 1990. The use of isocyanate as a bonding agent to improve the mechanical properties of polyethylene-wood fiber composites. Intern. J. Polym. Mats. 14:223-234.

Raj, R.G. and B.V. Kokta. 1995. Effect of aging cycle on mechanical properties of HDPE-pretreated wood fiber composites. Woodfiber-plastic composites: virgin and recycled wood fiber and polymers for composites. Eds. Caulfield et al. pp. 220-226.

Rehn, P. and W. Viöl. 2003. Dielectric barrier discharge treatments at atmospheric pressure for wood surface modification. Holz als Roh- und Werkstoff. 61(2):145-150.

Reinsch V.E. and S.S. Kelley. 1997. Crystallization of poly (hydroxybutyrate-co-hydroxyvalerate) in wood fiber-reinforced composites. J. Appl. Polym. Sci. 64(9):1791-1795.

Rezai, E. and R.R. Warner. 1997. Polymer-grafted cellulose fibers. I. Enhanced water absorbency and tensile strength. J Appl Polym Sci. 65:1463-1469.

Rietveld, J. X. and M. J. Simon. 1992. Processability and properties of wood flour filled polypropylene. Inter. J. Polymeric Mats. 18:213-235.

Richter, K., W.C. Feist, and M.T. Knaebe. 1994. The effect of surface roughness on the performance of finishes. Research and work reports, EMPA wood dept. Swiss Federal Lab. for Materials Testing and Research. 83 p.

Sain, M. and B.V. Kokta. 1993a. Study on molecular interaction in polyfunctional maleimide modified polypropylene/pulp composites by ESCA, FTIR, and DSC. J. Adh. Sci. Tech. 7(7):745-749.

Sain, M. and B.V. Kokta. 1993b. Toughened thermoplastic composite. I. Cross-linkable phenol formaldehyde and epoxy resin-coated cellulosic-filled polypropylene composites. J. Appl. Polym. Sci. 48:2181-2196.

Sain, M.M, B.V. Kotka, and C. Imbert. 1994. Structure property relationships of wood fiber filled polypropylene composite. Polym. Plastic. Tech. Eng. 33(1):89-104.

Sakai, K., M. Matsunaga, K. Minato, and F. Nakatsubo. 1999. Effects of impregnation of simple phenolic and natural polycyclic compounds on physical properties of wood. J. Wood Sci. 45:227-232.

Sapieha, S., P. Allard, and Y.H. Zang. 1990. Dicumyl peroxide-modified cellulose/LLDPE composites. J. Appl. Polym. Sci. 41(9-10):2039-2048.

SAS Institute Inc. 2004. What's New in SAS® 9.0, 9.1, 9.1.2, and 9.1.3. SAS Institute Inc., Cary, NC, USA. 301 p.

Scheikl, M. and M. Dunky. 1998. Measurement of dynamic and static contact angles on wood for the determination of its surface tension and the penetration of liquids into the wood surface. Holzforschung. 52(1):89-94.

Sharma, P.K. and K.H. Rao. 2002. Analysis of different approaches for evaluation of surface energy of microbial cells by contact angle goniometry. Adv. Colloid Interf. Sci. 98:341-463.

Sharples A. 1966, Introduction to polymer crystallization. Edward Arnold LTD. London. 138 p.

Shupe, T.F., C.Y. Hse, E.T. Choong, and L.H. Groom. 1998. Effect of wood grain and veneer side on loblolly pine veneer wettability. Forest Prod. J. 48(6):95-97.

Simonsen, J., R. Jacobsen, and R. Rowell. 1998. Wood-fiber reinforcement of styrene–maleic anhydride copolymers. J. Appl. Polym. Sci. 68:1567–1573.

Sjöström E. 1981. Wood chemistry; Fundamentals and applications. Academic Press, Inc. London. 223 p.

Sjöström, E. and R. Alen. 1999. Analytical methods in wood chemistry, pulping, and papermaking. Springer-Verlag Berlin Heidelberg New York. 316 p.

Skeist I., 1989, Handbook of adhesives. 3rd Edition. Reinhold publishing corporation chapman & hall LTD. New York. 779 p.

Smook G.A. 1992. Handbook for pulp and paper technologists. 2nd Edition. Angus Wilde Publication, Vancouver, B.C. 396 p.

Society of the Plastics Industry (SPI). 1991. Plastics engineering handbook of the Society of the Plastics Industry. Ed. Berins, M.L. 5th Edt. Van Nostrand Reinhold, New York. 885 p.

Špírková, M., J. Budinski-Simendic, M. Ilavský, P. Špaček, and K. Dušek. 1993. Formation of poly(urethane-isocyanurate) networks from poly(oxypropylene)diols and diisocyanate. Polym. Bulletin. 31:83-88.

Stark, N.M. 1999. Wood fiber drived from scrap pallets used in polypropylene composites. Forest Prod. J. 49(6):39-46.

Sundholm J. 1999. Mechanical pulping. Gummerus Printing. Finland. 427 p.

Takase, S. and N. Shiraishi. 1989. Studies on composites from wood and polypropylenes. II. J. Appl. Polym. Sci. 37:645-659.

Tappi. 1988. Tappi test method T204 om-88 Solvent extractives of wood and pulp. Tappi. Atlanta, GA.

Teo, L.S., C.Y. Chen, and J.F. Kuo. 1997. Fourier transform infrared spectroscopy study on effects of temperature on hydrogen bonding in amine-containing polyurethanes and poly(urethane-urea)s. Macromols. 30:1793-1799.

Thorsen, W.J., W.H. Ward, and M.M. Millard. 1979. Wool shrinkage control and surface modification by ozone. J. Appl. Polym. Sci. 24:523-546.

Thwe, M.M. and K. Liao. 2002. Effects of environmental aging on the mechanical properties of bamboo-glass fiber reinforced polymer matrix hybrid composites. Composites A. 33(1):43-52.

Trivedi, B.C. and B.M. Culbertson. 1982. Maleic anhydride. Plenum Press. New York. 871 p.

Verhey, S.T. and P.E. Laks. 2002. Wood particle size affects the decay resistance of woodfiber/thermoplastic composites. Forest Prod. J. 52(11/12):78-81.

Wålinder, M. 2000. Wetting phenomena on wood: factors influencing measurements of wood wettability. Dissertation. Dept. Manuf. Sys., KTH-Royal Insti. Tech. Stockholm, Sweden. 62 p.

Wålinder, M.E.P. and G. Ström. 2001. Measurement of wood wettability by the Wilhelmy method. Part 2. determination of apparent contact angles. Holzforschung. 55:33-41.

Wang G. and I.R. Harrison. 1994. Study of the preferential crystallization of polypropylene on the surface of wood fibers. In: Proc. 52nd Annual Tech. Conf. ANTEC 94. Part 2. pp. 1474-1475.

Wang, C. and L.M. Hwang. 1996a. Transcrystallization of PTFE Fiber/PP composites (I) crystallization kinetics and morphology. J. Polym. Sci.: Part B: Polym. Phys. 34:47-56.

Wang, C. and L. Hwang. 1996b. Transcrystallization of PTFE fiber/PP composites (II). Effect of transcrystallinity on the interfacial strength. J. Polym. Sci. Part B: Polym. Phys. 34:1435-1442.

Wang, R., M. Takeda, K. Mukai, and M. Kido. 2001. AC non contact mode atomic force microscopy of pure water wetting on natural mica and SUS304 steel. J. Japan Inst. Mats. 65(12):1057-1065.

Westerlind, S. Bo, and J.C. Berg. 1988. Surface energy of untreated and surface-modified cellulose fibers. J. Appl. Polym. Sci. 36(3): 523-534.

Wilkinson, M.C. and M.P. Aronson. 1973. Applicability of the drop-weight technique to the determination of the surface tension of liquid metals. J. Chem. Soc. Faraday Trans. 69:474-480.

Wolcott M.P., S. Yin, and T.G. Rials. 2000. Using dynamic mechanical spectroscopy to monitor the crystallization of PP/MAPP blends in the presence of wood. Composite Interfaces. 7(1):3-12.

Wolcott M.P. 2003. Formulation and process development of flat-pressed wood-polyethylene composites. Forest Prod. J. 53(9):25-32.

Wu, J., D. Yu, C. Chan, J. KIM, and Y. Mai. 2000. Effect of fiber pretreatment condition on the interfacial strength and mechanical properties of wood fiber/PP composites. J. Appl. Polym. Sci. 76:1000-1010.

Wua, C.M, M. Chena, and J. Karger-Kocsisb. 2001a. Effect of micromorphologic features on the interfacial strength of iPP/Kevlar fiber microcomposites. Polymer. 42:199-208.

Wua, C.M., M. Chena, and J. Karger-Kocsisb. 2001b. Interfacial shear strength and failure modes in sPP/CF and iPP/CF microcomposites by fragmentation. Polymer. 42:129-135.

Xue, P., and X.M. Tao1. 2005. Morphological and electromechanical studies of fibers coated with electrically conductive polymer. J. Appl. Polym. Sci. 98:1844-1854.

Yin S., T.G. Rials, and P.M. Wolcott. 1999. Crystallization behavior of polypropylene and its effect on wood fiber composite properties. In: Proc. 5th intern. Conf. Wood-plastic Composites. pp. 139-145.

Young, R. A., F. Denes, L. Nielsen and X. Tu. 1995. Improvement of biobased fiber-plastic composite properties through cold plasma treatments. Woodfiber-Plastic Composites: Virgin and recycled wood fiber and polymers for composites. Eds. Caulfield et al. pp. 220-226.

Young, R.A., F. Denes, L. Nielsen, and X. Tu. 1996. Improvement of bio-based fiber-plastic composite properties through cold plasma treatments. Woodfiber-plastic composites. Virgin and recycled wood fiber and polymers for composites. May 1-3, 1995, Madison, WI. pp. 227-234.

Zwillinger D.(ed.) 2003. CRC: Standard mathematical tables and formulae. 31st edit., Chapman & Hall / CRC Press, Inc., Boca Raton. 910 p.

VITA

The author was born in Yechun, Kyungbuk, Korea, in 1967. In 1993, he received his Bachelor of Science degree at Youngnam University in forestry. In 1995 and 2002, he received his Master of Science degrees both in forest products from Youngnam University and University of Idaho, respectively. He started graduate work in the School of Renewable Natural Resources at Louisiana State University in August 2003. He is currently a candidate for the degree of Doctor of Philosophy in forestry to be awarded at the Summer Commencement, 2006.